

**Nitroalkene Repression of Homologous Recombination as a Treatment for Triple
Negative Breast Cancer**

by

Alparslan Asan

B.S., University of Washington, 2013

Submitted to the Graduate Faculty of
the School of Medicine in partial fulfillment
of the requirements for the degree of
Doctor of Philosophy

University of Pittsburgh

2019

UNIVERSITY OF PITTSBURGH
SCHOOL OF MEDICINE

This dissertation was presented

by

Alparslan Asan

It was defended on

April 19, 2019

and approved by

Christopher Bakkenist, Associate Professor, Pharmacology & Chemical Biology

Adrian Lee, Professor, Pharmacology & Chemical Biology

Da Yang, Assistant Professor, Pharmacy

Bruce Freeman, Professor, Pharmacology & Chemical Biology

Dissertation Director: Carola Neumann, Associate Professor, Pharmacology & Chemical
Biology

Copyright © by Alparslan Asan

2019

Nitroalkene Repression of Homologous Recombination as a Treatment for Triple Negative Breast Cancer

Alparslan Asan, PhD

University of Pittsburgh, 2019

Triple-negative breast cancer (TNBC) is a heterogenous disease accounting for ~20% of all breast cancer (BC) cases. It is characterized by high genomic instability making it an aggressive BC subtype with higher rates of metastatic disease compared to other BC subtypes. In ~15% of TNBC, genomic instability is caused by loss of function mutations in *BRCA1/BRCA2* genes leading to homologous recombination (HR) deficiency which increases sensitivity for PARP inhibitor (PARPi) therapy. Therefore, there has been a great interest in extending the utility of PARP inhibitors to patients who are wildtype for *BRCA1/BRCA2*. The nitro-fatty acid (NFA) 10-nitro-octadec-9-enoic acid (OA-NO₂) was identified as an inhibitor of RAD51, an enzyme essential in HR. NFAs alkylate protein cysteines via Michael addition reaction and Cys319 in RAD51 is a specific target of OA-NO₂. Thus, to mimic a *BRCA* mutant phenotype in wildtype *BRCA* TNBC cells, OA-NO₂ was combined with a PARPi (olaparib or talazoparib) and other antineoplastic DNA-damaging therapies including doxorubicin, cisplatin and γ -irradiation (IR). Talazoparib combined with OA-NO₂ displayed high levels of synergistic growth inhibition of MM231 TNBC cells *in vitro* and *in vivo*: mice treated with talazoparib plus OA-NO₂ had significantly decreased tumor growth rates when compared to vehicle, talazoparib or OA-NO₂ alone. Also, OA-NO₂ inhibited IR-induced RAD51 foci formation and enhanced H2A histone family member X (H2AX) phosphorylation in TNBC cells. Additional analyses of fluorescent DSB reporter activity with both static-flow cytometry and kinetic live-cell studies, enabling

temporal resolution of recombination, revealed that OA-NO₂ does not affect non-homologous end-joining (NHEJ). Rather, OA-NO₂ inhibits post-resection DNA DSB repair pathways HR, single-strand annealing (SSA) and alternative end-joining (Alt-EJ). In conclusion, RAD51 Cys-319 is a functionally significant site for adduction of soft electrophiles such as OA-NO₂ and suggests further investigation of lipid electrophile-based combinational therapies for TNBC.

Table of Contents

Preface.....	xiii
1.0 Introduction.....	1
1.1 DNA Repair.....	1
1.1.1 DNA Repair Overview.....	1
1.1.2 Direct Repair, Base Excision Repair, Mismatch Repair and Nucleotide Excision Repair	2
1.1.3 Double-stranded Break (DSB) Repair	4
1.1.3.1 Non-Homologous End Joining.....	6
1.1.3.2 Homologous Recombination	8
1.1.3.3 Other Post-resection DSB repair pathways: Single-strand annealing (SSA) and Alternative End Joining (alt-EJ).....	11
1.1.4 Homologous Recombination and Cancer.....	12
1.1.5 Poly (ADP-ribose) polymerase (PARP).....	13
1.1.6 Targeting DNA Damage Response (DDR) Components in Cancer.....	13
1.1.7 Targeting Homologous Recombination in Cancer.....	15
1.2 Breast Cancer.....	17
1.2.1 Breast Cancer Overview.....	17
1.2.2 Triple-Negative Breast Cancer	19
1.2.3 Current Therapies for TNBC	19
1.2.4 BRCAness in TNBC.....	20
1.2.5 Evaluation of BRCAness in TNBC.....	20

1.2.6 PARP inhibitors	23
1.3 Electrophilic Fatty Acids	25
1.3.1 Interaction of Electrophiles with Nucleophiles.....	26
1.3.2 Electrophilic Fatty Acid Formation	27
1.3.3 Electrophilic Fatty Acids as Signaling Mediators	28
1.3.4 Electrophilic Fatty Acids in TNBC.....	28
2.0 Materials and Methods.....	30
2.1 Reagents and Cell Lines.....	30
2.2 OA-NO ₂	30
2.3 OA-NO ₂ <i>in vivo</i>	31
2.4 Plasmids.....	31
2.5 Clonogenic Survival Assays	32
2.6 DSB Repair Assays.....	32
2.7 Cell Cycle Analysis	33
2.8 Kinetic DSB Repair Assays.....	33
2.9 Immunostaining and Imaging	34
2.10 Western Blotting.....	34
2.11 Immunoprecipitation.....	35
2.12 Biotinylated OA-NO ₂ Affinity Capture of RAD51	35
2.13 DNA Binding Assays	36
2.14 γ -irradiation	36
2.15 Statistical Analysis.....	36

3.0 Impact of OA-NO₂ on Triple Negative Breast Cancer Cell Growth as a Single Agent and in Combination with DNA Targeted Therapies	38
3.1 Effects of OA-NO₂ on TNBC DNA Damage <i>in vivo</i>.....	38
3.2 Effects of OA-NO₂ in Combination with Chemotherapeutic Drugs and PARP Inhibition on TNBC Cells <i>in vitro</i>	40
3.3 OA-NO₂ Induces Heightened γH2AX and Sensitizes TNBC Cells to Ionizing Radiation (IR)	43
3.4 Discussion	46
4.0 Impact of OA-NO₂ on Double-Strand Break Repair Pathways	47
4.1 OA-NO₂ Inhibits Homologous Recombination	47
4.2 OA-NO₂ has no Effect on Non-Homologous End Joining.....	49
4.3 OA-NO₂ Inhibits Single Strand Annealing (SSA) and Alternative End Joining (Alt-EJ)	52
4.4 Discussion	54
5.0 Inhibition of RAD51 by OA-NO₂.....	55
5.1 OA-NO₂ Inhibits RAD51 Foci Formation in TNBC Cells	55
5.2 OA-NO₂ Targets RAD51 Cysteine 319	58
.....	60
5.3 OA-NO₂ Abrogates RAD51-DNA Interaction	61
5.4 Discussion	66
6.0 Pre-Clinical Studies Investigating Combinational Treatments of OA-NO₂ and PARP Inhibitors in TNBC	69

6.1 Talazoparib Inhibits MDA-MB-231 Cell Growth More Potently Than Olaparib in Combination With OA-NO ₂	69
6.2 Talazoparib in Combination with OA-NO ₂ Reduces Relative Tumor Growth <i>in vivo</i>	71
6.3 Discussion	73
7.0 Testing Other Nitro-Fatty Acid Derivatives.....	75
7.1 Identifying Other Nitroalkenes to be Investigated	75
7.2 The Effects of Nitroalkene Derivatives on TNBC Cell Growth	76
7.3 The Effects of Nitroalkene Derivatives on HR Efficiency	78
7.4 Discussion	80
8.0 Conclusions and Future Directions	81
8.1 Conclusions	81
8.2 Future Directions.....	84
Appendix – List of Potential OA-NO ₂ Targets in DNA Repair Pathways.....	87
Bibliography	91

List of Tables

Table 1. Breast cancer molecular subtypes and correlations with surface receptor expression. ..	18
Table 2. Chemical structures and characteristics of lipids used.	59
Table 3. Chemical structures of additional electrophilic nitro-fatty acid derivatives tested against TNBC cells.....	76

List of Figures

Figure 1. DNA repair overview.	1
Figure 2. Overview of double-strand break (DSB) DNA repair pathways.....	5
Figure 3. Regulation of DSB repair pathways.....	6
Figure 4. Schematic overview of non-homologous end joining repair (NHEJ).	7
Figure 5. Schematic overview of homologous recombination (HR) repair.....	10
Figure 6. Potential clinical utility of using biomarkers in triple negative breast cancer (TNBC).22	
Figure 7. PARP inhibitors in clinical development.	24
Figure 8. The Michael Addition reaction.....	25
Figure 9. Post-translational modification of a protein (nucleophile) by a nitroalkene (electrophile).	27
Figure 10. OA-NO ₂ inhibits tumor growth and induces DNA damage in TNBC cells <i>in vivo</i>	39
Figure 11. Antiproliferative effects of OA-NO ₂ in combination with chemotherapeutic drugs and PARPi.	42
Figure 12. OA-NO ₂ induces increased γ H2AX in irradiated TNBC cells.	44
Figure 13. Clonogenic formation of TNBC cells following OA-NO ₂ and IR treatment.	45
Figure 14. OA-NO ₂ inhibits HR in U2OS cells.....	48
Figure 15. OA-NO ₂ does not inhibit NHEJ in U2OS cells.....	50
Figure 16. OA-NO ₂ effects on HR and NHEJ in U2OS cells measured via live cell fluorescence imaging.	51
Figure 17. OA-NO ₂ inhibits DSB repair pathways SSA and Alt-EJ.	53
Figure 18. OA-NO ₂ inhibits RAD51 foci formation.	56

Figure 19. Overexpression of RAD51 partially rescues HR inhibition by OA-NO ₂	57
Figure 20. OA-NO ₂ binds to RAD51 at Cys319.....	60
Figure 21. OA-NO ₂ inhibits RAD51-DNA interaction in an <i>in vitro</i> fluorescent polarization (FP) based DNA binding assay.....	62
Figure 22. OA-NO ₂ removes RAD51 from DNA in an <i>in vitro</i> FP-based assay.	64
Figure 23. OA-NO ₂ represses HR and causes genomic instability and death in TNBC cells.	65
Figure 24. Crystal structure of pre-synaptic RAD51 filament on single-stranded DNA.....	68
Figure 25. Synergistic growth inhibition of MDA-MB-231 (MM231) cells is obtained when talazoparib is combined with OA-NO ₂	70
Figure 26. Talazoparib in combination with OA-NO ₂ reduces relative tumor growth compared to vehicle, PARPi or OA-NO ₂ <i>in vivo</i>	72
Figure 27. Clonogenic outgrowth comparison of MM231 cells treated with increasing concentrations of nitro-fatty acid derivatives.	77
Figure 28. HR inhibition by NFA-8 and NFA-5 are compared to HR inhibition by OA-NO ₂	79

Preface

Acknowledgments

I would like to thank my advisor Dr. Carola Neumann, for her guidance throughout the years of my training. Her dedicated mentorship helped me become a better scientist, through perseverance and commitment to results. I would also like to thank my co-mentor Dr. Bruce Freeman who supported me generously and with utmost compassion. He guided me to become a better leader as well as a great team member. I would like to give a special “thank you” to Dr. John Skoko who guided me to becoming the most rigorous and methodical scientist I can be. His support and vision have been vital for this project to succeed.

I would like to thank my committee members: Dr. Christopher Bakkenist, Dr. Adrian Lee and Dr. Da Yang. Their valuable insights and suggestions as well as their feedback helped me to successfully complete my thesis aims as well as making the right adjustments. Their feedback from the very beginning shaped this dissertation and drove the entire project forward most efficiently.

Lastly, I would like to thank the entire 4th floor of MWRI, the Freeman Lab and the entire cohort of Molecular Pharmacology graduate students. Anywhere from learning how to use a new instrument to giving valuable feedback on my presentations, these people helped me overcome many challenges during my training.

Abbreviations

DR: Direct reversal

MMR: Mismatch repair

NER: Nucleotide excision repair

BER: Base excision repair

DSB: Double-stranded break

MGMT: *O*⁶-methylguanine DNA methyltransferase

SSB: Single-stranded break

ROS: Reactive oxygen species

PARP: poly- (ADP ribose) polymerase

RPA: Replication protein A

RFC: Replication factor C

PCNA: Proliferating cell nuclear antigen

DDR: DNA damage response

ATM: Ataxia telangiectasia mutated

NHEJ: Non-homologous end joining

HR: Homologous recombination

DNA-PKcs: DNA-dependent protein kinase catalytic subunit

CtIP: CtBP-interacting protein

BRCA1: Breast cancer early onset gene 1

ATP: adenosine triphosphate

BRCA2: Breast cancer early onset gene 2

SSA: Single-strand annealing

Alt-EJ: Alternative end-joining

γ H2AX: Phosphorylated histone H2AX

ATR: Ataxia telangiectasia and Rad3-related

PARPi: PARP inhibition

TNBC: Triple negative breast cancer

ER: Estrogen receptor

PR: Progesterone receptor

HER2: human epidermal growth factor receptor-2

PTM: Post-translational modification

PUFA: poly-unsaturated fatty acid

OA-NO₂: 10-nitro-octadec-9-enoic acid (nitro-oleic acid)

OA: Octadec-9-enoic acid (oleic acid)

SA-NO₂: 10-nitro-octadecanoic acid

NFA5: 6/7-nitro-octadec-6-enoic acid

NFA8: 7/8-nitro-nonadec-7-enoic acid

NFA12: 5/6-nitro-eicos-5-enoic acid

NFA21: 14-nitro-pentadec-14-enoic acid

To my parents, Habip and Aşkın, my sisters Hilal and Yasemin, and my niece Rüya.

1.0 Introduction

1.1 DNA Repair

1.1.1 DNA Repair Overview

The multitude of exogenously and endogenously-stimulated DNA-damaging events requires that DNA damage be vigilantly detected and efficiently repaired. Several DNA repair mechanisms have been identified that ameliorate deleterious genomic perturbations such as direct reversal (DR), mismatch repair (MMR), nucleotide excision repair (NER), base excision repair (BER) and double-stranded break (DSB) repair [1] (Fig. 1).

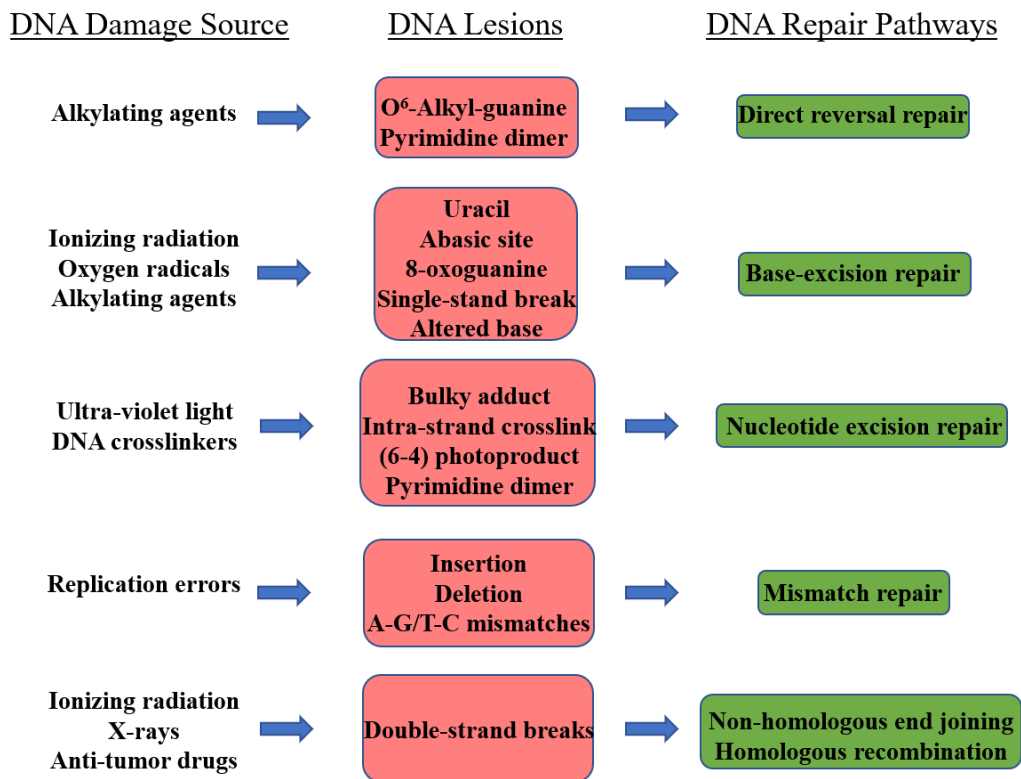


Figure 1. DNA repair overview.

1.1.2 Direct Repair, Base Excision Repair, Mismatch Repair and Nucleotide Excision Repair

DNA damaging agents that do not directly induce DSBs lead to the DNA repair pathways DR, BER, MMR or NER based on the kind of DNA lesion produced (Fig. 1).

Direct repair removes alkyl groups from specific oxygen positions of methylated guanine and thymine bases that result from normal cellular metabolism and carcinogens [2]. The DNA repair protein involved in this process is called *O*⁶-methylguanine DNA methyltransferase (MGMT) and its role is to transfer a methyl group from the *O*⁶ position onto itself. This then marks MGMT for degradation [3]. If the production of MGMT is impaired, there is an abundance of alkyl adducts and this leads to impaired pairing of bases during replication.

BER is the most commonly utilized repair mechanisms in cells. In cells, most single-stranded breaks (SSBs) result from reactive oxygen species (ROS) that are produced endogenously. It corrects SSBs that result from oxidation, alkylation, and deamination of bases [4]. BER uses glycosylases to remove impaired bases by cleaving N-glycosidic bonds that results in an abasic (AP) site [5]. AP endonuclease/Redox Factor 1 (APE1) and additional proteins that it recruits then prepares this site for addition of new bases [4]. PARP1 [poly-(ADP ribose) polymerase 1] is a BER protein that is involved in detecting damage. It decondenses the chromatin in the damaged area and recruits additional repair proteins [6]. PARP is a nuclear enzyme that catalyzes the transfer of ADP-ribose from NAD⁺ to mark proteins involved in chromatin architecture and DNA metabolism [7]. If left unrepaired, SSBs can lead to DSBs.

MMR ensures high fidelity DNA replication. It corrects errors that polymerases fail to identify [8]. During replication, MMR corrects the newly produced daughter strand using the parental strand as a template. MMR mainly repairs mismatches that occur in single nucleotides.

The errors occur during normal replication but can be exasperated by endogenously produced ROS as well as exogenous agents [9]. The main players involved in MMR are MSH2:MSH6 as well as MSH2:MSH3 nuclear protein complexes for recognizing damage, replication protein A (RPA) for stabilization and recruitment of replication factor C (RFC) and proliferating cell nuclear antigen (PCNA) that are important for protection of the damage site. DNA exonuclease (Exo1) removes the damaged area and a DNA polymerase (Pol δ) replaces it with Ligase I which ligates the new DNA product [8]. DSBs can occur if there is damage to the parental strand since MMR only accounts for the repair of the daughter strand [1].

NER repairs damage that is induced by UV light which leads to adjacent pyrimidine base crosslinking. NER also deals with damage done by mutagenic chemical compounds such as platinum agents which lead to crosslinks between purine bases and bases that are in different strands [10]. NER accounts for large adducts that are produced by such damage. Proteins involved in NER are transcription factor IIIH (TFIIH) complex involving helicases XPB and XPD, stability proteins RPA and XPA, endonucleases XPG and XPF as well as DNA excision repair protein ERCC1 [11]. In later steps, proteins such as DNA polymerases δ and ϵ and Ligase I are also involved for completion of the repair [12]. NER malfunction is linked with breast cancer, with NER protein levels reduced in tumor samples compared to normal tissue [13]. Additionally, certain polymorphisms in NER genes, which are more likely to be found in African American women, are associated with increased risk of breast cancer [14].

1.1.3 Double-stranded Break (DSB) Repair

DNA DSBs are the most pathogenic forms of DNA damage, as the loss of genomic material and mutations promote genomic variability and disequilibrium. In normal cells, DSBs are very rare, occurring about 10 times a day per cell [15]. DSBs can occur during replication fork stalls due to unrepaired base damage and when two separate SSB events occur in locations that are close to each other between two DNA strands [16]. Endogenous sources of DSBs are rare but can happen when the phosphate backbones of two complementary DNA strands break at the same time due to cellular oxidative damage [17]. Exogenous DSB inducers include topoisomerase poisons (e.g. doxorubicin), ionizing radiation (IR), DNA base crosslinking agents (e.g. cisplatin) and radiomimetic drugs (e.g. bleomycin) [18, 19]. High doses of IR induce DSBs in addition to SSBs [20].

Access to DNA broken ends is achieved by chromatin restructuring initiated by phosphorylation cascade by the DNA damage response (DDR) [21]. Upon damage, the Mre11-Rad50-NBS1 (MRN) complex binds to the DSB [22]. This complex recruits a regulator of DDR, ataxia telangiectasia mutated (ATM), which carries out many required protein phosphorylation events [23]. Of interest, histone variant H2AX is phosphorylated by ATM in response to DSBs, which is an early event for all DSB repair pathways [24].

There are two main pathways that cells utilize in order to repair DSBs: non-homologous end joining (NHEJ) and homologous recombination (HR) (Fig. 2). While error-prone NHEJ is faster and more frequently used, HR repair mechanisms maintain the highest fidelity of the genome by carrying out repair processes via using newly synthesized homologous sister chromatid as a template. HR repair protects cells from the deleterious genomic instability caused by DSBs. It corrects for the loss of genetic material through homologous template searches that maintain the

genomic landscape [25]. An overview of DSB repair is summarized in Figure 2. Which pathway is used depends on what phase of the cell cycle the cell is in, the availability of key repair proteins, and whether the ends of the breaks are prone to being easily joined by NHEJ [15, 26, 27]. NHEJ is mostly active during G0 and G1 and HR is mostly active during G2 and S phase (Fig. 3). This is important when developing targeted inhibitors to prevent cancer cell DNA repair, since cancer cells are more frequently in phase G2/S compared to normal cells. An inhibitor of HR is more likely to be targeted to cancer cell DNA repair mechanisms in contrast to normal cells.

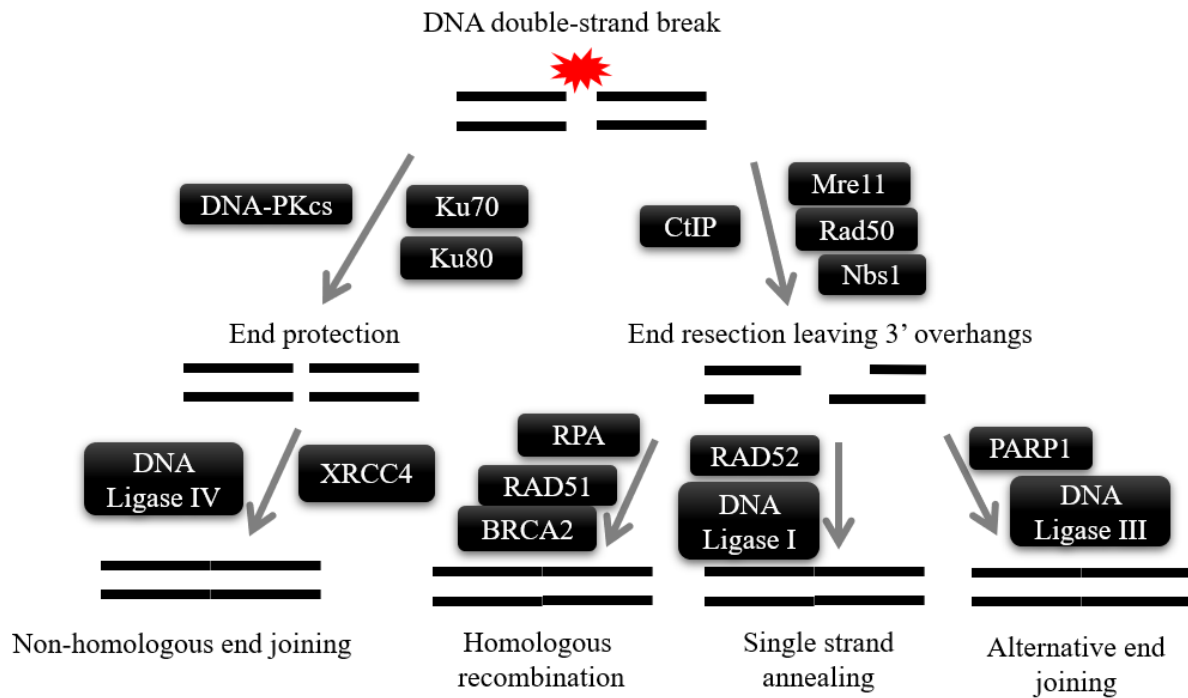


Figure 2. Overview of double-strand break (DSB) DNA repair pathways.

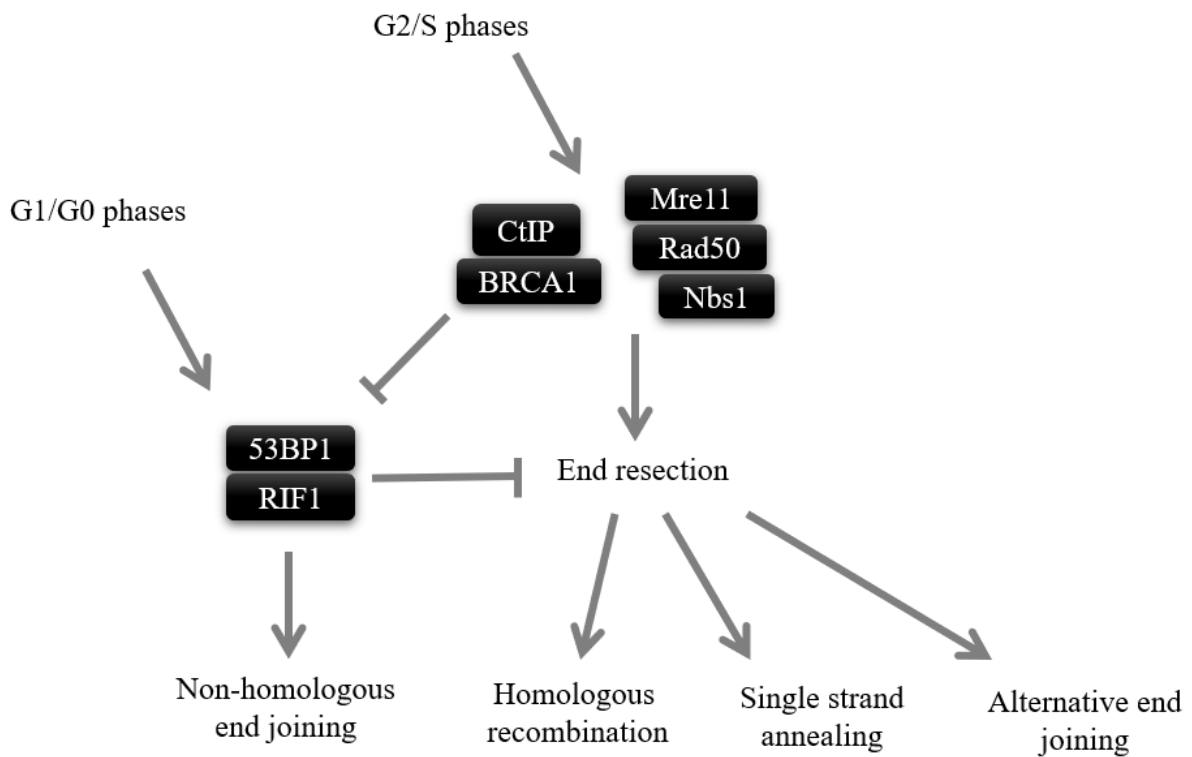


Figure 3. Regulation of DSB repair pathways.

1.1.3.1 Non-Homologous End Joining

NHEJ is the main pathway of DSB repair in mammalian cells. It also plays a major role in the development of the immune system. It is essential to V(D)J recombination to promote antigen diversity in mammalian cells [28]. NHEJ does not depend on DNA end resection in contrast to HR. It does not use homologous template for repair and the ligation of broken DNA ends which can be mutagenic due to loss of information [29].

Steps for NHEJ include detection, alignment, protection and joining of broken DNA ends. A protein heterodimer called Ku70/Ku80 binds to these broken ends and recruits additional protection components to the site [30]. 53BP1 and RIF1 are also end-protection factors. Ku70/Ku80 recruits DNA-dependent protein kinase catalytic subunit (DNA-PKcs) to the broken ends [1]. Both Ku70/Ku80 and DNA-PKcs protect DNA ends from nucleolytic degradation,

potentiate DNA end ligation by tethering the two ends together and recruit other NHEJ factors [31, 32]. A protein complex involving XRCC4, Ligase IV and XLF are activated by DNA-PK phosphorylation which then create a bridge between the break ends for stability and ligation (Fig. 4) [33, 34].

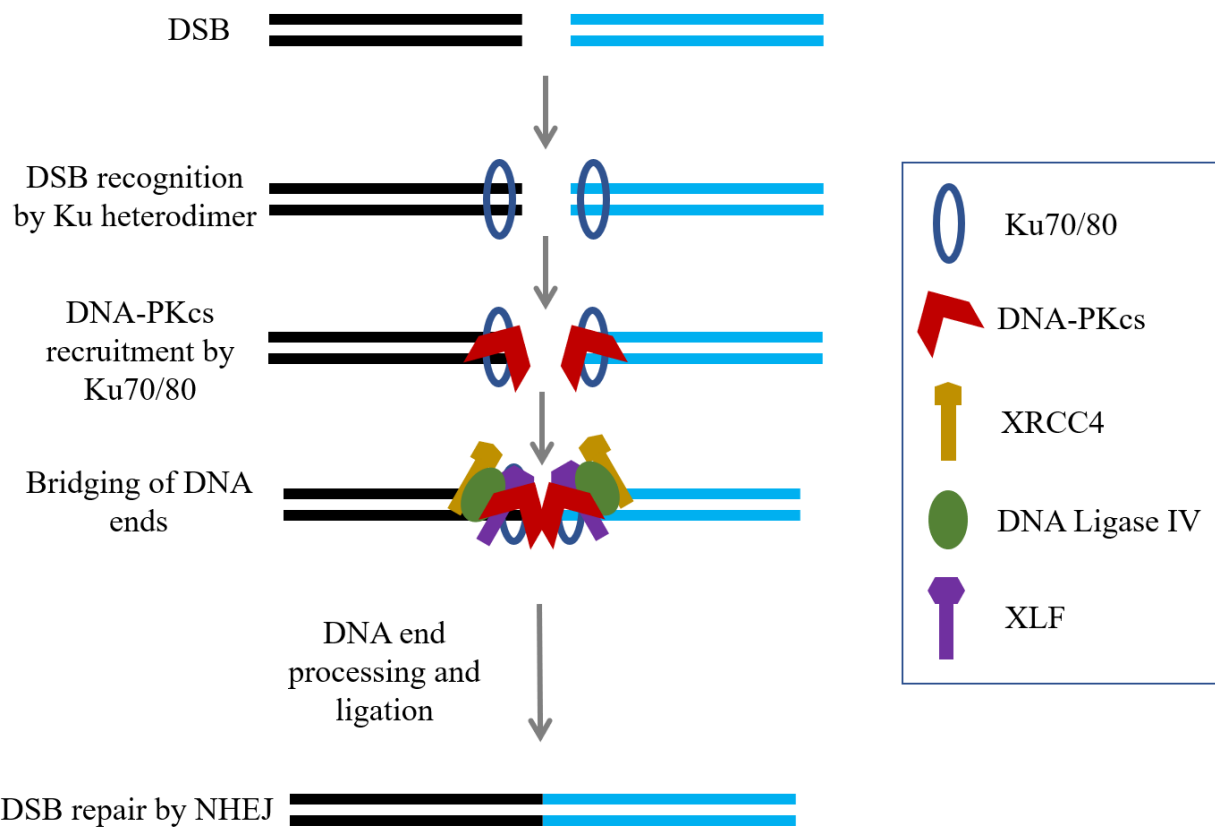


Figure 4. Schematic overview of non-homologous end joining repair (NHEJ).

1.1.3.2 Homologous Recombination

HR is involved in essential cellular processes such as DNA repair and DNA replication. In addition to its role in DNA DSBs, HR is also required for resolving stalled replication forks during replication [35]. In contrast to NHEJ, HR requires intact homologous templates to carry out repair processes [36].

DNA end resection is required to commit to HR in repairing DSBs. NHEJ initiators 53BP1 and RIF1 are always in competition for DSBs with HR initiators CtBP-interacting protein (CtIP) and its binding partner product of breast cancer early onset gene 1 (BRCA1) [37]. The onset of the S phase favors HR (Fig 3). BRCA1 promotes the phosphatase PP4C to dephosphorylate 53BP1 which leads to RIF1 release [38]. Together with the MRN complex, CtIP promotes end-resection of the 5' DNA ends to produce 3' single-stranded (ss) DNA overhangs, eliminating the occurrence of NHEJ. This occurs during S phase, where homology search is most efficacious due to the newly sensitized sister chromatids that are used as templates. In the process of end resection, the endonuclease MRE11 utilizes phosphorylated CtIP to resect DNA on the 5' end approximately 20 nucleotides away from the break [39]. Exonucleases Exo1 and DNA2 are then required to induce nicks farther away from the DSB to support unwinding of the DNA by the helicase BLM [40].

The ssDNA 3' overhangs generated upon nucleolytic resection quickly get coated by a trimeric RPA complex composed of 70-, 32- and 14-kDa subunits. Next, RPA gets displaced by the adenosine triphosphate (ATP)-dependent recombinase RAD51 in a process facilitated by breast cancer early onset gene 2 (BRCA2) [41]. RAD51 is a critical component of HR, which facilitates the homology search and strand-exchange to repair DSBs by forming a nucleoprotein helical filament [42]. There are numerous proteins that are involved in the recruitment of RAD51 to the site. BRCA2 is recruited to the damage site with the help of BRCA1 and partner and localizer of

BRCA2 (PALB2) [43]. The binding of BRCA1 and the BRCA2/PALB2 complex is oppressed due to ubiquitylation during G1 phase and is promoted during S phase by ubiquitin specific peptidase 11 (USP11) [44]. BRCA2 has multiple RAD51 binding sites and 8 of these are the BRC repeats in addition to a separate binding site close to the C-terminal [45, 46]. RAD51-bound BRCA2 translocates to the DSB site and facilitates the removal of trimeric RPA proteins. BRCA2 also functions in biasing RAD51 towards binding ssDNA as opposed to double-stranded (ds) DNA as well as decreasing the ATPase activity of RAD51. This further stabilizes RAD51 filament formation because filaments formed around dsDNA has deleterious effects and RAD51 is only stable on ssDNA in the ATP form, where the ADP form dissociates it from the DNA [47]. There are several proteins that share structural similarities to RAD51 namely XRCC2, XRCC3, RAD51B, RAD51C, RAD51D, DMC1 and SWSAP1. All work in concert with RAD51 to stabilize and assist RAD51 in DNA homology search and strand exchange [48-50]. Another protein that is involved in promoting HR is RAD52. Its role in human HR has been unresolved for a long time but recently it has been implicated to have a regulatory role in RPA displacement [51]. Of note, RAD52 is not required in the presence of BRCA2 [52].

SsDNA with bound RAD51 filament is called the presynaptic complex, and this complex searches for DNA sequence homology for a repair template. This search is biased by proximity. Since the sister chromatid is located very close to the damage site, it is most often used as the template [53]. This triggers strand invasion from the presynaptic complex to the DNA template. The 3' end of the invading strand is then used as a prime for DNA synthesis [54] (Fig. 5). RAD51 dissociation from ssDNA is facilitated by the PCNA-associated recombination inhibitor (PARI) and helicase RECQ5.

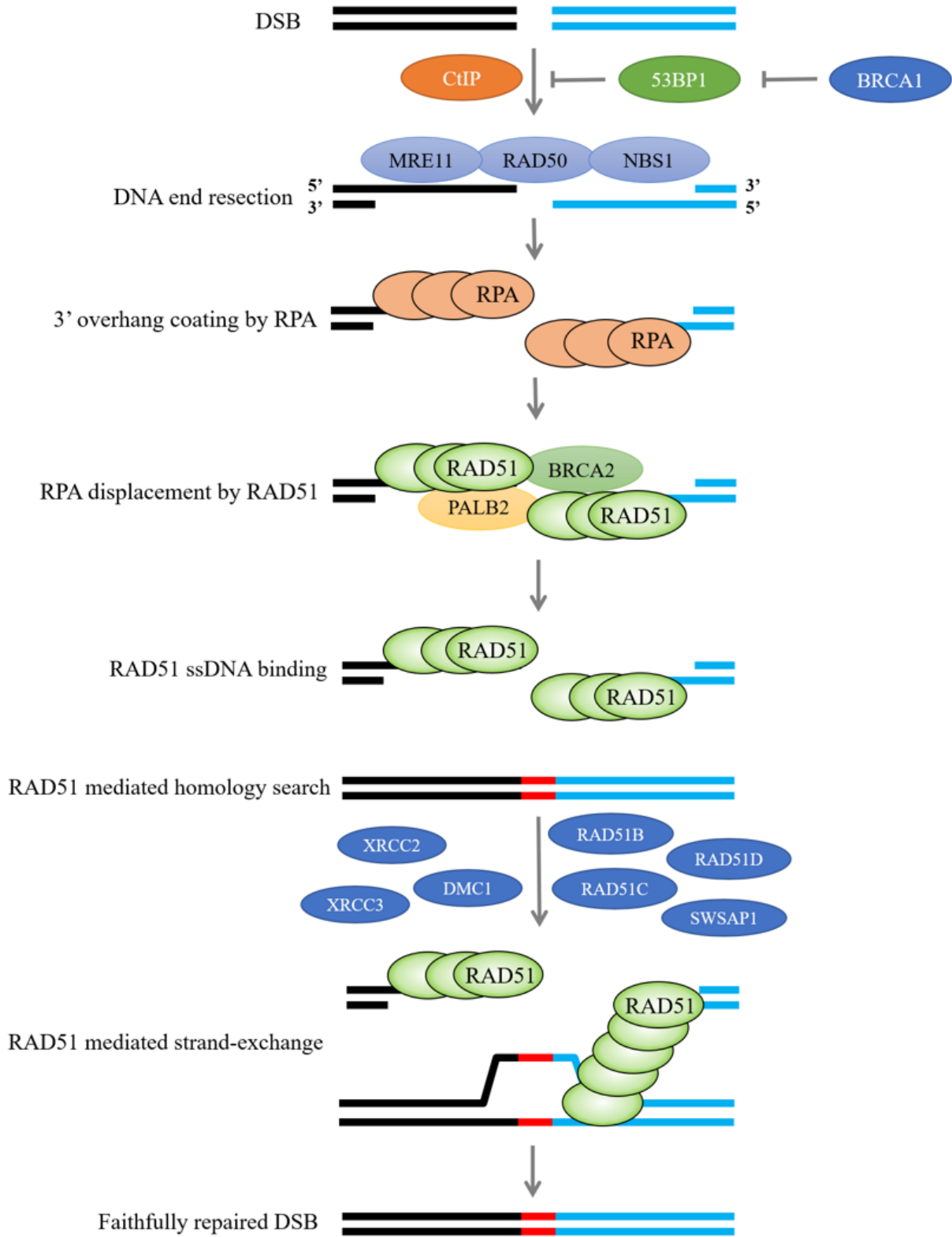


Figure 5. Schematic overview of homologous recombination (HR) repair.

1.1.3.3 Other Post-resection DSB repair pathways: Single-strand annealing (SSA) and Alternative End Joining (alt-EJ)

Resected DSB ends can also be repaired by SSA and alt-EJ. These pathways are rather mutagenic compared to HR [26, 55].

Upon end resection, SSA anneals homologous repeat sequences at the DSB site. Like HR, SSA requires bound RPA proteins. However, SSA doesn't require RAD51 to carry out repair and does not utilize strand invasion [56]. It relies on RAD52 to carry out annealing complementary sequences and uses ERCC1 to remove nonhomologous 3' overhangs via nucleolytic cleavage. ERCC1 performs this function through forming a complex with XPF and the nucleolytic function of this complex is enhanced by RAD52 [57]. This cleavage results in a deletion between homologous repeats, which is what makes this pathway potentially mutagenic. In addition to RAD52, RAD1-RAD10 (ERCC4-ERCC10) are involved in SSA in mammalian cells [58]. Additional components of this pathway in humans are unknown, including which specific polymerases and ligases are required for the completion of an SSA event. RAD52 has a more limited function in humans due to the presence of BRCA2 [59]. There is evidence that RAD52 impairment is synthetically lethal in cells with deficiencies in BRCA1, PALB2 and BRCA2 [60]. This suggests RAD52 can act as a compensatory protein to RAD51-dependent homology search which makes it a potential therapeutic target.

Alt-EJ was viewed as a compensatory pathway for NHEJ [61] until recently, when it was shown that alt-EJ competes with HR in post-resection DSB DNA repair [62]. Alt-EJ diverges from HR post-resection where DNA ends are processed by RAD51 in HR, whereas PARP1 has been identified to be processing resected ends in alt-EJ [63]. Exactly how PARP1 helps perform this function is unknown. Like SSA, alt-EJ is a backup pathway for DSB repair in the absence of

functional HR [62, 64]. The studies that identify SSA and alt-EJ as being compensatory mechanisms for HR highlight the necessity to target these pathways in therapeutic strategies prioritizing HR inhibition.

1.1.4 Homologous Recombination and Cancer

Cancer broadly represents uncontrolled cell growth and division. The hallmarks of cancer are increasing proliferation, prevention of growth suppression, evasion of cell death, acquired infinite replication capability, evasion of immune responses, acquired angiogenesis, and invasion of other sites through metastasis [65]. Cancerous cells acquire these features through increasing numbers of mutations and epigenetic changes. Thus, genome instability is an important factor for cancer cells to acquire uncontrolled cell growth and division. Mutations in DNA repair pathways can have such implication in cells.

Homologous recombination genes BRCA1 and BRCA2 are important tumor-suppressor genes implicated in breast and ovarian cancers [66, 67]. Approximately 15% of all familial breast cancers are associated with mutations in these two genes [68]. Rare mutations in other HR proteins such as PALB2, RAD51C, RAD51D have been implicated in familial breast and ovarian cancer [69-71].

1.1.5 Poly (ADP-ribose) polymerase (PARP)

There are 17 PARP proteins in humans [72], representing a family of multidomain enzymes that have functions related to cellular stress responses. PARP1 is the most studied PARP enzyme and has a role in DNA repair. PARP-2 and PARP-3 also have overlapping DNA repair roles but are studied to a lesser extent [73]. PARP1 binds SSBs and using its catalytic domain, it PARylates [process of adding poly (ADP-ribose) chains] itself and surrounding proteins. This modification then recruits additional SSB repair components such as XRCC1 to the site of damage to induce chromatin remodeling to facilitate DNA repair processes. Although PARP is best described by its role in BER and thus in the repair of SSBs, it is also involved in DSB repair via the alt-EJ pathway.

1.1.6 Targeting DNA Damage Response (DDR) Components in Cancer

DDR has evolved to signal presence of DNA damage and induce downstream repair processes including cell cycle checkpoint activation and DNA repair processes, as well as cell senescence and apoptosis upon extensive DNA damage [74]. DDR signaling proteins DNA-PKcs, ATM and ATR play critical roles in DNA DSB repair. Therefore, targeting key DDR proteins have been sought after in the cancer setting.

DNA-PKcs is critical for NHEJ repair as described earlier. Inhibition of DNA-PKcs have shown to chemosensitize cancer cells to IR and topoisomerase II poisons such as etoposide in combination therapies [75]. There are various inhibitors of DNA-PKcs being investigated in Phase I trials as monotherapies as well as in combination with topoisomerase II inhibitors for Chronic Lymphocytic Leukemia (CLL) (NCT02316197) and advanced solid tumors (NCT02644278).

ATM activates downstream DNA DSB repair processes and is the kinase that phosphorylates histone H2AX on serine 139 (γ H2AX). Another important protein that ATM modulates is CHK2, which is involved in G1-S phase checkpoint activation [76]. A specific inhibitor of ATM, KU59493, sensitizes cancer cells to IR therapy and the DNA DSB initiating chemotherapeutic agents camptothecin, doxorubicin and etoposide [77]. Another ATM inhibitor AZD0156 (AstraZeneca) is being investigated in a Phase I clinical trial as a monotherapy as well as in combination with olaparib and other cytotoxic chemotherapies in patients with advanced malignancies (NCT02588105).

Ataxia telangiectasia and Rad3-related (ATR), a key protein involved in sensing DNA SSBs, is also associated with DSBs through its interactions with RPA [78, 79]. Among many other substrates, ATR activates CHK1 which an important regulator of the G2-M and S cycle checkpoints [80]. An ATR inhibitor, VX-970, demonstrated promising pre-clinical data showing sensitization of lung cancer cells to chemotherapeutics such as cisplatin both *in vitro* and *in vivo* [81]. A phase II clinical trial is ongoing investigating it as a potential treatment for advanced solid tumor (NCT03718091). Additionally, possible targeted therapies are being pursued to treat ATM-deficient tumors with ATR inhibitors in combination with cisplatin treatments in lung cancer. Preclinical studies show that ATM deficiency could be a predictive biomarker for ATR targeting therapies [82]. Lastly, the ATR inhibitor AZD6738 induces CD8⁺ T cell activity in KRAS-mutant mice models receiving IR therapy implicating immunotherapeutic potential of ATR inhibition [83].

1.1.7 Targeting Homologous Recombination in Cancer

Although it is implied that HR deficiency leads to genomic instability and the development of cancer, it is important to emphasize that the lack of HR can also halt cancer cell progression [84]. Since HR has major roles in DNA repair and replication, cancer cells heavily rely on HR to resist DNA targeted cancer therapeutics. The anti-neoplastic platinum agent cisplatin is commonly used as a cancer therapeutic. It causes DNA crosslinks which require cancer cells to correct by relying on DNA repair. In response, cancer cells upregulate HR pathway in order to prevent death from platinum agents [85]. Furthermore, ovarian cancer patients with HR deficiencies benefit from platinum therapy at a greater extent and have increased survival rates compared to patients proficient in HR [86]. Therefore, it is important to identify patients who are HR-deficient. In addition to platinum therapies, HR-deficient patients can benefit from treatments involving PARP inhibition (PARPi). PARPi induce DSBs in replicating cells [87]. In HR-proficient cells, DSBs caused by PARPi are subsequently repaired. However, in cells with HR defects, strand breaks caused by PARPi are not repaired, leading to cell death. This phenomenon is referred as ‘synthetic lethality’. Beyond BRCA1 and BRCA2 deficiencies, cells that have defects in other HR repair proteins also benefit from PARPi. Collectively, cells with HR defects are said to have a ‘BRCAness’ phenotype. Induction of synthetic lethality by PARPi in cells with the BRCAness phenotype suggest an effective treatment alternative to chemotherapy approaches in patients with HR defects.

In addition to the strategy of treating HR-deficient cells with PARPi, another strategy involving DNA repair is targeting HR components of HR-proficient cancer cells to induce a BRCAness phenotype. Targeting proteins in the DNA DSB repair pathways can lead to cancer cell killing if combined with DNA damaging agents such as topoisomerase poisons, DNA crosslinking

agents, ionizing radiation and PARPi. One downside to this approach is that the induced BRCAness is not cancer cell specific. However, there are differences between cancer cells and normal cells that are both HR-proficient. For example, cancer cells have increased replication stress due to the downregulation of aberrant cell cycle checkpoints [35]. This leads to an increased need for intact HR function. Additionally, cancer cells, due to their replicating nature, are more likely to be in G2/S phase compared to normal cells which makes HR inhibition more toxic to cancer cells in contrast to normal cells. Therefore, potentiating DNA-targeted therapies with HR inhibitors represents a viable treatment strategy for HR-proficient patient populations. Efforts have been made to target the MRN complex, BRCA1/2, RAD51, ATR/CHK1 and ATM/CHK2 pathways. Targeting the MRN complex sensitizes cancer cells to IR and cisplatin [88, 89]. Although not through small molecule inhibition, repression of BRCA1/2 have been achieved through PI3K inhibition (BKM120) by inducing transcriptional repression of BRCA1/2 [90]. This led to the initiation of a phase-I clinical trial of BKM120 and olaparib (PARPi) studying patients with recurrent triple negative breast cancer (TNBC) and high-grade serous ovarian cancer (NCT01623349).

RAD51 inhibition is being extensively studied as a promising HR repression strategy [91]. While RAD51 is essential for high fidelity repair of DSBs to maintain genomic homeostasis, overexpression of RAD51 in cancer can have detrimental consequences. RAD51 overexpression correlates positively with breast cancer tumor grade and triple negative breast cancer (TNBC) metastatic patient samples [92, 93]. Overexpression of RAD51 inhibits chemotherapeutic efficacy in cancer patients by rendering cancer cells more resistant to DNA damaging agents. Responses to neoadjuvant chemotherapy are inversely correlated with BRCA1-, γ H2AX- and RAD51-foci before treatment as well as RAD51-foci numbers following treatment [94, 95]. Efforts have been

made to develop viable RAD51 inhibitors, but no safe small molecule Rad51 inhibitors have progressed through preclinical toxicology and pharmacokinetics evaluation prior to Phase 1/2 trials. B02, a small molecule that inhibits DNA strand exchange activity of RAD51, sensitized MDA-MB-231 TNBC human cell line to cisplatin in a mouse xenograft model [96, 97]. RI-1, another RAD51 inhibitor, binds cysteine 319 residue of RAD51 irreversibly which blocked its filament formation on ssDNA. However, this irreversible covalent interaction can have toxic side effects and although the compound was later upgraded to a reversible interactor with better pharmacologic properties, its progression came to a halt due to the high IC₅₀ needed for RAD51 inactivation [98]. Lastly, IBR120, another RAD51 inhibitor which disrupts RAD51 multimerization, has been shown to be highly toxic to TNBC cancer cells but is going through additionally chemical refinements to lower its IC₅₀ before moving past preclinical studies [99].

1.2 Breast Cancer

1.2.1 Breast Cancer Overview

In 2018, there was an estimated 266,120 new cases of invasive breast cancer diagnoses and 41,400 breast cancer deaths in the US [100]. This makes breast cancer the leading cause of death among all types of cancers in women [101]. Although early detection and advances in therapies have resulted in an increase in survival rates, an urgent need for novel therapies exists for the treatment of metastatic breast cancer, which remains largely incurable [102].

Breast cancer is a heterogenous disease with multiple biological subtypes (Table 1). Immunohistochemistry and gene expression profiling are mainly used to classify different

subtypes. Clinical decisions are made based on these subtypes, despite the advancement of omics technologies such as whole genome sequencing and transcriptomics that can better resolve the heterogeneity of this disease by providing more specific targets for therapy [103]. Using gene expression profiling, breast cancer is broadly sub-classified into luminal ER positive (luminal A and luminal B), HER2 enriched and basal-like [104, 105]. Additionally, breast cancer can be sub-classified based on surface receptor expression. These receptors are estrogen receptor (ER), progesterone receptor (PR), and human epidermal growth factor receptor-2 (HER2). Approximately 70% of breast cancer patients express estrogen receptor- α (ER α). Mortality rates in this subset has been dramatically decreased since the advent of endocrine therapies such as Tamoxifen and aromatase inhibitors. Additionally, around 15% of patients have cancers with overexpression in human epidermal growth factor receptor-2 (HER2). These patients are candidates for HER2-targeted treatments such as Trastuzumab (Herceptin), and others [106]. In contrast, triple-negative breast cancer (TNBC) patients lack these surface receptors and are unresponsive to endocrine and HER2-targeting treatments.

Table 1. Breast cancer molecular subtypes and correlations with surface receptor expression.

Molecular subtype	ER	PR	HER2
Luminal A	positive	positive	negative
Luminal B	positive	positive/negative	negative
	positive	positive/negative	positive
HER2	negative	negative	positive
TN or basal-like	negative	negative	negative

ER: Estrogen receptor, HER2: human epidermal growth factor receptor 2, PR: progesterone receptor

1.2.2 Triple-Negative Breast Cancer

TNBC lacks the ER and PR receptors with no amplification of HER2. It is highly heterogenous and is found in about 15-20% of all breast cancers [107]. There has been little therapeutic progress since the advent of chemotherapy in TNBC. Conventional chemotherapy is the first-line therapy for all TNBC patients and lacks targeted therapies such as hormone or anti-HER2 treatments available to other subtypes. TNBC generally shows the worst prognosis among all subtypes of breast cancer patients [108]. It demonstrates a peak of recurrence during the first three years and the majority of deaths occur within the first 5 years [109].

1.2.3 Current Therapies for TNBC

Systemic chemotherapy remains the first line treatment for TNBC. Among all breast cancers, TNBC has the highest response rate to DNA damaging chemotherapy due to high genomic instability [110]. Taxanes and anthracyclines are among the most effective chemotherapy options for TNBC patients [111]. However, TNBC is the most aggressive subtype and relapses within 3 to 5 years after chemotherapy [112]. TNBC also has a higher predisposition to metastasize to lung, liver and brain, leading to significantly shorter overall survival compared to other subtypes [113]. Less than 30% of patients with metastatic disease live past 5 years [114].

1.2.4 BRCAness in TNBC

BRCA1/2 deleterious mutations are found in 10-20% of TNBC patients according to The Cancer Genome Atlas (TCGA) and other registries [115]. The presence of mutations in BRCA1 and BRCA2 genes increase the risk of breast cancer to up to 70% and is closely associated with TNBC [116]. Conversely, 80% of patients who have a BRCA1 mutation are diagnosed with TNBC [117]. In addition to BRCA mutant tumors that are defined by having homologous recombination deficiencies, recently, a wider subclassification of TNBC tumors is made by defining tumors that share phenotypic similarities with BRCA mutant tumors. This is referred as the BRCAness phenotype [117].

TNBC tumors with wild-type (WT) BRCA genes that exhibit the BRCAness phenotype also have deficiencies in the HR pathway. Tumors with the BRCAness phenotype share common mutational signatures in their DNA with BRCA mutant tumors [118]. Specifically, having a pattern of genome-wide mutation called ‘signature 3’ is closely associated with having the BRCAness phenotype in ~1000 different breast cancer tumors [119]. Mutations (either germline or somatic) in breast cancer tumor samples with BRCAness phenotype includes DSB repair pathway components such as ATM, ATR, PALB2, RAD51C, RAD51D, and CHK2 [120]. Lastly, BRCA1 promoter methylation in TNBC tumor samples also exhibit BRCAness [121].

1.2.5 Evaluation of BRCAness in TNBC

In order to identify tumors with HR deficiency, various predictive biomarker assays have been developed. One of the most widely recognized biomarkers for HR defects measures the cells’ ability to form nuclear RAD51 foci. In this assay, freshly acquired breast tumors are irradiated and

their ability to form RAD51 foci is quantified. It was shown that tumors with HR deficiency could be diagnosed irrespective of whether they have germline BRCA mutations or not. By using RAD51 foci as an assessment of HR functionality, 50% more HR-defective tumors were identified that could benefit from specific DNA repair targeting therapies [122, 123]. A requirement to this approach is the need for performing this assay on fresh tumor tissue. Other assays include sequencing-based methods. The HRD assay, developed by Myriad Genetics, uses a single-nucleotide polymorphism (SNP) based profiling system where a high HRD score correlates to having a HR defect. Interestingly, in a 2014 study, high HRD scores were seen in tumor samples regardless of breast cancer subtype suggesting DNA repair targeting therapies can extend beyond the TNBC subtype [121]. Another assay is called HRDetect which is a whole-genome sequencing based platform that detects BRCA1 and BRCA2 mutations up to 98.7% accuracy [124]. Additionally, a diagnostic test developed by Myriad Genetics called the BRCAAnalysis CDx, is the first FDA approved approach for metastatic breast cancer patients to identify their BRCA status. It uses sequencing and deletion/duplication analyzing methods to determine mutation status of BRCA1 and BRCA2 genes. Lastly, a diagnostic test called FoundationOne CDx developed by Foundation Medicine is the first of its kind to carry out genomic profiling for all solid tumors. It is capable of identifying gene mutations, copy number alterations, structural rearrangements and promoter mutations evaluating a total of 341 genes that are associated with cancer [125]. These developments in the field of precision medicine open new venues for identifying breast cancer patients with deficiencies in specific DNA repair pathways, thus better facilitating the development and use of novel small molecule inhibitors that can target the pathways cancer cells use to evade conventional therapies (Fig. 7).

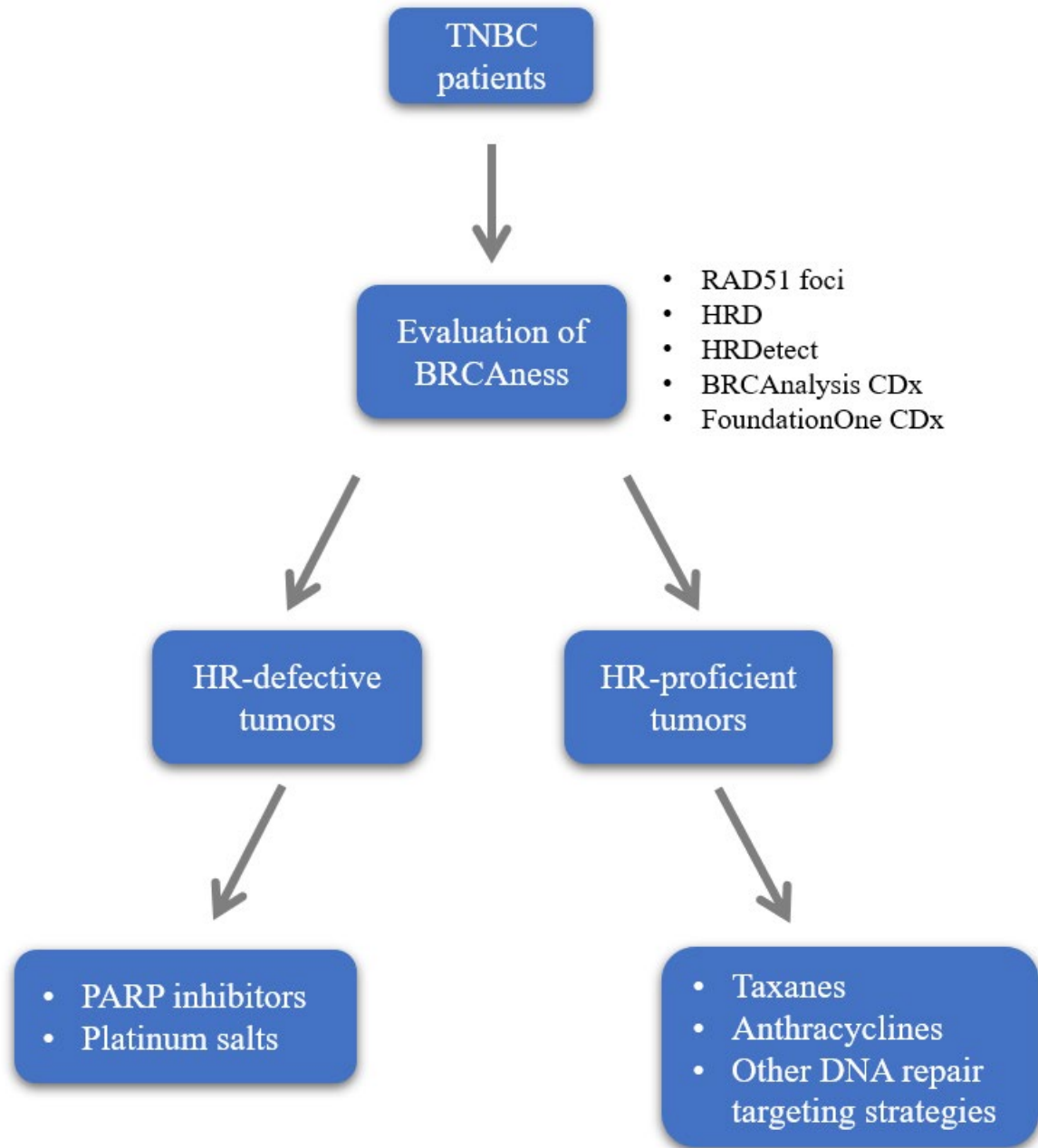


Figure 6. Potential clinical utility of using biomarkers in triple negative breast cancer (TNBC).

1.2.6 PARP inhibitors

PARPi has been viewed to be a vital strategy for a subset of TNBC patients, ones with HR deficiency (HRD). By inhibiting PARP in patients with BRCAness phenotype, DSBs that cannot be repaired are anticipated to induce synthetic lethality [126]. A phase III clinical trial called OlympiAD tested this idea in metastatic breast cancer [127]. In this study, olaparib, a PARP inhibitor, was used as monotherapy and compared with the physician's choice of chemotherapeutic agent in metastatic HER2-negative breast cancer with germline *BRCA1/2* mutations. Patients who were treated with olaparib had a 2-fold increase in response rate and a longer progression free survival (PFS) of ~7 months, as well as lower toxicity. In addition to the OlympiAD study, another phase III trial, EMBRACA, compares PARPi (talazoparib) monotherapy with the physician's choice of chemotherapy in metastatic TNBC. This study revealed talazoparib monotherapy to be significantly superior in PFS (3 months longer) and overall response rates (ORR) [128]. After these results, PARPi was approved for breast cancer patients with *BRCA1/2* mutations.

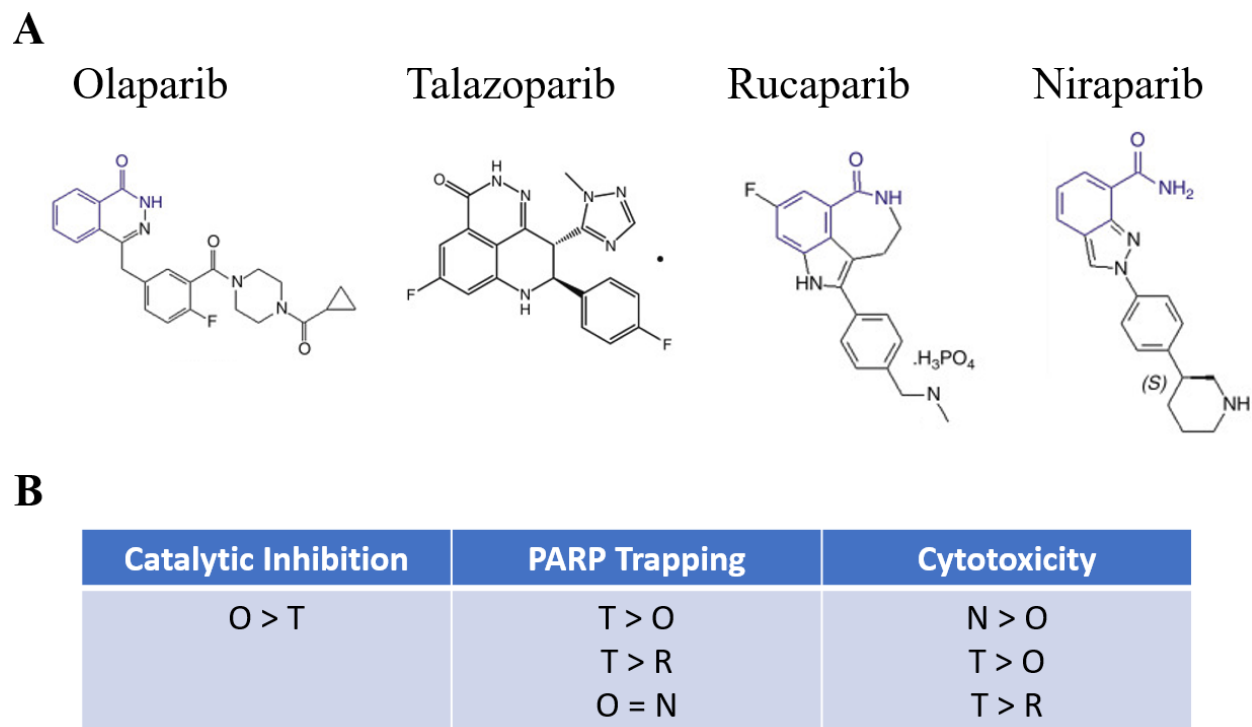


Figure 7. PARP inhibitors in clinical development.

(A) Chemical structures of PARP inhibitors currently being pursued in clinical development. (B) Differences between PARP inhibitors and their mechanisms of actions. T: talazoparib, O: olaparib, R: rucaparib, N: niraparib. “>”: more potent, “=”: equally potent.

Other PARP inhibitors are presently being studied for breast cancer therapy. These are veliparib, talazoparib, rucaparib and niraparib. The mechanisms by which they inhibit PARP activity and their overall cytotoxicity differ due to their structural differences (Fig. 8). Two different mechanisms of action for PARP inhibition exist. One is the catalytic inhibition, via inhibitor binding with the catalytic subunit of PARP, thus blocking the transfer ADP-ribose moieties to acceptor proteins. The second mode of inhibition stems from trapping PARP on the DNA damage site thus preventing the recruitment of essential repair proteins [129]. Talazoparib is described as the most specific PARP1 inhibitor in contrast to olaparib which inhibits both

PARP1 and PARP2. Additionally, Talazoparib has the most potent PARP trapping activity, when compared with other PARP inhibitors [130].

Currently, PARPi is also being explored in combination with other treatments for breast cancer therapy in clinical trials. These include platinum, taxanes, and DNA repair inhibitors (ATM and ATR). The rationale behind this is that by targeting two repair pathways simultaneously, otherwise resistant cancer cells with high genomic instability will die. A phase I study investigates olaparib in combination with an ATR inhibitor AZD6738 in breast cancer patients with BRCA mutations (NCT02264678). This study includes a subset of TNBC patients who don't have BRCA mutations. A phase II study is investigating olaparib in combination with a WEE1 (a key regulator of cell cycle progression) inhibitor AZD1775 in TNBC patients (NCT03330847).

1.3 Electrophilic Fatty Acids

An electrophile is an ion or a molecule that can accept electrons from electron-rich donor molecules (nucleophiles) to make a covalent bond. The reaction that takes place to form this covalent bond is termed Michael Addition [131].

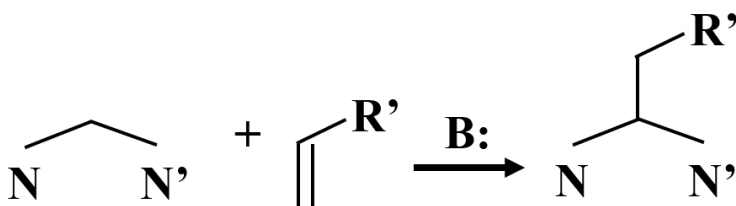


Figure 8. The Michael Addition reaction.

The N and N' are substituents of the nucleophile and R' is a substituent of the electrophile. R' is usually a ketone but it can also be a nitro group.

In addition to post-translational modifications (PTM) such as phosphorylation, acetylation, ubiquitinylation and SUMOylation, electrophiles can react with nucleophiles to induce PTMs. Electrophilic fatty acids are such electrophiles.

1.3.1 Interaction of Electrophiles with Nucleophiles

Covalent bonds that occur between electrophiles and nucleophiles can be irreversible or reversible. These two conditions are based on the Pearson concept of hard and soft acids and bases [132]. Hard electrophiles such as formaldehyde react with hard nucleophiles such as amino groups. In contrast, soft electrophiles such as electrophilic fatty acids react with soft nucleophiles such as protein thiols [133]. A soft electrophile is defined by the electrophile having a more diffuse charge density. Therefore, the soft-soft interaction of nitroalkenes and protein thiols are reversible in nature [134].

By virtue of their electrophilic nature, fatty acid nitroalkenes mediate PTMs of hyper-reactive nucleophilic cysteine thiols in proteins as well as other nucleophiles such as glutathione (GSH) and imidazolyl (His) residues. These reactions occur via the Michael Addition reaction [135] (Fig. 10).

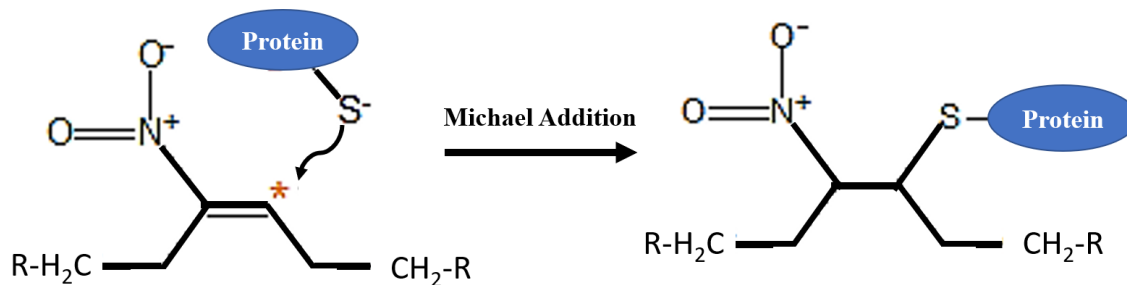


Figure 9. Post-translational modification of a protein (nucleophile) by a nitroalkene (electrophile).

The asterisk indicates the carbon that has reduced electron density due to the electron-withdrawing nitro group.

1.3.2 Electrophilic Fatty Acid Formation

Fatty acids (FAs) are typically 16-22 carbon long hydrocarbon chains with a terminal carboxyl group. FAs can be either saturated or unsaturated. Saturated FAs have no double bonds whereas unsaturated FAs have at least one double bond. FAs with at least two unsaturated bonds are called poly-unsaturated FAs (PUFAs). The most distal carbon in FAs is called the omega (ω) carbon. PUFAs are named according to how far away their double bond is from the ω carbon. For example, essential PUFAs linoleic acid (LA) and α -linolenic acid (ALA) are omega-6 and omega 3 PUFAs respectively [136]. These FAs are essential because they cannot be produced within the body and must be acquired through diet [136]. PUFAs are oxidized or nitrated through enzymatic or non-enzymatic reactions. Fatty acid nitroalkenes or electrophilic fatty acids are endogenously-detectable products of nitric oxide and nitrite-dependent metabolic and inflammatory reactions with unsaturated fatty acids. Nitration of PUFAs result in FAs with double bonds that have high electrophilic nature due to the strong electron-withdrawing activity of the nitro group. The resulting FA-NO₂ in electrophile capable of reacting with nucleophiles to induce PTMs [137]. Of

note, FA-NO₂ containing triacylglycerides can be formed via FA-NO₂ incorporation into triacylglycerides as well as via the direct nitration of esterified unsaturated fatty acids [138].

1.3.3 Electrophilic Fatty Acids as Signaling Mediators

Nitroalkenes have many protein targets in the cell including NF- κ B, Keap1/Nrf2, PPAR γ and HSF-1, thus modulating protein structure and function and mediating pleiotropic cytoprotective and anti-inflammatory signaling responses [139, 140].

NF- κ B is important for proliferation and survival of cells as well as mediating inflammatory responses [141]. Nitroalkenes repress NF- κ B signaling by inhibiting its DNA binding. Nitroalkene 10-nitrooctadec-9-enoic acid (OA-NO₂) binds the p65 subunit of NF- κ B [142]. Keap1/Nrf2 pathway regulates cytoprotective responses to oxidative and electrophilic stress [143]. Nitroalkenes react with Keap1 cysteines to regulate this pathway [144]. The nuclear receptor PPAR γ regulates lipid homeostasis and adipocyte differentiation [145]. Nitroalkenes bind a PPAR γ cysteine residue in the ligand binding domain and act as a nuclear receptor ligand [146].

1.3.4 Electrophilic Fatty Acids in TNBC

Emerging evidence has revealed that triple negative breast cancer cell growth, migration and invasion are suppressed by the electrophilic nitro-fatty acid derivative OA-NO₂ through modulation of NF- κ B signaling, while non-tumorigenic breast epithelial cells were resistant to the effects of OA-NO₂ because of more intact mechanisms for maintaining redox homeostasis (increased GSH levels) and increased expression of multi-drug resistance protein-1 (MRP1), an

exporter of GS-NO₂-OA adducts. In comparison to the nontumorigenic human breast epithelial cells MCF-10A and ER⁺ breast cancer cells MCF-7, OA-NO₂ was a more potent inhibitor of TNBC cells MDA-MB-231 and MDA-MB-468. [147]. OA-NO₂ inhibited NF-κB signaling, by alkylating functionally-significant thiols in a) the inhibitor of NF-κB subunit kinase β (IKK β), thus limiting downstream IκKα phosphorylation and (b) the NF-κB RelA protein, thus preventing DNA binding and promoting RelA polyubiquitination and proteasomal degradation. In addition, OA-NO₂ inhibited TNBC cell migration and invasion as well as tumor growth in mouse xenografts [147]. These studies suggest that OA-NO₂ treatment can be exploited therapeutically in TNBC and possible other cancers warranting further investigations.

2.0 Materials and Methods

2.1 Reagents and Cell Lines

HEK 293T, MDA-MB-231, MDA-MB-468, Hs578T and BT-549 cells (American Type Culture Collection) were cultured at 37° C with 5% CO₂ in Dulbecco's modified Eagle's medium containing (DMEM) (Gibco) supplemented with 5% FBS (HyClone), 100 units/ml penicillin, 100 mg/ml streptomycin (Gibco), non-essential amino acids (Gibco) and 2 mM l-glutamine (Gibco). Doxorubicin (Selleckchem), cisplatin (Sigma) or olaparib (Selleckchem) were dissolved in DMSO or DMF (cisplatin). Nitro-oleic acid (10-octadeca-9-enoic acid) (OA-NO₂) and biotinylated OA-NO₂ were synthesized as previously described[142, 148]. Pure OA-NO₂ was diluted in DMSO and added to cells after solvation in assay media. Relative cell numbers were compared by measuring the luminescent signal generated by ATP using the CellTiter-Glo (Promega) assay. Cells were plated in a 96-well plate at 5,000 (MDA-MB-231) or 6,600 (BT549 or Hs578T) cells per well. Cells were treated with doxorubicin, cisplatin, or olaparib at the indicated concentrations for 72 h in the presence or absence of 2 μM OA-NO₂, which was replenished every 24 h.

2.2 OA-NO₂

Nitro-oleic acid (10-octadeca-9-enoic acid) (OA-NO₂) was synthesized as previously described[149, 150]. Biotin-OA-NO₂, biotin-SA-NO₂, and biotin-OA were synthesized by conjugation of OA-NO₂ or respective lipids to biotin-poly (ethylene glycol)-amine (Pierce,

#21346) as described. Pure OA-NO₂ was diluted in DMSO and added to cells after solvation in assay media.

2.3 OA-NO₂ *in vivo*

Animal use in this study was approved by and conducted according to the guidelines of the University of Pittsburgh IACUC. MDA-MB-231 cells (0.5×10^6) were injected into the mammary fat pad (left 4th gland) of 6-wk-old female nude mice in a volume of 20 μ L sterile saline. When tumors reached an average volume of 100 mm³, mice were randomized into groups and administered vehicle (tricaprylin) + 15 mg/kg OA or vehicle + 15 mg/kg OA-NO₂ every day by gavage (200 μ L) for 4 wk. The surgical procedure has been previously described [151].

2.4 Plasmids

The direct repeat green fluorescent protein (DR-GFP) reporter and I-SceI pCAGGS plasmids were a kind gift from Prof. Maria Jasin [152, 153]. pLVX Neo-RAD51 was cloned by PCR amplification of RAD51 with PCR primers incorporating SpeI (5') and BamHI (3') restrictions sites. The PCR product was then ligated into the corresponding restrictions sites of pLVX-Neo (Clontech) and transformed into DH5 α Max efficiency cells (Invitrogen). pLVX Neo RAD51 cysteine to serine mutant plasmids (137, 312, or 319) were produced using the QuikChange II site-directed mutagenesis kit (Agilent) using pLVX Neo-RAD51 as a template.

2.5 Clonogenic Survival Assays

Cells were trypsinized and seeded onto 6-well plates at a density of approximately 500 cells per well and incubated at 37°C with 5% CO₂. Cells were incubated in DMEM containing 5% FBS with or without increasing concentrations of OA-NO₂ (0.1% DMSO final solvent concentration) for 1 h prior to irradiation treatment. Next, cells were dosed with 0 or 2 Gy (breast cancer cells) or 0 to 8 Gy (MEFs). Media containing OA-NO₂ was immediately replenished post-irradiation. Then, media was exchanged every other day and the cells were fixed (PFA) after 10 days. Colonies were stained with 1% crystal violet (Sigma) in 10% ethanol and washed with distilled water. Quantification of colonies was carried out using ColonyArea plugin (Daniel Abankwa, <http://www.btk.fi/research/research-groups/abankwa/downloads/>) in ImageJ.

2.6 DSB Repair Assays

Measurements of HR and NHEJ assays were performed as previously described [152, 154]. HR activity was measured by counting GFP-positive cells by flow cytometry at the MWRI flow cytometry core using a BD LSRII (BD Biosciences). RAD51 overexpressing cells were generated by stable transfection of pLVX RAD51 IRES Neo and selection with geneticin (Invitrogen).

2.7 Cell Cycle Analysis

Propidium iodide (PI) stained DNA content was measured as an indication of cell cycle phase in PRDX1-proficient and deficient MDA-MB-231 cells as well as OA-NO₂ treated breast cancer cells. 10⁶ unsynchronized cells were harvested by trypsinization and following inactivation of trypsin, cells were pelleted and washed with ice cold 1xPBS (Gibco). Cells were fixed in 70% ethanol by adding ethanol dropwise with swirling and incubated for 20 min at 4° C. Cells were then centrifuged at 2000 rpm and the supernatant removed. Pellets were washed with ice cold PBS then treated with 500 µl RNase A (50ng RNAase/µl) for 15 min at 37° C. Next, propidium iodide (Sigma) (50 ng PI/ µl) was added and incubated for 30 min at 4° C in a dark chamber. Samples were later analyzed at the Flow Cytometry Core at MWRI utilizing a BD LSRII (BD).

2.8 Kinetic DSB Repair Assays

U2OS cells were prepared as above, but 5 h following compound treatment, cells were transferred into the Incucyte Zoom (Essen) live-cell imaging automated fluorescence microscope at 37° C with 5% CO₂. Cell confluence and green object count per mm² were determined using Incucyte Zoom software. Green object count per field was normalized to cell confluency to correct for OA-NO₂-induced effects on cell proliferation.

2.9 Immunostaining and Imaging

To analyze RAD51 foci formation, cells were plated on CultureWell 16-well chambered cover glass (MIDSCI) coated with poly-L-lysine (Sigma) at a density of 10,000 cells per well and were incubated overnight in 5% FBS media. The next day, cells were treated with OA-NO₂ for 1 h, then irradiated with 5 Gy and then further incubated with OA-NO₂ for 6 more hours. Cells were later fixed with 10% formalin for 20 min at 4° C and immunostained overnight at 4° C with antibodies for RAD51 (H-92) (Santa Cruz) at 1/100 dilution or phosphorylated γ H2AX (JBW301) (EMD Biosciences) at 1/200 dilution. Secondary antibodies for RAD51 (Goat anti-Rabbit Alexa Fluor 488) or γ H2AX (Goat anti-Mouse Alexa Fluor 546) were incubated at 25° C for 1 h (1/2000). Z-stack images were acquired using a Nikon A1R confocal microscope with 60x oil objective and acquisition was done using NIS elements software.

2.10 Western Blotting

Cell lysates were prepared in 50 mM Tris, 150 mM NaCl, 1% Triton X-100, 0.5 mM EDTA, 0.5 mM EGTA and 10% glycerol supplemented with catalase (30 μ g/ml), 100 mM N-ethylmaleimide (NEM) and protease (Halt protease inhibitors, Fisher Scientific) and phosphatase inhibitors (50 mM NaF, 1 mM NaVO₄ and 40 mM β -glycerophosphate). Lysates were sonicated for 5 min (30 sec pulse/30 sec delay) at 4° C, and then centrifuged to pellet insoluble material. Laemmli sample buffer (BioRad) supplemented with β -mercaptoethanol was added to 40 μ g sample and incubated for 5 min at 95° C. Protein lysates were separated on 10% tris-glycine gels and transferred onto nitrocellulose.

2.11 Immunoprecipitation

One million HEK 293T cells were transiently transfected with Fugene 6 (Promega) and 2 μg pQCXIP (EV) or FLAG-RAD51 pQCXIP plasmids. After 24 hours cells were irradiated with between 0 and 10 Gy. Lysates were prepared as for Western blotting above. Protein concentrations were quantified by BCA assay kit (Fisher Scientific). 500 μg of cell lysate was incubated with 10 μL of acid treated Anti-FLAG M2 Affinity Gel and 400 μL lysis buffer at 25° C for 3 h with rotation. Tubes containing precipitated proteins were centrifuged and washed four times in lysis buffer and once in 1x TBS. Laemmli sample buffer (BioRad) supplemented with β -mercaptoethanol was added to the sample and incubated for 10 min at 95° C, then loaded onto a 10% tris-glycine gel.

2.12 Biotinylated OA-NO₂ Affinity Capture of RAD51

HEK 293T were transiently transfected with Fugene 6 (Promega) and 5 μg RAD51 expressing vectors (wild-type, C312S, or C319S). Cells were treated 24 h later with 5 μM biotin-OA-NO₂ or biotin-SA-NO₂ for 1 h in 5% FBS medium. Cells were prepared as above. Precipitation of biotinylated OA-NO₂ was accomplished with 8 μl of streptavidin agarose beads with 1 mg total cell lysates incubated for 16 h at 4° C. Detection of RAD51 was accomplished by immunoblot with RAD51 antibody (1:2000) with actin antibody (1:3000) probed as loading control.

2.13 DNA Binding Assays

Reactions were performed in black 96-well plates (Greiner) in 50 μ L reaction volumes in 20 mM HEPES pH 7.5, 10 mM MgCl₂, 0.25 μ M BSA, 2% glycerol, 30 mM NaCl and 4% DMSO. Purified RAD51 protein (Abcam) and OA (negative control) or OA-NO₂ was pre-incubated for 5 min at 25 °C. 2 mM ATP and 100 nM 5'-Alexa Fluor 488 ssDNA poly-dT (Integrated DNA technologies) were added to the reaction and incubated for 90 min at 37 °C. DNA binding was measured using fluorescence polarization (FP) on a Tecan Spark 20M (ex/em, 480 nm/535 nm). Fluorescence quenching was detected as above in the absence of RAD51 protein.

2.14 γ -irradiation

Experiments were conducted on cells dosed with 0 to 10 Gy utilizing a Gammacell 40 Exactor γ -Irradiator (Best Medical) with a dose rate of 69 R/min.

2.15 Statistical Analysis

Data represent the mean \pm SEM from 3 independent experiments unless otherwise noted. A p value < 0.05 was considered statistically significant. Non-linear curves were generated in GraphPad Prism 7.0 (GraphPad Software, La Jolla, CA, USA) for statistical analysis. EC₅₀ values and standard error were calculated from three independent experiments utilizing a non-linear dose response variable slope model. Significance was tested by one-way ANOVA for multiple groups

with Tukey posttest or by t-test when groups were less than three. RAD51 foci number was analyzed with ImageJ. Nuclear boundaries were individually identified in more than 50 cells per treatment group in three independent experiments.

3.0 Impact of OA-NO₂ on Triple Negative Breast Cancer Cell Growth as a Single Agent and in Combination with DNA Targeted Therapies

3.1 Effects of OA-NO₂ on TNBC DNA Damage *in vivo*

Current data indicates that OA-NO₂ regulates multiple pathways in TNBC cells that contribute to the aggressiveness of this cancer. For example, OA-NO₂ inhibits NF-κB signaling, by alkylating functionally-significant thiols in a) the inhibitor of NF-κB subunit kinase β (IKK β), thus limiting downstream IκKα phosphorylation and (b) the NF-κB RelA protein, thus preventing DNA binding and promoting RelA polyubiquitination and proteasomal degradation [155]. NF-κB is a group of transcription factors that are essential for stress response in cells. Some of the genes that are modulated by NF-κB are involved in the DDR. NF-κB is activated in response to DSB inducing cancer therapies cisplatin and IR [156, 157]. This motivated assessing whether OA-NO₂ enhances TNBC DNA damage *in vivo*.

MDA-MD-231 cells were implanted into the mammary gland of mice and when tumors reached a volume of 100 mm³, mice were treated with 15 mg/kg of the non-electrophilic fatty acid oleic acid (OA) or OA-NO₂ by gavage for 4 weeks.

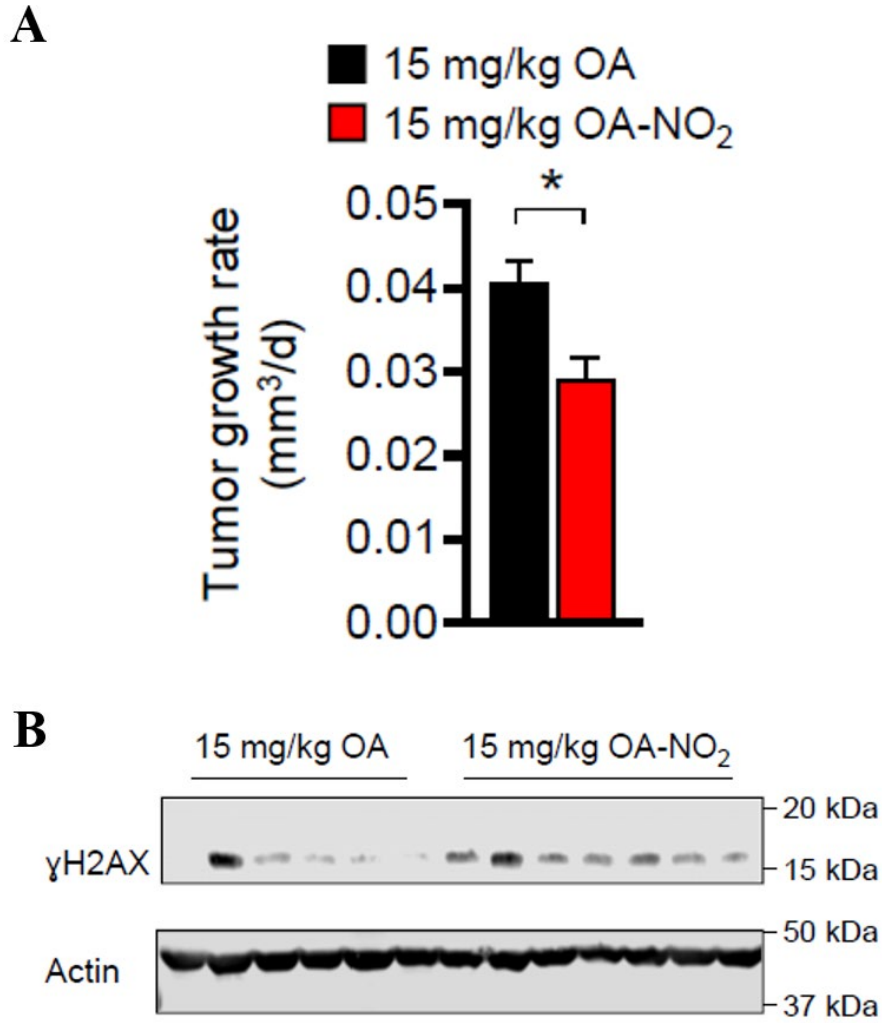


Figure 10. OA-NO₂ inhibits tumor growth and induces DNA damage in TNBC cells *in vivo*.

(A) MDA-MB-231 (MM231) cells (0.5×10^6) were orthotopically injected into 6-week-old mice and gavaged with 15 mg/kg OA (black) or OA-NO₂ (red) for 4 w when tumors reached a volume of 100 mm³. (B) Tumoral γH2AX was increased in OA-NO₂ treated mice compared to OA control mice by immunoblot (n = 6-7 per group).

Mice treated with OA-NO₂ had significantly decreased tumor growth rates when compared to OA treated animals (Fig. 11A). When a DSB occurs, there is a revealing response in chromatin which is the phosphorylation of a histone H2A variant called H2AX [158, 159]. Phosphorylated H2AX (γ H2AX) is therefore a part of the DNA damage response and increased γ H2AX reflects increased DNA damage in a cell [160]. Probing tumor levels of the DNA damage biomarker γ H2AX by immunoblot showed that OA-NO₂ treated mice generally displayed higher levels of γ H2AX (Fig. 11B) suggesting OA-NO₂ treatment directly causes DNA damage in TNBC cells *in vivo*.

3.2 Effects of OA-NO₂ in Combination with Chemotherapeutic Drugs and PARP Inhibition on TNBC Cells *in vitro*

The TNBC growth inhibitory effects of OA-NO₂ were then evaluated in combination with DNA damaging agents. The TNBC cell lines MDA-MB-231, BT-549 and Hs578T were treated with OA-NO₂ daily for 3 days and relative cell numbers were quantified by measuring the ATP-dependent luminescent signal generated using Ultra-Glo luciferase with the substrate luciferin. The EC₅₀ values for growth inhibition of TNBC cells ranged from 1.98 \pm 0.52 μ M (Hs578T) to 3.78 \pm 0.48 μ M (BT-549), with MDA-MB-231 cells displaying an EC₅₀ value of 3.66 \pm 0.14 μ M (Fig. 12A). We next tested the DNA damaging drugs doxorubicin and cisplatin in combination with daily treatment with 2 μ M OA-NO₂. OA-NO₂ enhanced growth inhibition of doxorubicin in MDA-MB-231 and Hs578T cells, by 7- and 5-fold, respectively (Fig. 12B). The growth of BT-549 cells was not affected. Co-treatment of OA-NO₂ with cisplatin showed a similar trend for MDA-MB-231 and Hs578T cells, displaying increased growth inhibition by 6- and 3-fold,

respectively, while growth inhibition of BT-549 cells was suppressed 1.4-fold (Fig. 12C). A subset of TNBC cells are sensitive to PARP inhibition and display a BRCAness phenotype in the presence of wild-type BRCA1 [161], so the PARP-1 inhibitor olaparib was evaluated to determine if a combination treatment with OA-NO₂ enhanced potency. MDA-MB-231 (high RAD51 expression, P53 mutant, BRCA1 wild-type), Hs578T (low RAD51 expression, P53 mutant, BRCA1 wild-type) and BT-549 (low RAD51 expression, P53 mutant, BRCA1 wild-type) cells all displayed enhanced growth inhibition when olaparib was combined with OA-NO₂ by 5-, 17- and 3-fold, respectively (Fig. 12D). Thus, standard TNBC chemotherapeutic drugs as well as targeted PARP-1 inhibition exhibited enhanced anti-proliferative effects when co-administered with OA-NO₂ in TNBC cells.

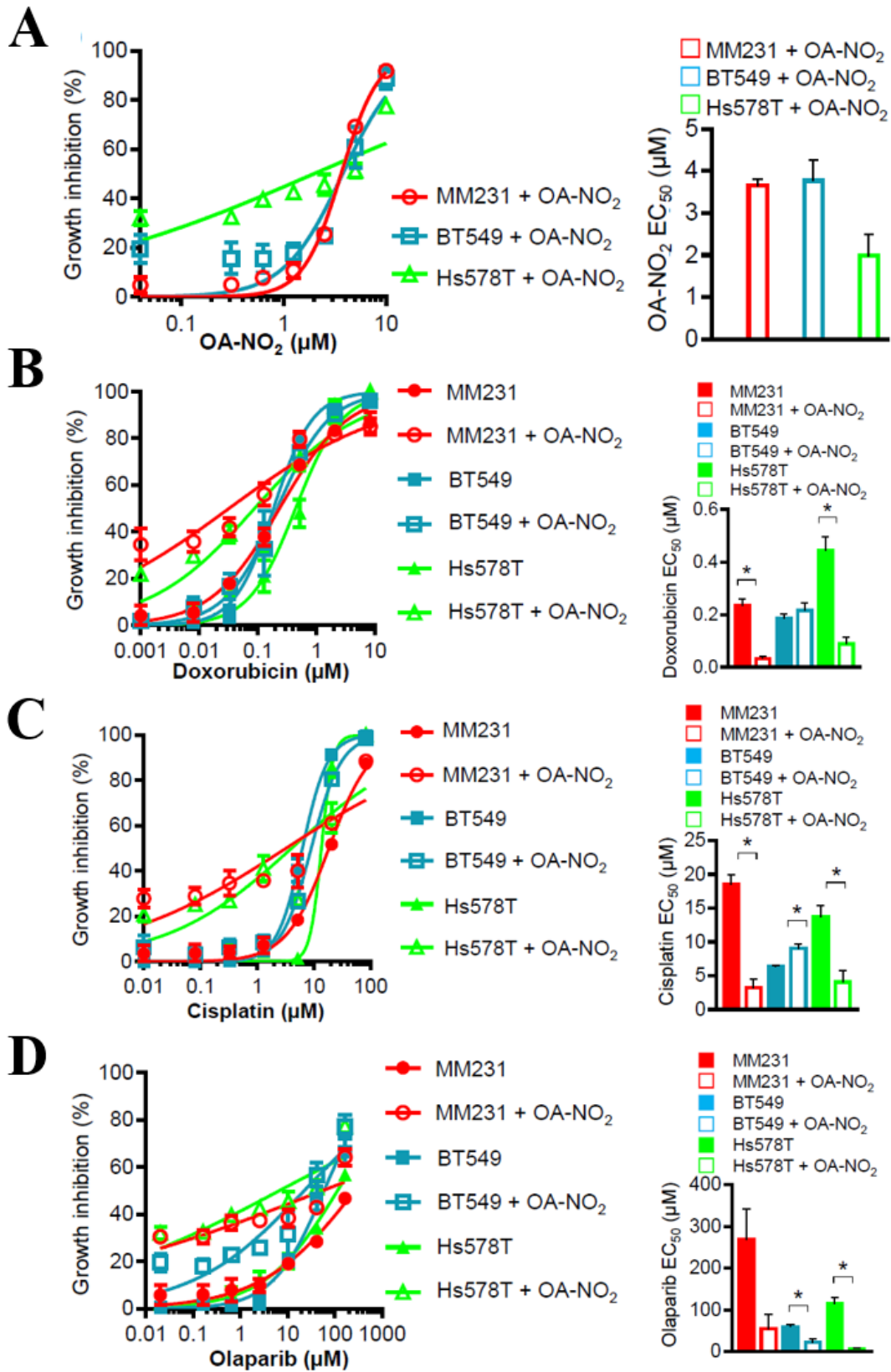


Figure 11. Antiproliferative effects of OA-NO₂ in combination with chemotherapeutic drugs and PARPi.

(A) MM231 (red), BT549 (blue) or Hs578T (green) cells were treated with increasing concentrations of OA-NO₂ and relative growth was measured by quantifying luminescent ATP levels (CellTiter-Glo). EC50 values indicate average + SEM, n=3. (B-D) MM231 (red), BT549 (blue) or Hs578T (green) cells were treated with increasing concentrations of doxorubicin, cisplatin or olaparib ± OA-NO₂ and measured as above.

3.3 OA-NO₂ Induces Heightened γ H2AX and Sensitizes TNBC Cells to Ionizing Radiation

(IR)

The heightened tumor γ H2AX levels *in vivo* and sensitization of TNBC cells to DNA damaging agents, especially in the context of olaparib-induced responses, led to further exploration of DNA damage repair modulation by OA-NO₂. Evaluation of nuclear γ H2AX staining to probe for DNA damage of MDA-MB-231 cells in the presence or absence of 5 Gy IR found OA-NO₂ to significantly increase nuclear γ H2AX localization in irradiated MDA-MB-231 cells compared to vehicle controls indicating increases in DSBs and overall DNA damage (Fig. 13A). Evaluation of the DNA damaging effects of OA and OA-NO₂ on non-transformed MCF10A and MDA-MB-231 cells following 5 Gy IR found nuclear γ H2AX staining was only increased in TNBC cells treated with OA-NO₂, not MCF10A cells (Fig 13B).

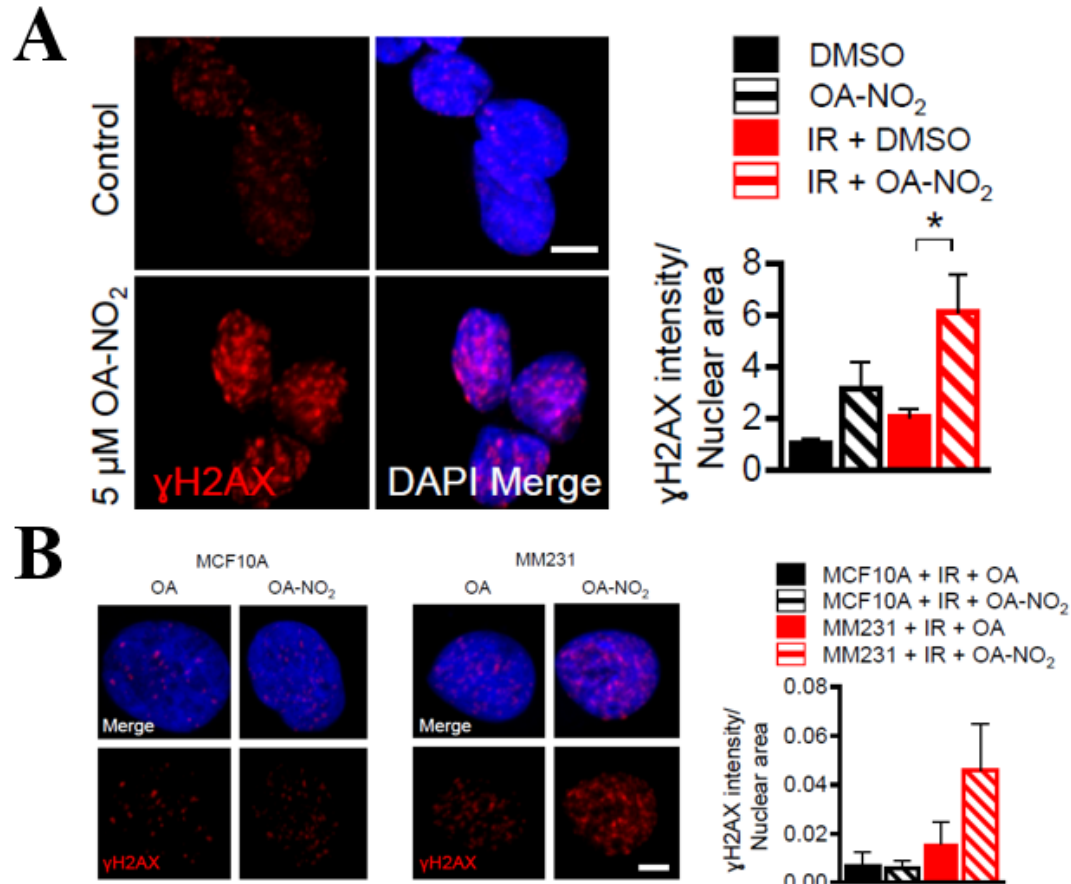


Figure 12. OA-NO₂ induces increased γ H2AX in irradiated TNBC cells.

(A) OA-NO₂ increased γ H2AX (red) in MM231 cells following irradiation with 5 Gy. Merged samples include DAPI stained nuclei (blue). Cells on 16-well coverslips were dosed with 5 Gy then and treated with 5 μ M OA-NO₂ or vehicle for 6 h prior to IF processing. The average percentages of cells with 5 or more foci from confocal z-stacked images are indicated from 0 or 5 Gy samples + SEM. (B) MCF10A (black) or MDA-MB-231 (MM231) (red) cells on 16-well coverslips were dosed with 5 Gy, then treated with 5 μ M OA (solid) or OA-NO₂ (striped) for 6 h prior to IF processing. The γ H2AX intensity per unit nuclear area of confocal z-stacked images are indicated from two experiments + range.

Increasing concentrations of OA-NO₂ also enhanced breast cancer cell death in a clonogenic assay following irradiation with 2 Gy IR (Fig. 14A). Cell cycle analysis of MDA-MB-231 cells confirmed that no significant changes to the cell cycle occurred. (Fig. 14B).

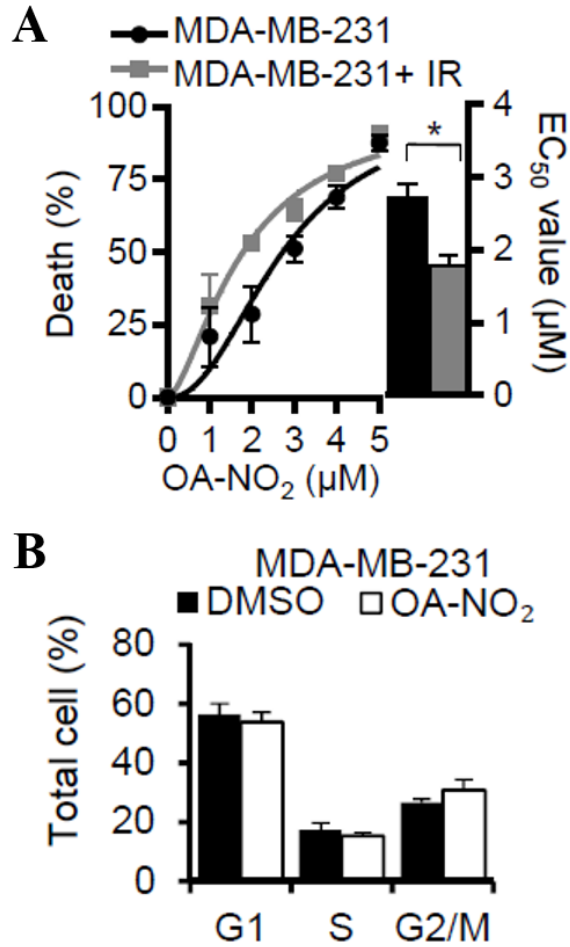


Figure 13. Clonogenic formation of TNBC cells following OA-NO₂ and IR treatment.

(A) Increasing concentrations of OA-NO₂ decrease clonogenic survival of TNBC cells following irradiation with 5 Gy. MDA-MB-231 cells were dosed with 5 Gy (■), then treated with 0 to 5 µM OA-NO₂ every other day for 10 days and compared to non-irradiated cells (□). EC₅₀ values indicate average + SEM, n=3. (B) OA-NO₂ or vehicle treated cells displayed a similar cell cycle profile by flow cytometric analysis of propidium iodide stained breast cancer cells.

3.4 Discussion

It is shown that the ability of OA-NO₂ to decrease cancer cell growth is partly due to its DNA damage inducing effect by heightening γ H2AX responses *in vivo* (Fig. 11). Therefore, it was tested whether OA-NO₂ can enhance the sensitivity of cancer cells to anti-cancer agents that induce DNA damage. The DNA damaging drugs cisplatin (DNA cross-linking agent), doxorubicin (DNA topoisomerase II inhibitor) and olaparib (PARP inhibitor) were co-treated with OA-NO₂ to test potential sensitization of TNBC cells to these drugs [19, 162, 163]. The results indicate that OA-NO₂ inhibits growth of the TNBC cell lines MM231, BT549 and Hs578T to a greater extent when co-administered with the clinically-relevant DNA-directed therapeutics doxorubicin, cisplatin or olaparib (Fig. 12). IR therapy, a potent DNA damage inducer through DSBs and SSBs, is given to most breast cancer patients with stage 1 invasive cancers. It was investigated whether OA-NO₂ had any beneficial effects on IR therapy. OA-NO₂ amplified the induction of DSB by IR (Fig. 13A). This suggests that OA-NO₂ can be a useful adjuvant for to breast cancer patients who are undergoing IR therapy to potentiate cancer cell killing. Additionally, OA-NO₂ amplified γ H2AX staining in MM231 cells specifically compared to non-tumorigenic epithelial breast cell line MCF-10A (Fig. 13B). This implies that such co-treatment of OA-NO₂ will have minimal off target toxicity to normal cells. Increasing concentrations of OA-NO₂ also enhanced breast cancer cell death in a clonogenic assay following irradiation with 2 Gy IR (Fig. 14A). This suggests that OA-NO₂ DNA effects are not short-lived and have inhibitory effects on cancer cell colony formation over a long period of 8 to 10 days. Combined, these results build a foundation for promising combinational regimens involving OA-NO₂ and DNA targeting therapies.

4.0 Impact of OA-NO₂ on Double-Strand Break Repair Pathways

4.1 OA-NO₂ Inhibits Homologous Recombination

The heightened tumor γ H2AX levels *in vivo* and *in vitro* as well as sensitization of TNBC cells to DNA damaging agents, especially in the context of olaparib-induced and IR-induced responses, led to further exploration of DNA damage repair modulation by OA-NO₂. Cell lines comprising machinery to measure four different DSB repair pathway efficiencies were used. These fluorescence-based reporter cell lines (DR-GFP for HR, EJ5-GFP for NHEJ, SA-GFP for SSA and EJ2-GFP for alt-EJ) were generated by Dr. Jeremy Stark [58].

OA-NO₂-dependent effects on HR DNA repair were investigated by utilizing a DR-GFP reporter assay. This analysis quantifies intracellular recombination of an integrated cDNA cassette of two tandem non-fluorescent GFP constructs following introduction of an I-SceI cleavage to the system by measuring the fluorescent GFP protein that is produced following successful recombination (Fig. 15A) [152]. Daily OA-NO₂ treatment of human osteosarcoma U2OS cells harboring the DR-GFP construct revealed that after I-SceI transfection, the number of GFP positive cells was significantly decreased by 2-fold when compared to native OA or vehicle control after 48 hours (Fig. 15B).

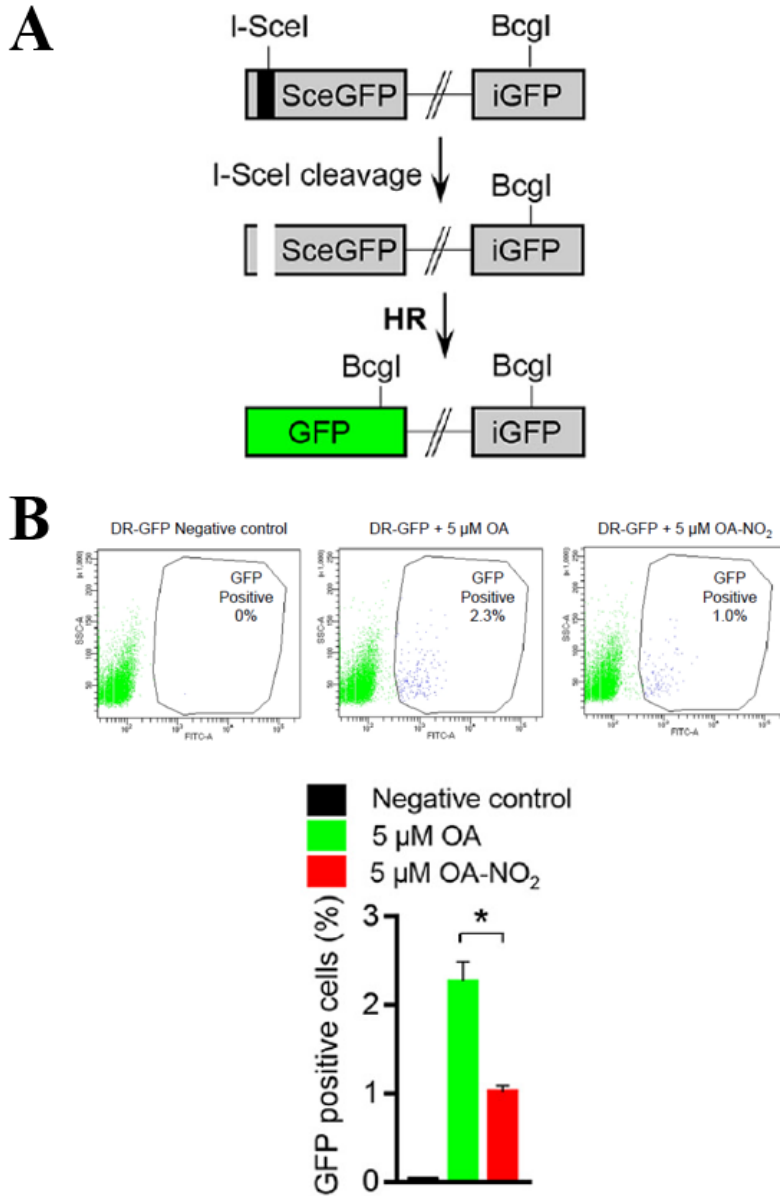


Figure 14. OA-NO₂ inhibits HR in U2OS cells.

(A) Scheme of the DR-GFP assay. (B) U2OS cells containing the HR reporter construct DR-GFP were transfected with an I-SceI plasmid and treated with vehicle (black), 5 μ M OA (green) or 5 μ M OA-NO₂ (red). Negative control cells did not have I-SceI present. Values indicate average and error bars represent SEM, $n \geq 3$. The number of GFP positive cells were detected by flow cytometry at 48 h.

4.2 OA-NO₂ has no Effect on Non-Homologous End Joining

The impact of OA-NO₂ on suppression of DSB repair through both the HR and NHEJ pathways was examined by utilizing the EJ5-GFP NHEJ reporter assay, which separates GFP cDNA from a transcriptional promoter with a puromycin gene flanked by two I-SceI cleavage sites (Fig. 16A) [58]. In contrast to the effects seen by DR-GFP-mediated HR measurements, EJ5-GFP U2OS cells showed no effect of OA-NO₂ on NHEJ. This was indicated by an absence of changes in the number of GFP positive cells following I-SceI cleavage after 48 h by flow cytometric analysis (Fig. 16B).

A novel strategy to measure the kinetics of changes in both HR and NHEJ in live cells utilized automated fluorescence microscopy to track the emergence of GFP positive cells over time in monolayers, as opposed to making static measurements of detached cells using flow cytometry. To account for changes in cell density over time, cell confluency was measured following treatment of DR-GFP U2OS cells with vehicle, 5 μ M OA or OA-NO₂ every 4 hours for 3 days (Fig. 17A-B). The emergence of GFP positive cells subsequent to I-SceI-induced cleavage was quantified and normalized to cell confluency over time to compare OA-NO₂ with OA and untreated cells. Daily administration of 5 μ M OA-NO₂ decreased the number of GFP-positive cells by 2-fold over 68 hours when compared to controls (Fig. 17C). In addition, EJ5-GFP U2OS cells showed no effect of OA-NO₂ on NHEJ indicated by live-cell fluorescence microscopy (Fig. 17D).

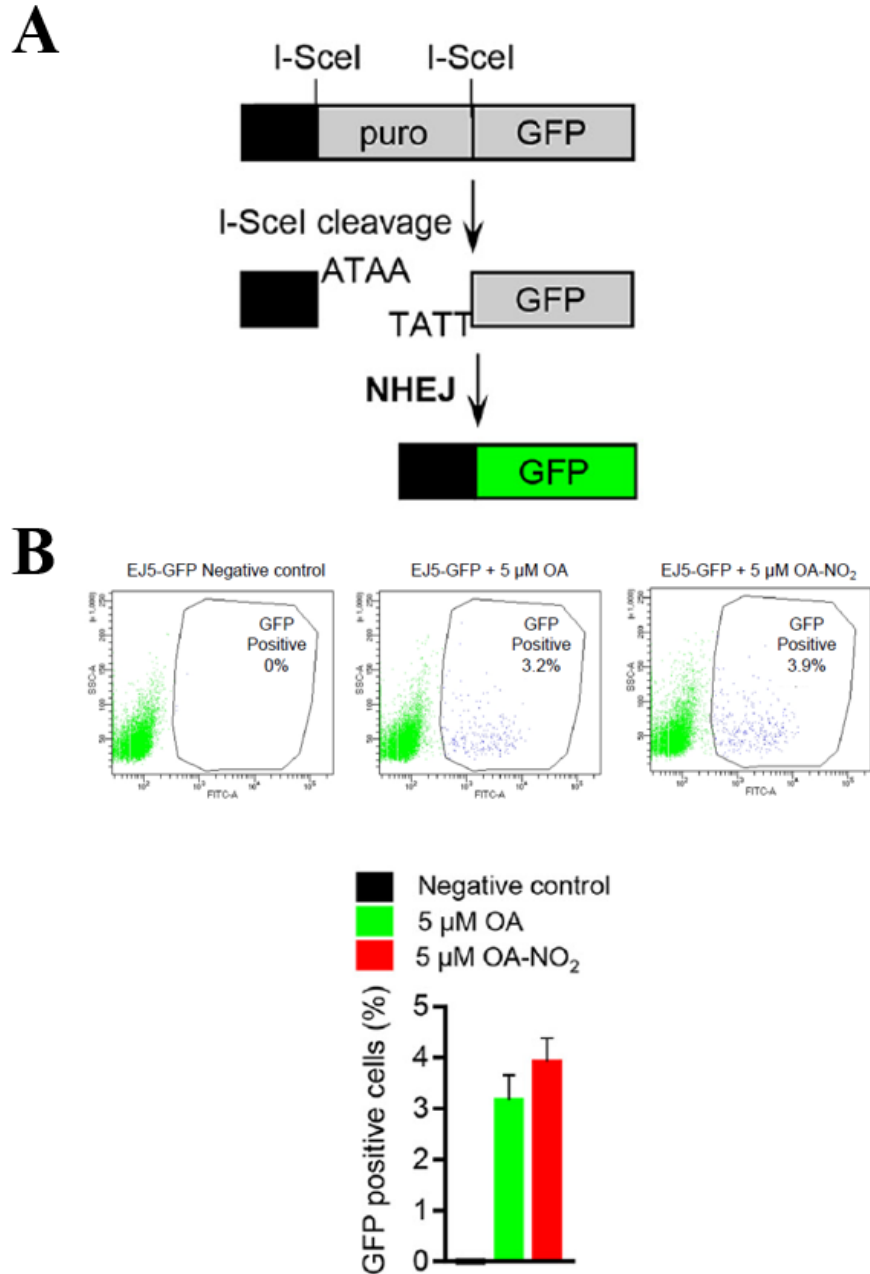


Figure 15. OA-NO₂ does not inhibit NHEJ in U2OS cells.

(A) Structure of the EJ5-GFP assay. (B) U2OS cells containing the HR reporter construct DR-GFP were transfected with an I-SceI plasmid and treated with vehicle (black), 5 μ M OA (green) or 5 μ M OA-NO₂ (red). Negative control cells did not have I-SceI present. Values indicate average and error bars represent SEM, $n \geq 3$. The number of GFP positive cells were detected by flow cytometry at 48 hours.

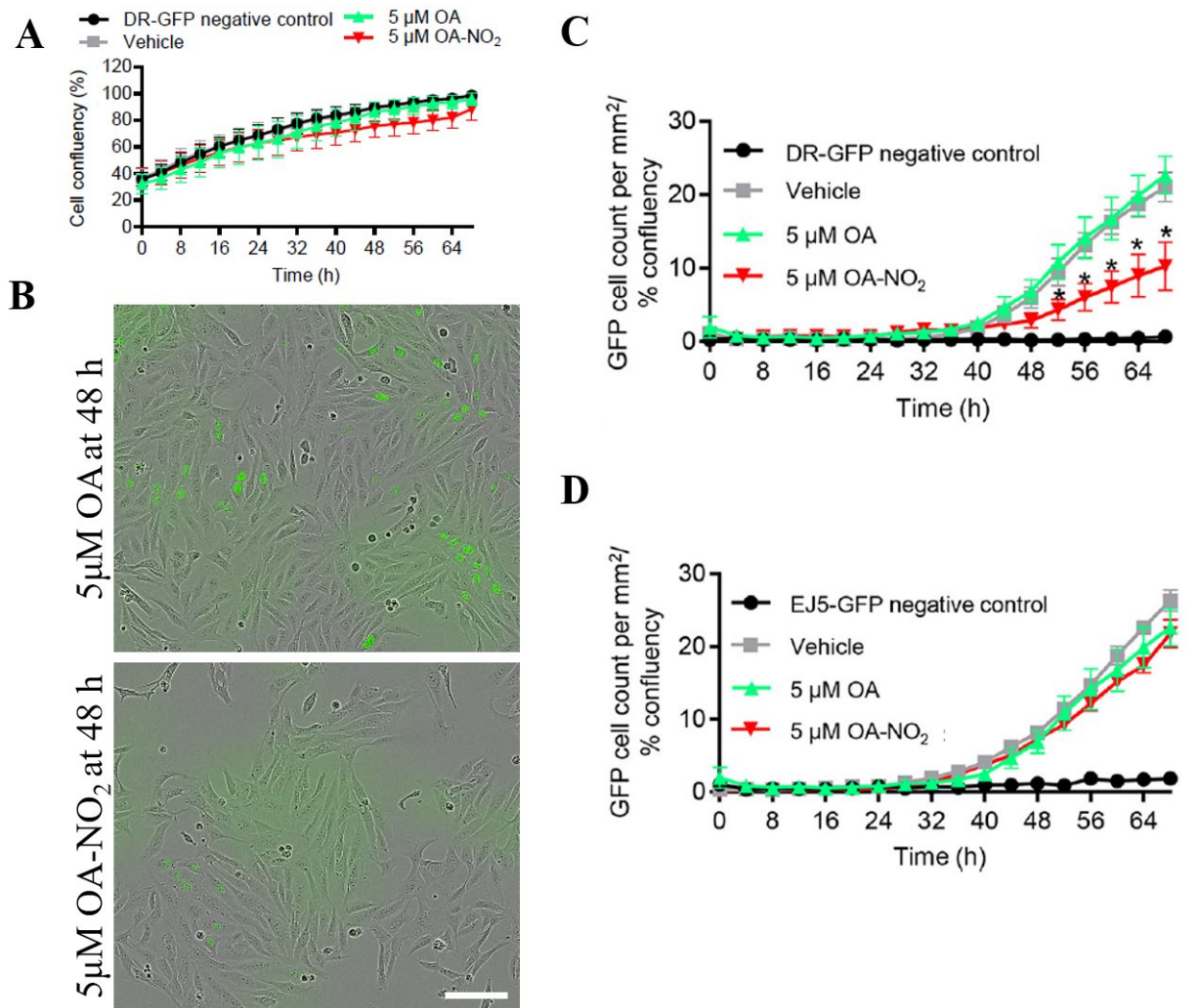


Figure 16. OA-NO₂ effects on HR and NHEJ in U2OS cells measured via live cell fluorescence imaging.

(A-B) U2OS cells containing the HR reporter construct DR-GFP were transfected with an I-SceI plasmid and treated with vehicle (gray), 5 μM OA (green) or 5 μM OA-NO₂ (red). Negative control cells did not have I-SceI present. Average + SEM, n ≥ 3. The number of GFP positive cells were detected by flow cytometry at 48 h. U2OS cell proliferation was measured by calculating cell confluency from brightfield images using live-cell imaging with the Incucyte Zoom over 68 hours at 37°C with 5% CO₂. (C-D) The emergence of GFP positive cells over 68 hours was quantified

using live-cell fluorescent microscopy. GFP positive cell counts were normalized to cell confluency and compared. Bar: 150 μm .

4.3 OA-NO₂ Inhibits Single Strand Annealing (SSA) and Alternative End Joining (Alt-EJ)

The impact of OA-NO₂ was further studied in two additional DSB repair pathways that also depend on DNA end resection like HR, SSA and alt- EJ. Both pathways were tested using GFP-based chromosomal reporter assays: SA-GFP and EJ2-GFP measured SSA and alt-EJ, respectively. The SA-GFP reporter assay utilizes I-SceI to generate DSBs. The reporter consists of the 5' GFP and SceGFP3' that have 266 bp homology. Repair occurs when a DNA strand of SceGFP3' is annealed to the complementary strand 5'GFP'. The annealing produces a 2.7 kb deletion in the chromosome. HR can also repair SA-GFP but will not restore a functional GFP gene, so this reporter is specific to SSA. Similarly, EJ2-GFP produces GFP+ products from alt-EJ events. The reporter contains an N-terminal tag expression tag that is fused to a GFP sequence. The coding sequence between the tag and GFP is disrupted by an I-SceI site and a DSB repair there only produces a functional GFP molecule with an alt-EJ event. Both SSA and alt-EJ are inhibited by OA-NO₂ in U2OS cells by ~4 fold and ~1.5 fold respectively (Fig 18. A-B). Comparing the amount of inhibition among SSA, alt-EJ and HR, OA-NO₂ most potently represses SSA.

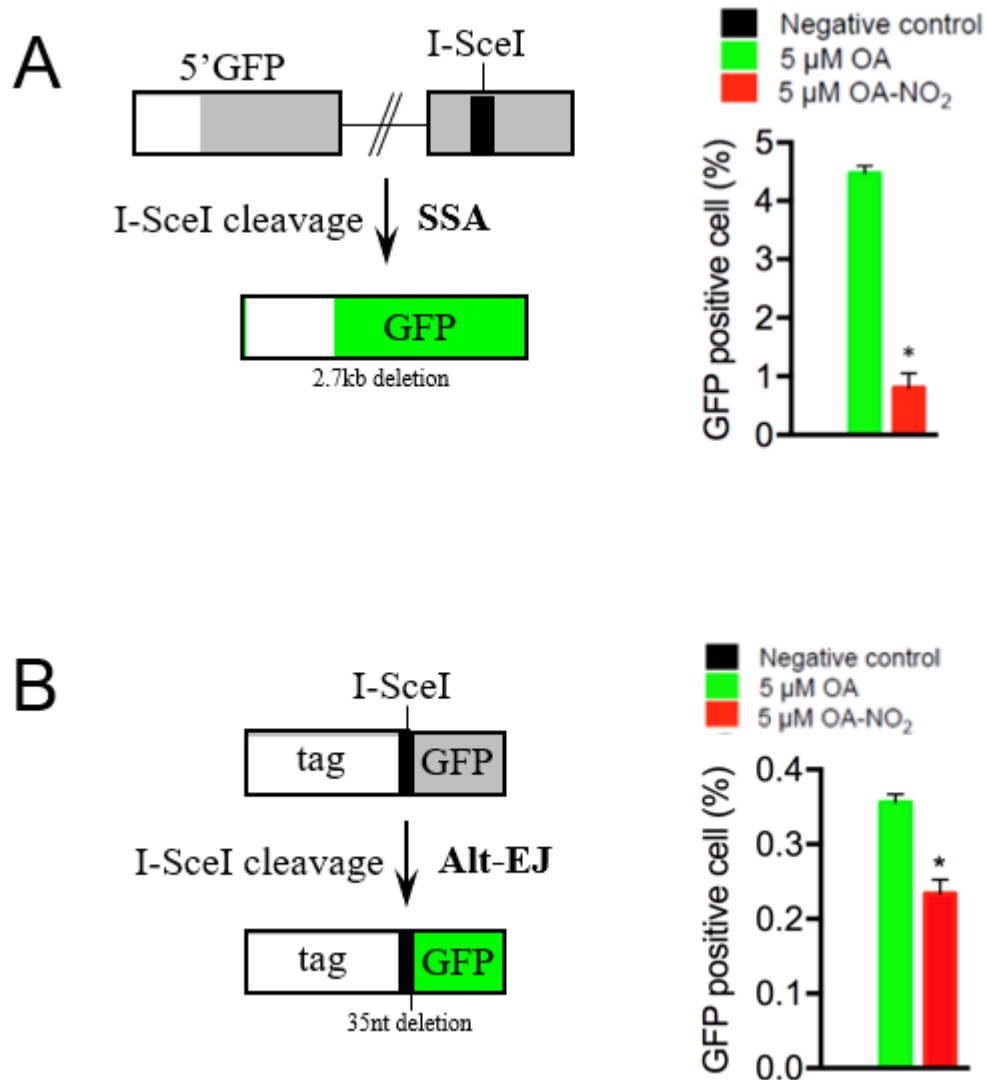


Figure 17. OA-NO₂ inhibits DSB repair pathways SSA and Alt-EJ.

(A-B) U2OS cells containing the SSA reporter construct SA-GFP or alt-EJ reporter construct EJ2-GFP were transfected with an I-SceI plasmid and treated with vehicle (black), 5 μM OA (green) or 5 μM OA-NO₂ (red). Negative control cells did not have I-SceI present. Average + SEM, n ≥ 3. The number of GFP positive cells were detected by flow cytometry at 48 h.

4.4 Discussion

HR is critical for cancer cell evasion of DNA-targeting therapeutics. In addition, HR is more frequently used by cancer cells since it is functional in cell cycle phases S/G2 and cancer cells are more frequently in these phases compared to normal cells [164]. On the other hand, NHEJ, the other major DSB repair pathway, is mostly inactive in non-replicating cells, making it a less active pathway in cancer cells. In support of this, breast cancer cells have elevated HR function but no change in NHEJ [165]. Additionally, cisplatin induced DNA crosslinks are ultimately repaired by HR and not through NHEJ [166, 167]. Similarly, doxorubicin induced topoisomerase II inhibition and olaparib induced PARP inhibition eventually create DNA DSBs that require HR for repair. Therefore, complementing current cancer therapies that target DNA with a drug that targets the HR pathway but not NHEJ pathway is potentially a very effective strategy to eliminate resistant cancer cells with minimal damage to normal cells. Based on fluorescent based cell reporter assays evaluating DNA repair, OA-NO₂ inhibits HR but not NHEJ (Fig. 15-17). In addition to HR inhibition, OA-NO₂ also inhibits SSA and alt-EJ (Fig 18). This is particularly important because SSA and alt-EJ are proposed to be the backup repair pathways for HR-deficient basal-like breast epithelial cancer cells to rely on for the repair of DNA DSBs [168, 169]. RAD51 inhibition has been shown to upregulate SSA activity in mammalian cells [58]. RAD52, the SSA pathway central protein, has been shown to compensate for lack of RAD51 function in BRCA1/2 deficient cells [60]. Additionally, alt-EJ has also been shown to function as a backup pathway for HR through polymerase θ -mediated repair [64]. Therefore, blocking only HR in cancer cells may not be sufficient as the other DNA DSB repair pathways are likely to compensate for HR inhibition. This identifies OA-NO₂ as a unique and effective drug to specifically target replicating cancer cells that rely on HR, SSA, and alt-EJ to evade cancer therapy.

5.0 Inhibition of RAD51 by OA-NO₂

5.1 OA-NO₂ Inhibits RAD51 Foci Formation in TNBC Cells

HR efficiency inhibition of DR-GFP U2OS cells but not NHEJ efficiency led to further exploration of post-resection DSB DNA damage repair modulation by OA-NO₂. As olaparib sensitivity is a hallmark of HR-deficient cells [170], it was evaluated whether OA-NO₂ impacted DNA repair by targeting RAD51 after the identification of a reactive cysteine that might serve as a target of OA-NO₂ [171]. To specifically probe DNA double-strand break repair, MDA-MB-231 cells were challenged with 5 Gy IR and RAD51 foci were quantified using an ImageJ plugin developed by the author. IR was used in order to create DSBs in the DNA [20]. Upon IR treatment, the percent of cells with positive RAD51 staining went from ~8% up to ~40%. The treatment of breast cancer cells with 5 μ M OA-NO₂ inhibited RAD51 foci formation, as reflected by a) the number of cells with more than 5 foci and b) responses of vehicle treated cells following IR (Fig. 19).

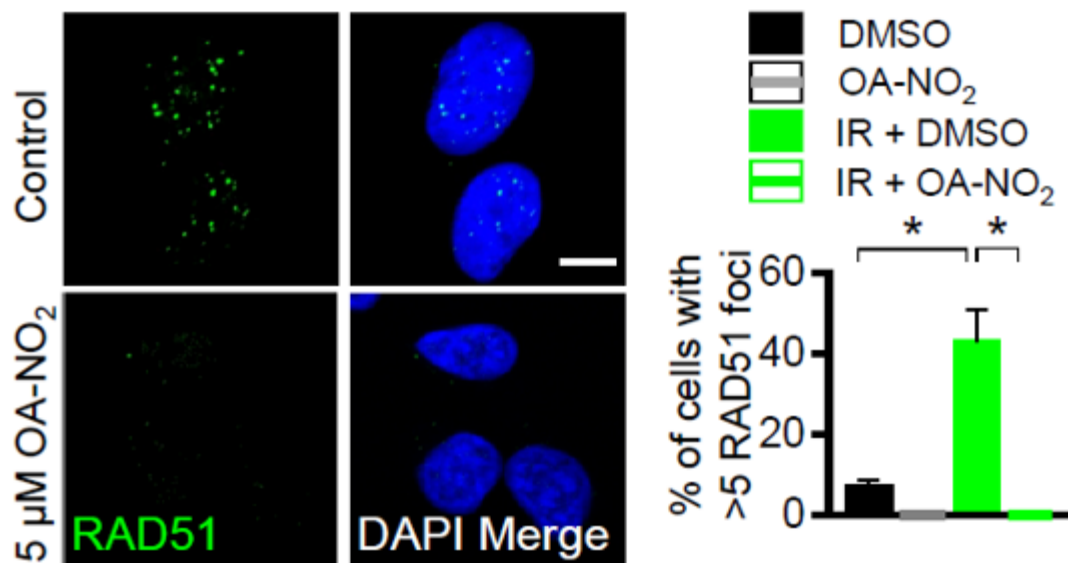


Figure 18. OA-NO₂ inhibits RAD51 foci formation.

OA-NO₂ diminished RAD51 foci formation (green) in MM231 cells following irradiation with 5 Gy. Merged samples include DAPI stained nuclei (blue). Cells on 16-well coverslips were dosed with 5 Gy then and treated with 5 μM OA-NO₂ or vehicle for 6 h prior to IF processing. The average percentages of cells with 5 or more foci from confocal z-stacked images are indicated from 0 or 5 Gy samples + SEM. Bar: 10 μm.

Effects of OA-NO₂ on RAD51 were further tested by overexpressing RAD51 in the HR reporter cells. HR activity, as measured by the percentage of GFP positive cells relative to OA control treatment, was significantly increased in U2OS DR-GFP reporter cells stably overexpressing RAD51 treated with 5 μM OA-NO₂ in comparison to control reporter cells, suggesting a rescue of the HR function (Fig. 20).

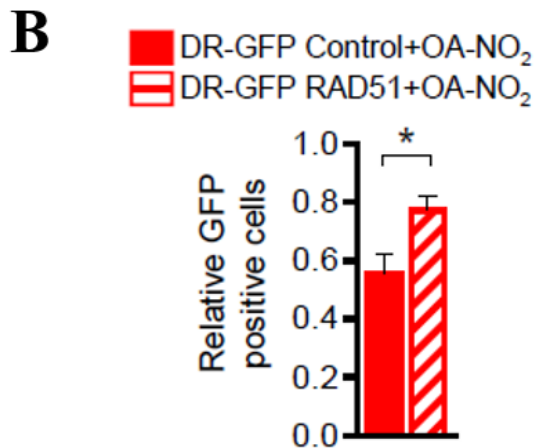
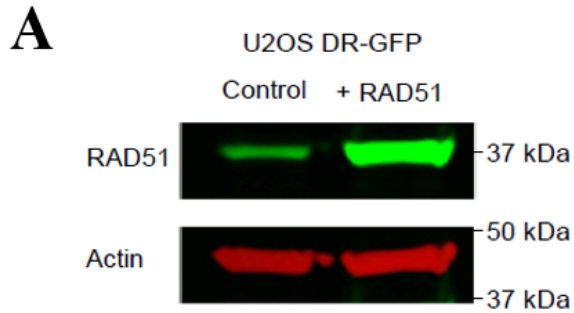


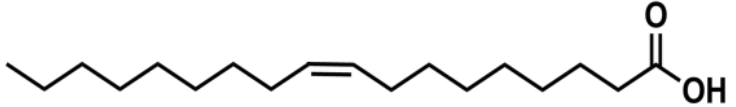
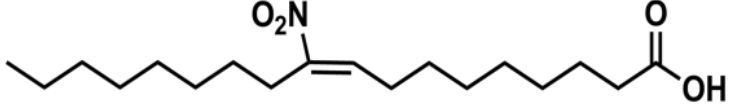
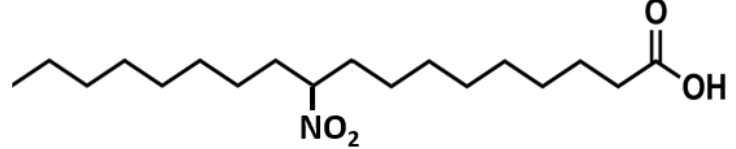
Figure 19. Overexpression of RAD51 partially rescues HR inhibition by OA-NO₂.

(A) U2OS cells containing the HR reporter construct DR-GFP were stably transfected with a control or RAD51 overexpression plasmid and protein expression for RAD51 and actin were detected by immunoblot. (B) U2OS cells containing the HR reporter construct DR-GFP were stably transfected with a control or RAD51 overexpression plasmid and the cells were investigated as above with 5 μ M OA-NO₂ in control (red) or RAD51 overexpressing cells (red striped).

5.2 OA-NO₂ Targets RAD51 Cysteine 319

Fluorophore adduction of Cys319 disrupts RAD51 filament formation *in vitro* [172]. Moreover, protein structural data (PDB: 1N0W) shows Cys319 is a solvent-exposed nucleophile within the RAD51 C-Terminus (Fig. 21A) that is susceptible to reaction with RI-1, a reagent also having Michael acceptor qualities [173]. Due to its electrophilic nature, it was hypothesized that OA-NO₂ would react with nucleophilic RAD51 Cys319. Indeed, biotin-OA-NO₂, but not the non-electrophilic biotin-oleic acid (OA) and biotin-10-nitro-octadecanoic acid (SA-NO₂) (Table 2), supported affinity precipitation of RAD51 from cell lysates with streptavidin-labeled beads (Fig. 21B). By comparing RAD51 Cys312Ser or Cys319Ser mutants for reactivity with biotin-OA-NO₂, it was revealed that there is a preferential reaction of OA-NO₂ with Cys319 (Fig. 21C). RAD51Cys312Ser and RAD51 WT controls were readily affinity precipitated by biotin-OA-NO₂, as opposed to RAD51Cys319Ser expressed in mutant cells. Of note, the RAD51-Cys312Ser mutant displayed enhanced precipitation of OA-NO₂, which may reflect interruption of a disulfide bond between RAD51-Cys312 and Cys319 or another intracellular protein that obscures Cys319. To define whether OA-NO₂ alkylates endogenous RAD51 in TNBC cells, biotin-OA-NO₂ was added to MDA-MB-231 and MDA-MB-468 cells. Biotin-OA-NO₂-RAD51 complex formation upon streptavidin precipitation was observed in lysates of both cell lines (Fig. 21D).

Table 2. Chemical structures and characteristics of lipids used.

Name	Structure	Electrophilic
Oleic acid (OA)		-
Nitro-oleic acid (OA-NO ₂)		+
Nitro-stearic acid (SA-NO ₂)		-

A IYDSPCLPEAEAMFAINADGVGDAKD

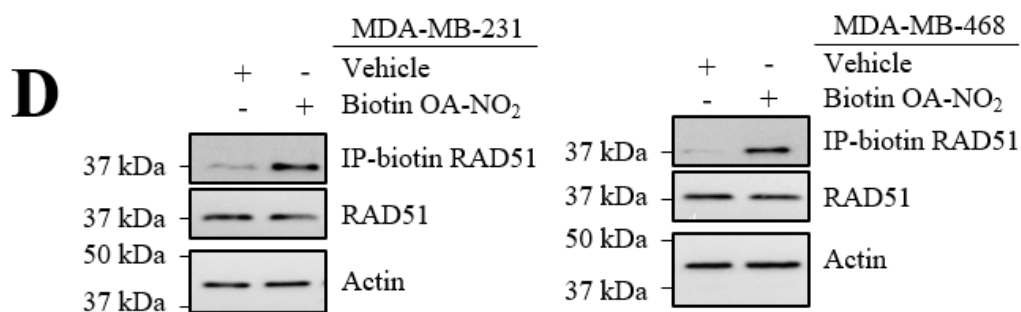
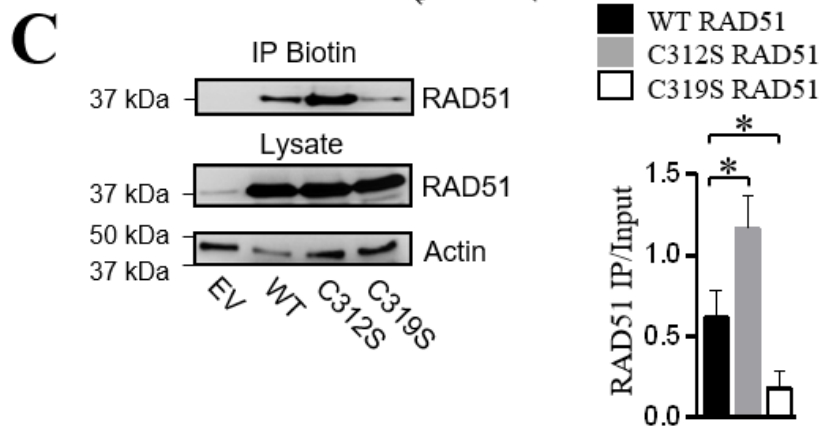
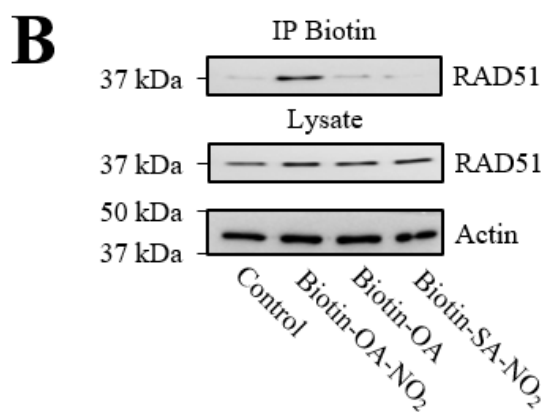


Figure 20. OA-NO₂ binds to RAD51 at Cys319.

(A) The crystal structure of RAD51 (PDB: 1N0W) demonstrates that RAD51 Cys319 is solvent exposed. (B) OA-NO₂ binds RAD51 *in vitro*. Purified RAD51 protein was incubated with control, biotinylated OA, OA-NO₂ or SA-NO₂ for 1 h and precipitated with streptavidin coated agarose and then detected by immunoblot. (C) OA-NO₂ binds to RAD51 Cys319 in cells expressing RAD51. 293T cells expressing WT or cysteine mutant RAD51 were incubated with biotinylated OA-NO₂ for 1 h and precipitated and detected. Three independent experiments were quantified and analyzed by one-way ANOVA * $p < 0.05$. (D) OA-NO₂ binds RAD51 in MM231 or MM468 cells. Cells were incubated with biotinylated OA-NO₂ and then lysates were precipitated with streptavidin coated agarose and detected by immunoblot.

5.3 OA-NO₂ Abrogates RAD51-DNA Interaction

In addition to RAD51 foci inhibition by OA-NO₂, measured via immunofluorescence, an *in vitro* DNA binding assay was performed to test whether OA-NO₂ can directly inhibit DNA binding capability of RAD51. The ability of OA-NO₂ to specifically disrupt RAD51 binding from DNA was probed by quantifying changes in fluorescence polarization of an Alexa Fluor 488 conjugated single-stranded oligonucleotide *in vitro*. RAD51 protein binding to Alexa Fluor 488 conjugated ssDNA will increase the polarization of light emitted by the fluorescent substrate (Fig 22A). OA-NO₂, but not OA, decreased the relative polarization of RAD51 in the presence of ATP and DNA (Fig. 22B). The inhibition of polarization increase suggests OA-NO₂ abrogates RAD51-DNA interaction. Control experiments found OA and OA-NO₂ did not cause non-specific effects through fluorophore quenching to decrease fluorescence polarization (Fig. 22C).

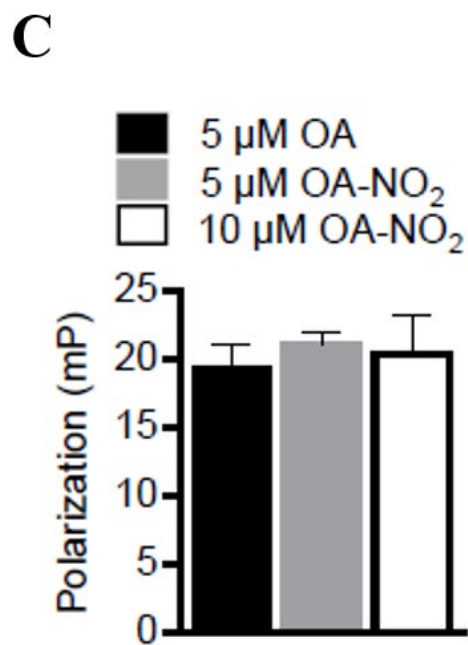
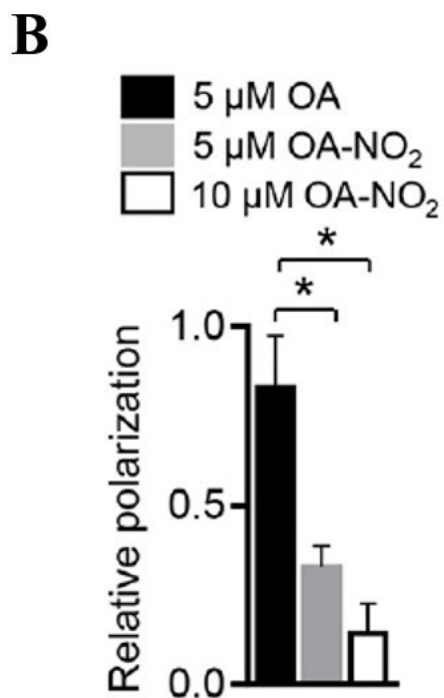
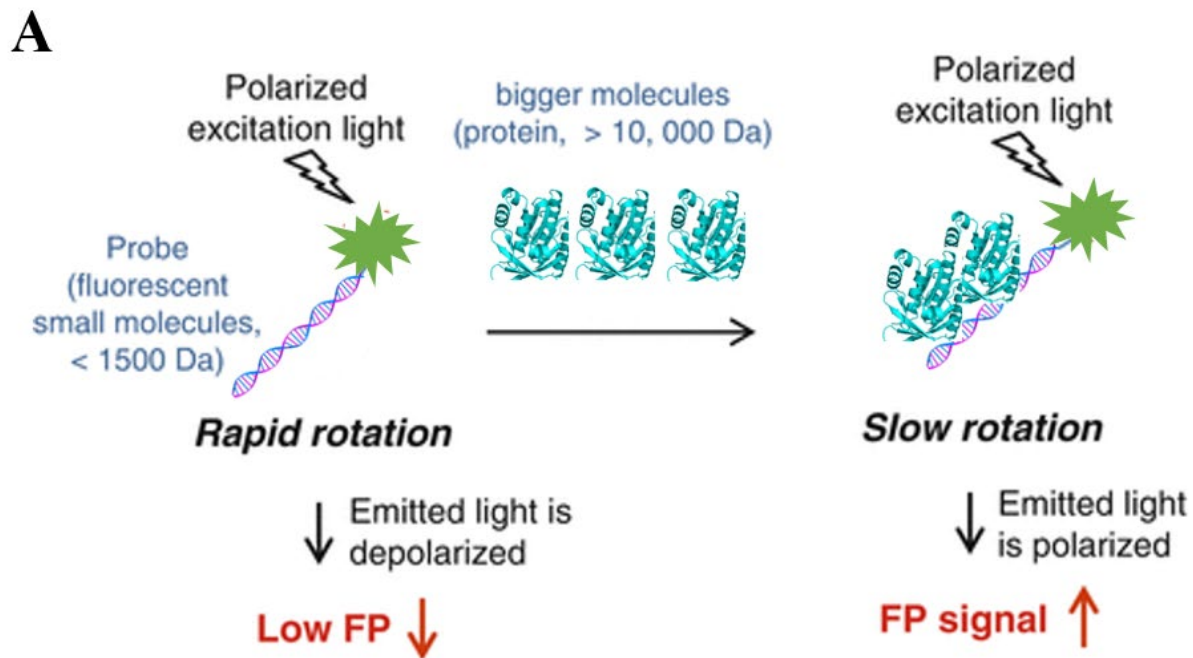


Figure 21. OA-NO₂ inhibits RAD51-DNA interaction in an *in vitro* fluorescent polarization (FP) based DNA binding assay.

(A) Schematic explaining DNA binding measurement as a function of fluorescent polarization.

(B) Alexa Fluor 488 conjugated DNA was incubated with purified RAD51, ATP and 5 μM OA

(black), 5 μM OA-NO₂ (gray) or 10 μM OA-NO₂ (white) and fluorescence polarization was quantified and normalized to a control lacking ATP. (C) Alexa Fluor 488 conjugated DNA was incubated with ATP and 5 μM OA (black), 5 μM OA-NO₂ (gray) or 10 μM OA-NO₂ (white) and fluorescence polarization was quantified to determine if non-specific fluorophore quenching was present.

Next, it was investigated whether DNA-bound RAD51 reacts with OA-NO₂ by testing an ability to decrease FP. This was explored using two conditions. First, OA-NO₂ (10 μM) was pre-incubated with human RAD51 protein (27 μM) for 5 minutes prior to adding Alexa 488 ssDNA strand into the mix (Fig 23A). Secondly, OA-NO₂ (10 μM) was added to the reaction mix 1 hour after RAD51 protein and Alexa 488 ssDNA incubation at 37 °C. Under these conditions, Alexa 488 ssDNA-RAD51 binding is achieved after 1 hr, as reflected by an increase in FP (Fig 23B). After addition of OA-NO₂, this interaction is significantly abrogated at 2 hr, as there is a decrease of FP (Fig 23B). This suggests that OA-NO₂ can access C319 of RAD51 monomers in a filament and dissociate RAD51 protein from ssDNA *in vitro*.

Overall, these data reveal that OA-NO₂ inhibited HR by forming adducts with RAD51 and possibly other additional target proteins to enhance sensitivity to DNA-directed cancer therapies (Fig. 24).

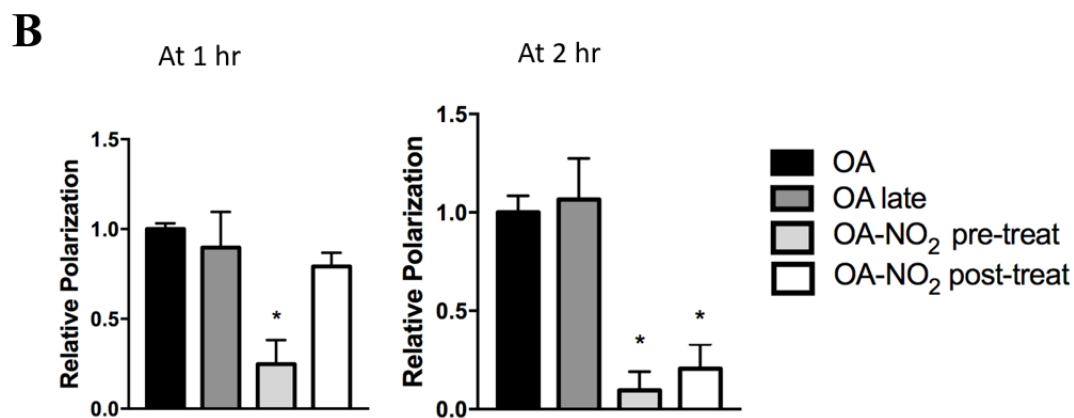
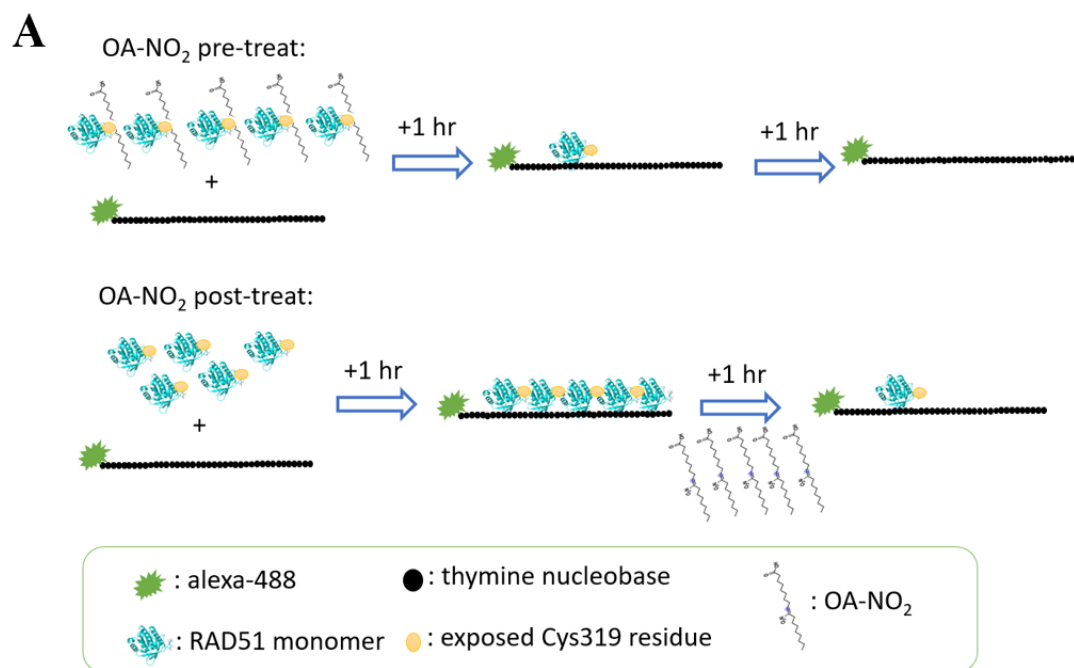


Figure 22. OA-NO₂ removes RAD51 from DNA in an *in vitro* FP-based assay.

(A) Schematic explaining DNA binding measurement comparing pre-treated and post-treated OA-NO₂ conditions as a function of fluorescent polarization. (B) Alexa Fluor 488 conjugated DNA was incubated with purified RAD51, ATP and RAD51 pre-incubated with 10 μ M OA (black), RAD51 post-incubated with 10 μ M OA (dark gray), RAD51 pre-incubated with 10 μ M OA-NO₂ (light gray) or RAD51 post-incubated with 10 μ M OA-NO₂ (white) and fluorescence polarization was quantified and normalized to a control lacking ATP.

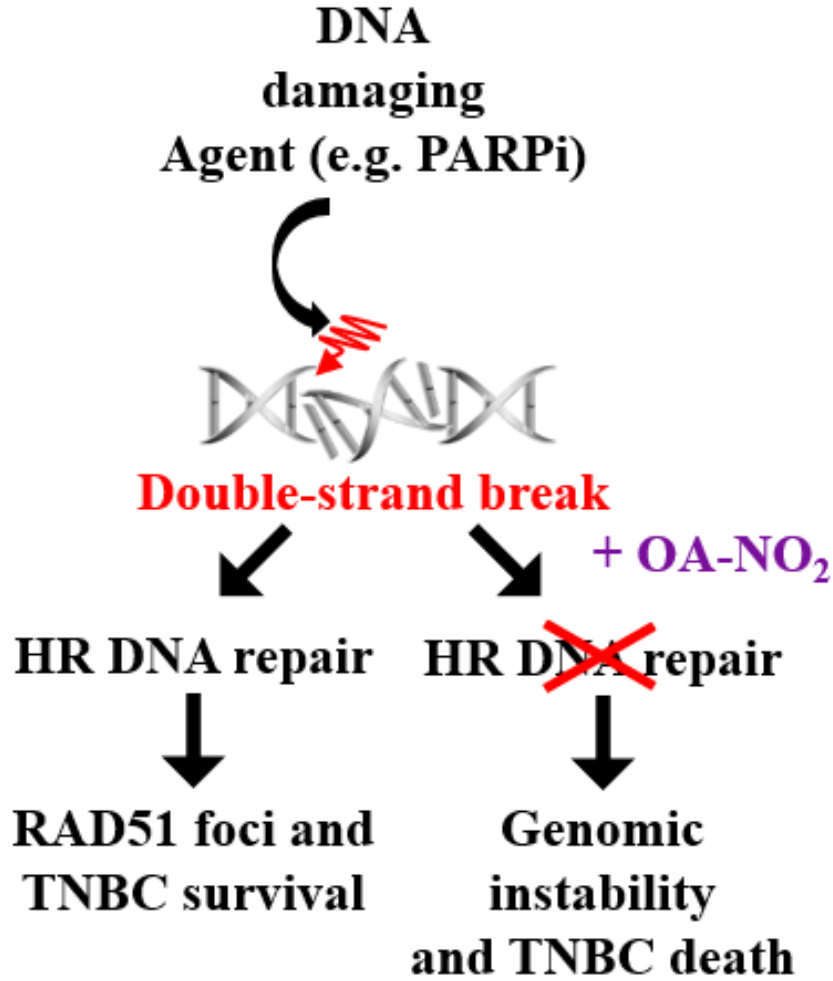


Figure 23. OA-NO₂ represses HR and causes genomic instability and death in TNBC cells.

5.4 Discussion

Targeting HR repair pathway proteins using small molecule inhibitors is an active area of research. Strategies being explored include targeting the MRN complex comprising MRE11, RAD50 and NBS1 as well as the RAD51 protein [174, 175]. Several studies have attempted to harness RAD51 inhibition in order to promote killing of cancer cells. Inhibition of RAD51 with small molecule inhibitors [e.g., DIDS [176], B02 [96, 177], RI-1 [173] and IBR2 [178] can sensitize cancer cells to DNA damaging agents like chemotherapeutics or IR. However, so far, no safe small molecule Rad51 inhibitors have progressed to Phase 1/2 trials. For example, RI-1 was identified in a high-throughput screen to potentiate RAD51 filament formation and HR activity, fortuitously adducting Cys319 [173]. However, RI-1 has multiple electrophilic centers in a complex biphenolic morpholino structure, thus inducing either irreversible Michael addition or crosslinking leading to incompatibility for *in vivo* applications due to toxicity. In contrast, OA-NO₂ is a soft electrophile that reacts with soft nucleophiles such as thiols leading via a reversible Michael addition.

RAD51 is a viable drug target. Overexpression of RAD51 has been reported in many types of cancer [179]. The elevated expression of RAD51 is positively correlated with breast cancer tumor grade and has been identified in several TNBC cell lines and metastatic patient samples [92, 93]. In BRCA-1 deficient tumors, RAD51 upregulation has been shown to be a mechanism to bypass BRCA1 need in response to IR [180]. It was previously reported that OA-NO₂ more selectively targets TNBC thiols, as opposed to non-tumorigenic breast epithelium, due to the more effective mechanisms for maintaining redox homeostasis in normal breast epithelium. The non-tumorigenic epithelial breast cell line MCF-10A was less sensitive than TNBC cells lines to OA-NO₂ treatment due to higher rates of MRP1-mediated efflux of OA-NO₂ [147]. For RAD51

filaments to form faithfully, the amino acids that are in parts of the protein where two RAD51 monomers make contact are deemed to have important conformational roles. The cysteine 319 (C319) residue in RAD51 is important for filament formation. Modesti et al. studied nucleation sites by synthesizing fluorescent human RAD51 proteins [172]. They conjugated Alexa 488 to cysteine residues in order to carry out their analyses. When they labelled RAD51 on the C319 residue with Alexa 488, RAD51 failed to carry out its recombinase activity. This suggests that C319 is essential for RAD51 function. Next, another group developed RI-1, a small molecule inhibitor of RAD51 and showed that it covalently binds to the RAD51 C319 residue to destabilize RAD51 oligomerization [173]. In addition, they also show RAD51 C319S mutant fails to bind DNA [98, 173]. Furthermore, the recently published crystal structure of the pre-synaptic RAD51 filament on ssDNA shows the C319 to be located between two RAD51 monomers, suggesting it is located in an important site for oligomerization [181]. This crystal structure also identifies C319 to be solvent exposed, highlighting its availability for solvent macromolecule interactions. The C319 residue in one monomer is surrounded by two positively charged arginine residues (R197 and R170) marking it as a candidate to be identified as a hyperreactive cysteine due to increased electronegativity. Lastly, C319 is also happens to be near the RAD51 ATP binding site (~14 angstroms). The aggregated data from the studies identify RAD51 C319 residue to be of functional significance. A pymol rendering of this crystal structure is shown in Figure 25. Post-translational thiol modification or pharmacological targeting of Cys319 may thus disrupt RAD51 function through multiple mechanisms. We have now identified that electrophilic nitroalkenes inhibit RAD51 foci formation, bind RAD51 C319 and impair RAD51 binding to ssDNA (Fig. 19-23). Thus, the administration of synthetic homologs of endogenously-occurring fatty acid nitroalkenes offers a viable option for inactivating RAD51. These results motivate further *in vivo* model system

and clinical studies to determine if endogenously-generated lipid electrophiles and exogenously-administered synthetic homologs might play a role in modulating DNA repair and other signaling responses that would lead to improved treatment of drug-resistant cancers.

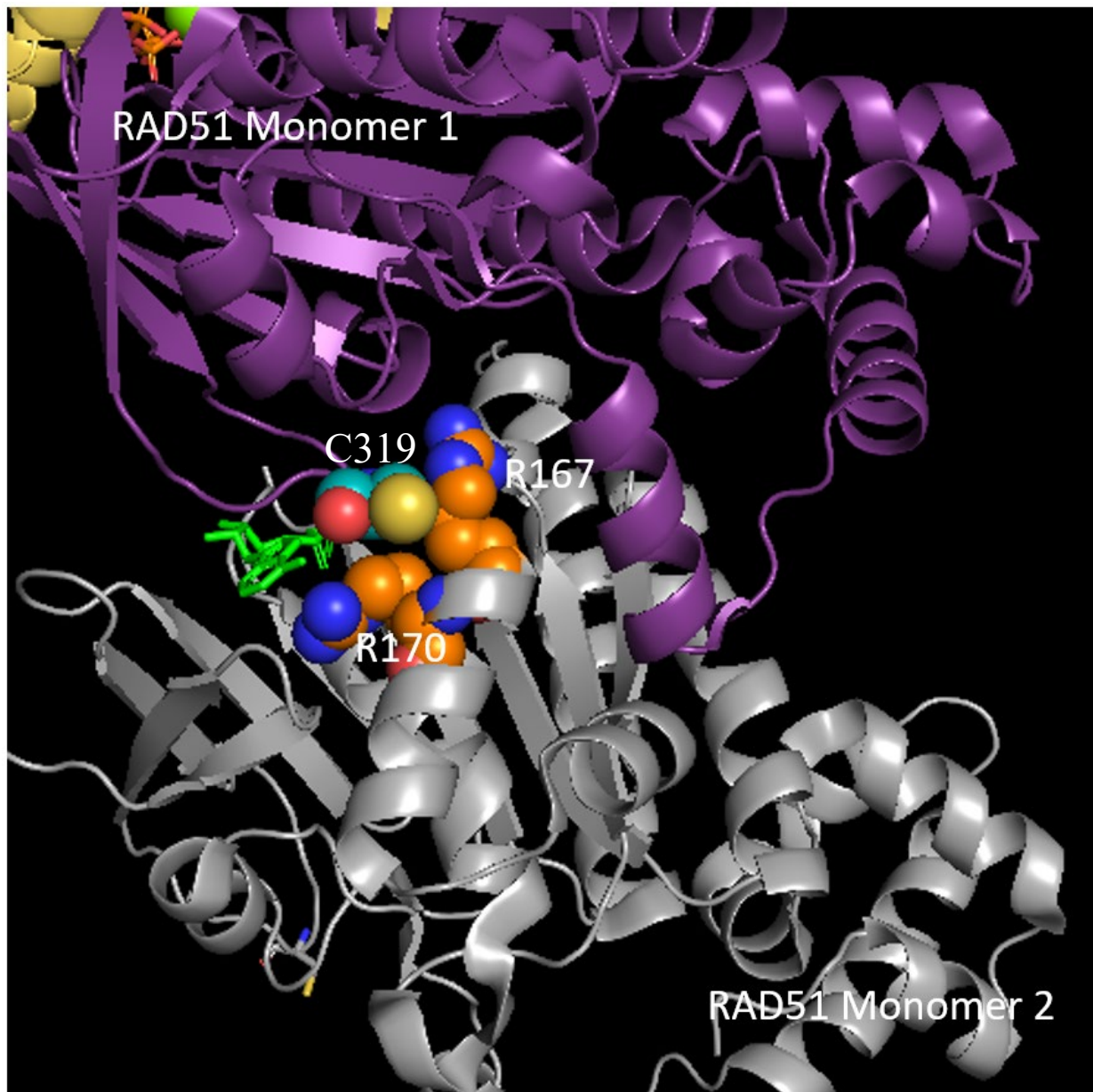


Figure 24. Crystal structure of pre-synaptic RAD51 filament on single-stranded DNA.

6.0 Pre-Clinical Studies Investigating Combinational Treatments of OA-NO₂ and PARP Inhibitors in TNBC

6.1 Talazoparib Inhibits MDA-MB-231 Cell Growth More Potently Than Olaparib in Combination With OA-NO₂

In pre-clinical studies, talazoparib (BMN 673) inhibited PARP both in its catalytic subunit as well as via PARP trapping mechanism [129, 182, 183]. Talazoparib's PARP trapping is 100 times more potent than other PARP inhibitors such as olaparib [184]. In addition to olaparib's FDA approval for BRCA-mutated breast cancer patients after the phase III OlympiAD trial, talazoparib was also approved for BRCA-mutated, HER2-negative breast cancer in October 2018 after favorable findings that came out of the phase III EMBRACA trial where talazoparib decreased risk of disease progression or death by 46% compared to physician's choice of chemotherapy in metastatic breast cancer patients with germline BRCA mutations [185]. Taking these results into consideration, synergistic outcomes were explored via *in vitro* combination treatments involving olaparib plus OA-NO₂ and talazoparib plus OA-NO₂ (Fig 26A, B). Increasing concentrations of either vehicle (OA) or OA-NO₂ were tested against increasing concentrations of olaparib and talazoparib. Next, synergism was evaluated using a median-drug effect analysis method. Combination indices (CI) were calculated from growth inhibition curves. The software Calcsyn was used to calculate CI to find out whether a combination was synergistic, additive or antagonistic. Talazoparib in combination with OA-NO₂ displayed greater synergistic growth inhibition of MM231 TNBC cells compared to olaparib (Fig 26C).

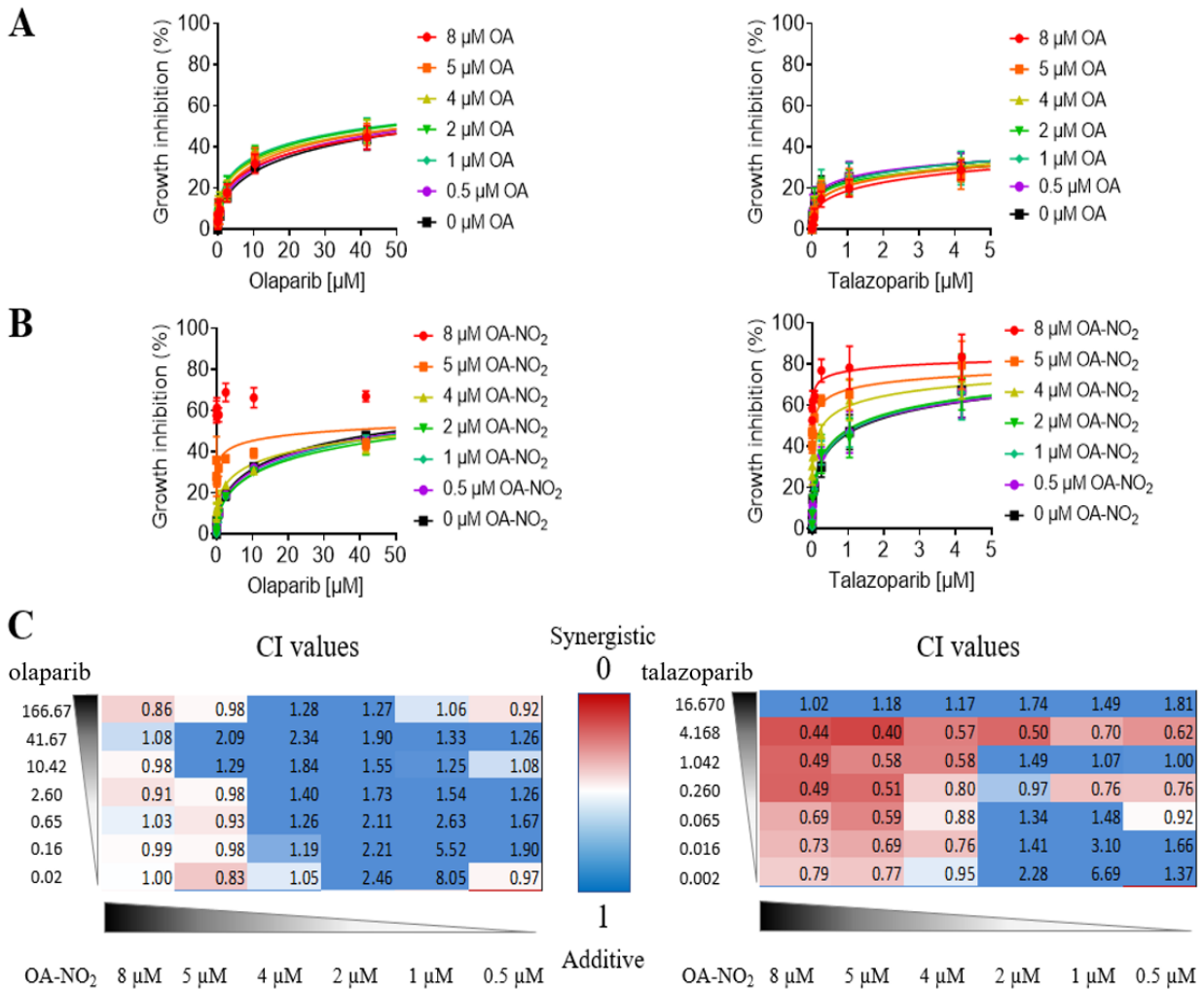


Figure 25. Synergistic growth inhibition of MDA-MB-231 (MM231) cells is obtained when talazoparib is combined with OA-NO₂.

MM231 cells were treated with increasing concentrations of control (A) OA or (B) OA-NO₂ and relative growth was measured by quantifying luminescent ATP levels (CellTiter-Glo). Error bars indicate SEM SEM, n=3. (C) Calcsyn software was used to calculate Chou-Talalay's Combination Indices in order to to compare synergistic outcomes of talazoparib and olaparib. Red indicates synergism.

6.2 Talazoparib in Combination with OA-NO₂ Reduces Relative Tumor Growth *in vivo*

Next, the efficacy of talazoparib plus OA-NO₂ was evaluated *in vivo* using a xenograft mouse model. In previous pre-clinical TNBC xenograft mouse models, talazoparib has been successfully demonstrated to be efficacious at the concentration of 0.3 mg/kg [186, 187]. This concentration was chosen for the combination *in vivo* study. 15 mg/kg OA-NO₂ was chosen based on previous favorable tumor growth inhibition experiments with no adverse side effects. MDA-MD-231 cells were implanted into the mammary gland of mice and when tumors reached a volume of 50 mm³, mice were treated with 15 mg/kg OA or 15 mg/kg OA-NO₂ in tricapylin plus vehicle (5% DMSO, 35% PEG, 65% saline) or 0.3 mg/kg talazoparib for 4 weeks when tumors reached a volume of 50 mm³. (Fig. 27A). Mice treated with talazoparib plus OA-NO₂ had significantly decreased tumor growth rates when compared to vehicle, PARPi or OA-NO₂ *in vivo* (Fig. 27B).

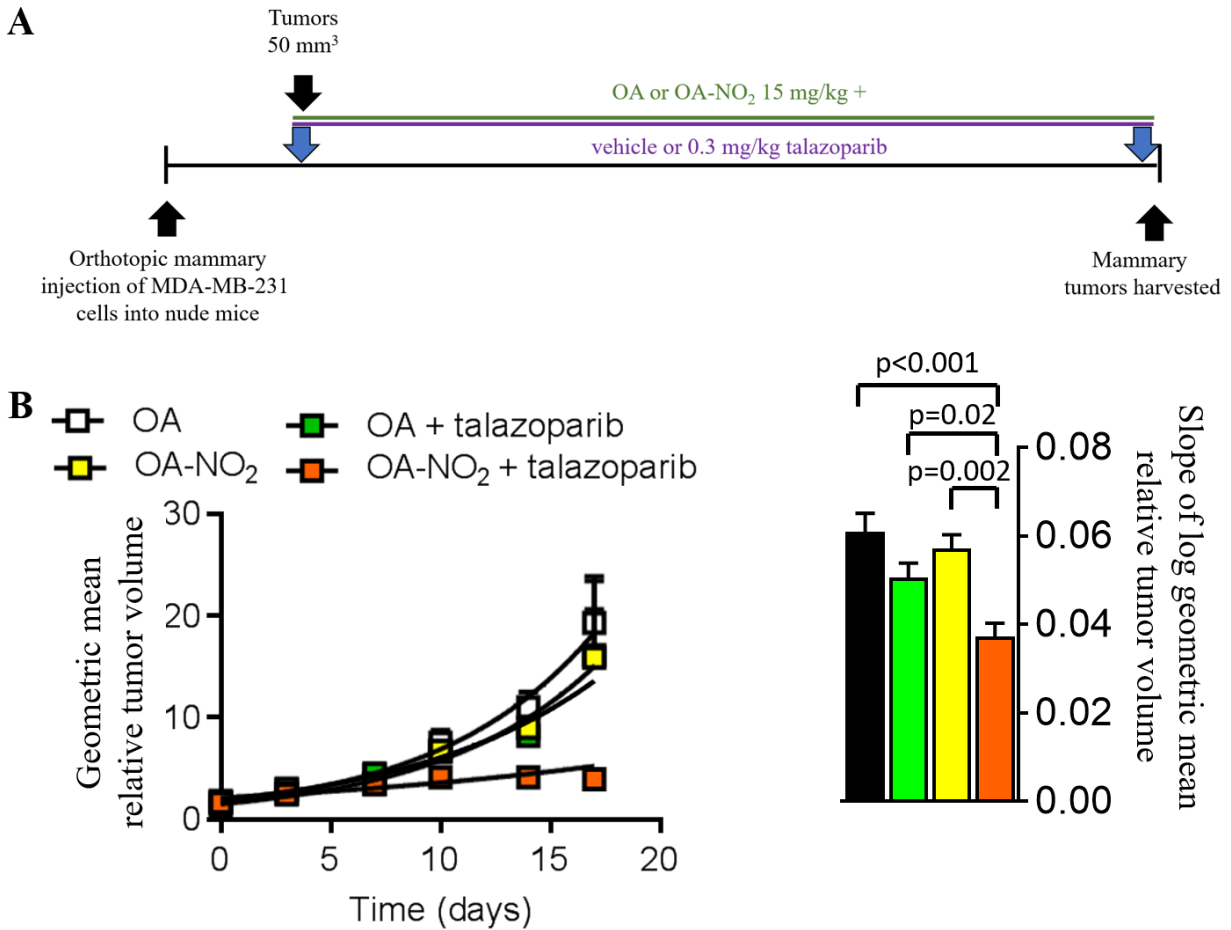


Figure 26. Talazoparib in combination with OA-NO₂ reduces relative tumor growth compared to vehicle, PARPi or OA-NO₂ *in vivo*.

(A) MDA-MB-231 (MM231) cells (10^6) were orthotopically injected into 6-week-old mice and gavaged with 15 mg/kg OA or 15 mg/kg OA-NO₂ in tricapylin plus vehicle (5% DMSO, 35% PEG, 65% saline) or 0.3 mg/kg talazoparib every day for 4 weeks when tumors reached a volume of 50 mm³. (n = 7 per group). (B) Multi-variant comparison that uses all the data points to compare curves. On the right, the curves are log transform to compare the slopes.

6.3 Discussion

PARPi as a targeted therapy is now approved for BRCA-mutated metastatic breast cancer with the notion that their tumors have defective HR pathways. However, there are several mechanisms whereby BRCA-mutant cells overcome this deficiency and acquire resistance to PARPi. Elevated RAD51 levels in TNBC cells lose their sensitivity to PARPi [188]. This provides a rationale for targeting other HR components in combination with PARPi, that may confer sensitivity to HR-proficient TNBC cells to PARPi. OA-NO₂, a potent RAD51 inhibitor, is combined with PARPi to test this hypothesis.

Due to talazoparib being more specific and potent than olaparib, OA-NO₂ plus olaparib was compared to OA-NO₂ plus talazoparib *in vitro*. OA-NO₂ sensitized HR-proficient TNBC cell lines to both PARPi drugs olaparib and talazoparib (Fig 26B). This suggests that the BRCAness phenotype induced by OA-NO₂ via inhibition of HR is a viable strategy to target HR-proficient TNBC cells. Additionally, talazoparib in combination with OA-NO₂ displayed higher levels of synergistic growth inhibition of MM231 TNBC cells compared to olaparib (Fig 26C). Using chemicals in *in vivo* studies often pose toxicity risks. Biological effects seen in *in vitro* studies were tested in an *in vivo* setting. There were no toxicities induced by OA-NO₂ treatment given to mice during the combinational therapy experiment involving OA-NO₂ and talazoparib. Mice treated with talazoparib plus OA-NO₂ had significantly decreased tumor growth rates when compared to vehicle, PARPi or OA-NO₂ *in vivo* (Fig. 27B). These results suggest that OA-NO₂ can induce BRCAness in the *in vivo* setting to HR-proficient TNBC mice tumors to sensitize them to PARPi. Of note, the clinical administration of intravenous and oral formulations of OA-NO₂ (IV IND, 122583; oral IND, 124524) is safe, having cleared multiple Phase I and drug-drug

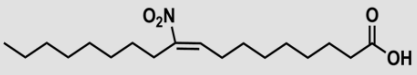
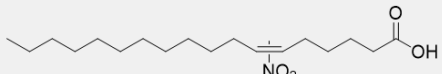
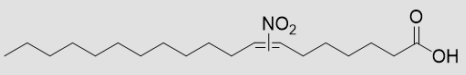
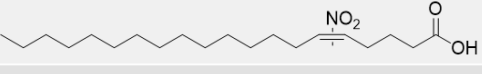
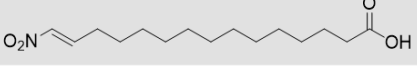
interaction studies, with an oral formulation now in multi-center Phase II trials for treating chronic inflammatory-related diseases.

7.0 Testing Other Nitro-Fatty Acid Derivatives

7.1 Identifying Other Nitroalkenes to be Investigated

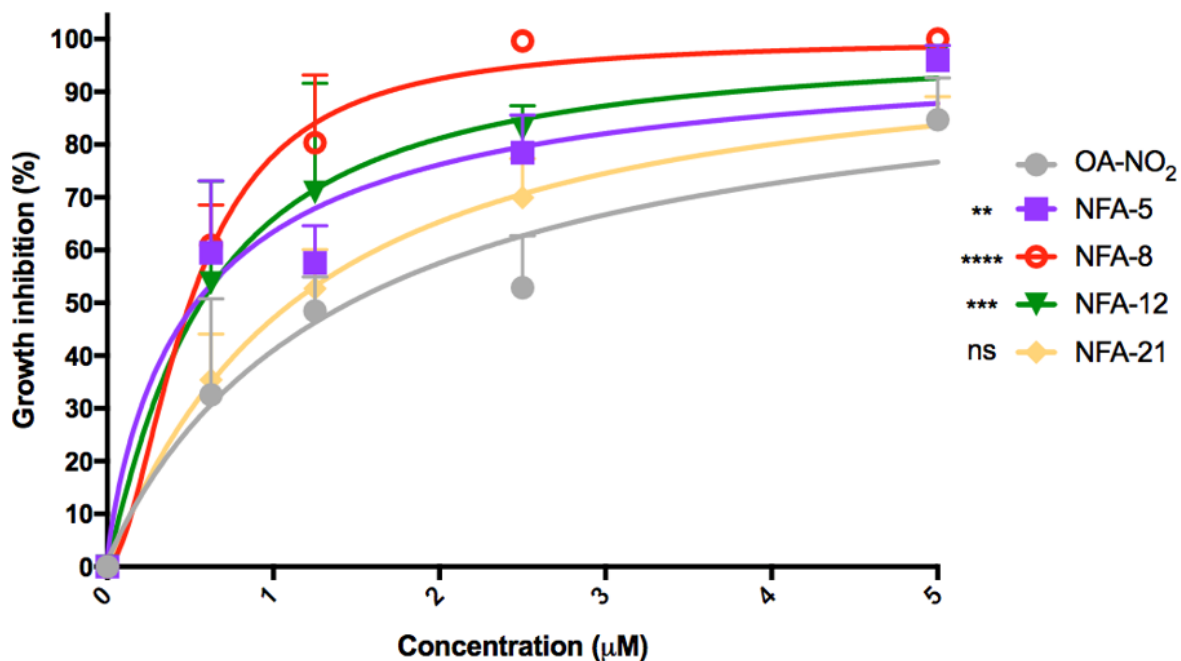
OA-NO₂ is electrophilic in nature due to the nitro group (-NO₂) on its double bond that is between C9 and C10. Therefore, the Michael reaction that takes place between the electrophilic carbon and biological nucleophiles such as thiols is 10 carbons away from the carboxyl group. In collaboration with computational biologists from the University of Pittsburgh, the RAD51 crystal structure was analyzed to investigate how well the OA-NO₂ fits into the pocket where C319 is located. It was hypothesized that a nitro-fatty acid (FA-NO₂) where the double bond is positioned closer to the carboxylate should yield a more rigid binding to the RAD51 monomer. A library of 22 unique alkyl nitroalkenes, where the nitroalkene substituent is positioned at varying positions along an acyl chain was screened, with 4 candidate derivatives were selected: 3 having double bonds positioned closer to the carboxylate and 1 having its double bond farther away from C10 (Table 3). It was hypothesized that NFA12, NFA8 and NFA5 having their double bonds at C5, C7 and C8 respectively would be more potent RAD51 inhibitors whereas NFA21 with the nitroalkene at C14 would be a less potent inhibitor of RAD51 as compared to OA-NO₂.

Table 3. Chemical structures of additional electrophilic nitro-fatty acid derivatives tested against TNBC cells.

Lipid ID	Lipid Name	Lipid Structure
OA-NO ₂	10-nitrooctadec-9-enoic acid	
NFA5	6/7-nitro-octadec-6-enoic acid	
NFA8	7/8-nitro-nonadec-7-enoic acid	
NFA12	5/6-nitro-eicos-5-enoic acid	
NFA21	14-nitro-pentadec-14-enoic acid	

7.2 The Effects of Nitroalkene Derivatives on TNBC Cell Growth

The impact of nitroalkene derivatives that have the electrophilic nitroalkene at different positions along an acyl was investigated for an ability to inhibit cell proliferation of the TNBC cell line MDA-MB-231. Increasing concentrations of OA-NO₂ were compared to increasing concentrations of NFA5, NFA8, NFA12 and NFA21 in a clonogenic assay where OA was the negative control. NFA5, NFA8, and NFA12 (IC₅₀ values 0.55 μM, 0.49 μM, 0.58 μM respectively) enhanced breast cancer cell death more potently than OA-NO₂ (IC₅₀ value of 1.5 μM). In contrast, there was not a significant difference in potency of cell growth inhibition between NFA21 (IC₅₀ value of 1.12 μM) and OA-NO₂. Compared with OA-NO₂, These results suggest that if the electrophilic carbon is positioned vicinal to the carboxylate, nitroalkenes become more potent inhibitors of TNBC cell growth.



	OA-NO ₂	NFA-5	NFA-8	NFA-12	NFA-21
IC50 (μM)	1.50	0.55	0.49	0.58	1.12

Figure 27. Clonogenic outgrowth comparison of MM231 cells treated with increasing concentrations of nitro-fatty acid derivatives.

(A) Increasing concentrations of OA-NO₂, NFA-5, NFA-8, NFA-12 and NFA-21 decrease clonogenic survival of TNBC cells. MM231 cells were treated with 0 to 5 μM nitroalkenes every day for 10 days and compared with each other. IC50 values indicate average + SEM, n=3.

7.3 The Effects of Nitroalkene Derivatives on HR Efficiency

NO₂-FA effects on HR DNA repair was investigated by utilizing a DR-GFP reporter assay. This analysis quantifies intracellular recombination of an integrated cDNA cassette of two tandem non-fluorescent GFP constructs following introduction of an I-SceI cleavage to the system by measuring the fluorescent GFP protein that is produced following successful recombination [152]. Daily 1 μM NFA8 treatment of U2OS cells harboring the DR-GFP construct revealed that after I-SceI transfection, the number of GFP positive cells was decreased by 5-fold when compared to 1 μM OA-NO₂ after 48 hours (Fig. 29A-B). The concentration of 1 μM was picked due to the toxicity of the NFA8 to cells at higher concentrations.

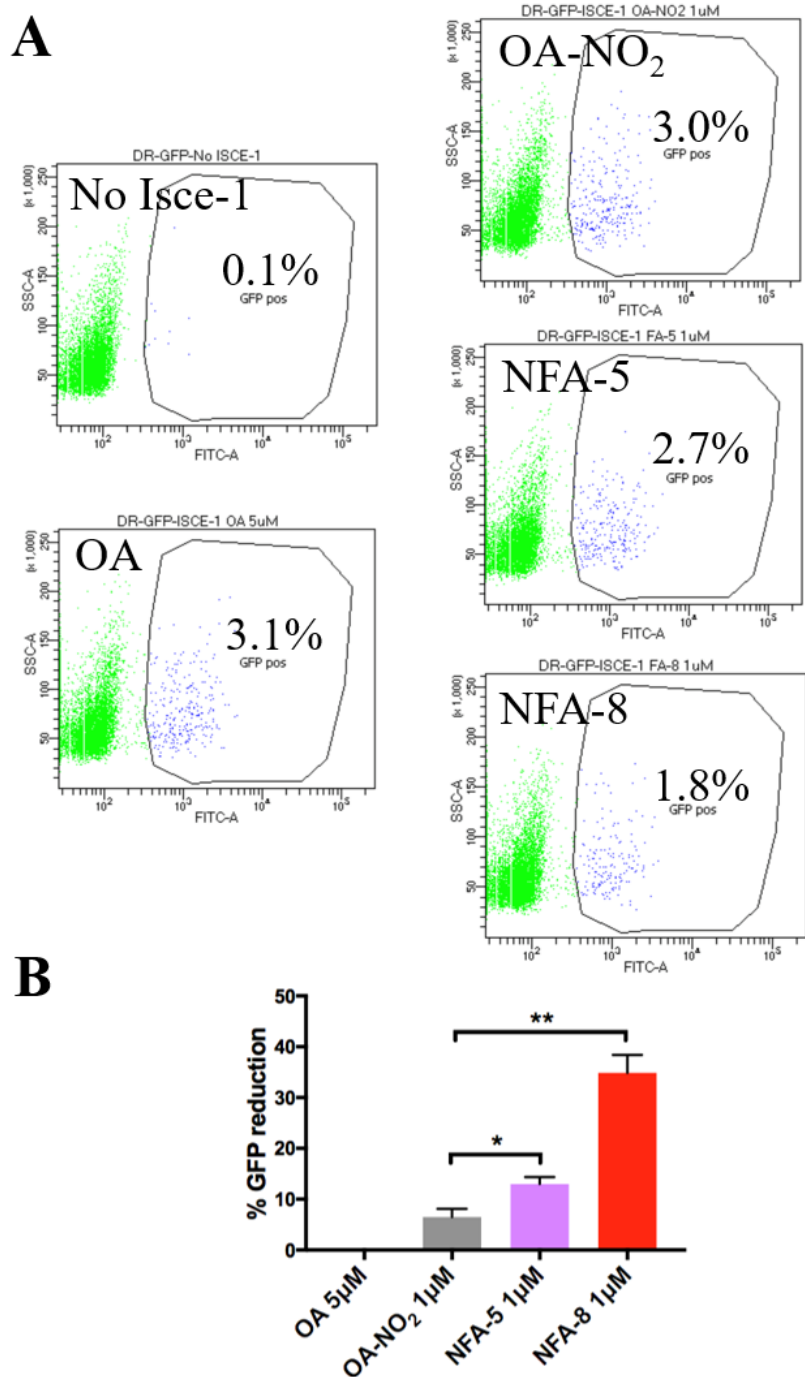


Figure 28. HR inhibition by NFA-8 and NFA-5 are compared to HR inhibition by OA-NO₂.

(A-B) U2OS cells containing the HR reporter construct DR-GFP were transfected with an I-SceI plasmid and treated with vehicle (black), 5 μ M OA (green) or 5 μ M OA-NO₂ (red). Negative control cells did not have I-SceI present. Values indicate average and error bars represent SEM, n \geq 3. The number of GFP positive cells were detected by flow cytometry at 48 h.

7.4 Discussion

Most small molecule inhibitors that are developed pre-clinically fail in the clinic for two reasons. They either do not work or they are too toxic at the doses required for them to be administered. Therefore, it is critical to test structurally similar drugs in the pre-clinical setting to identify potentially more potent and specific inhibitors of druggable targets. This study shows that as the electrophilic carbon gets closer to the carboxyl group, the potency at which the FA-NO₂ derivatives inhibit TNBC cell growth increases. This can also be described as the derivatives that have a longer acyl chain between the electrophilic nitroalkene and the omega terminus of the fatty acid are more potent inhibitors of TNBC cell growth. The clonogenic assay results correlate with the DR-GFP assay results where the same nitroalkenes were able to inhibit HR efficiency at greater potencies than the ones that had their electrophilic carbon closer to the omega end of the fatty acids. These favorable results could be due to the omega end acyl chains' ability to stabilize the nitroalkenes' binding on their nucleophile targets such as the RAD51 C319. These results suggest that the location of the electrophilic carbon on a fatty acid in respect to how far they are from the carboxylate as well as the omega terminus affect an ability to interact with their targets. Knowing the pleiotropic nature of these compounds, this opens a new venue for developing drugs to favor targets of interest within the cell. For example, OA-NO₂ induces angiogenesis under hypoxic conditions via upregulation of HIF-1 α [189]. This would not be a preferable off-target effect in the cancer setting. Therefore, it would be useful to test compound NFA-8 and other derivatives' specificity on targets such as HIF-1 α to test if the modifications introduced to OA-NO₂ favor cancer treatment settings.

8.0 Conclusions and Future Directions

8.1 Conclusions

Breast cancer is the most common type of cancer in females [190]. TNBC, generally defined by tumors lacking expression of estrogen receptor (ER), progesterone receptor (PR) accounting for 15-20% of all breast cancers [109]. In contrast to other subtypes, there is a lack of approved targeted therapy available in TNBC treatment leaving systemic chemotherapy as the first line of therapy. Most TNBC patients ultimately develop resistance to chemotherapy which results in worse clinical outcomes and more aggressive tumor behavior compared to other subtypes [191, 192]. There is an urgent need for novel approaches to treating TNBC. A viable option is to discover drugs that can confer sensitization to the currently used DNA damaging therapeutics.

There has been recent progress in developing targeted therapies for TNBC. One such approach is targeting PARP1 [193]. It has been found that ~20% of TNBC tumors have either a germline or somatic BRCA mutation which is the subset of patients hypothesized to have sensitivity to PARP inhibitors [115]. In addition to BRCA mutants, tumors with defects in other components of the HR pathway have been described to have the “BRCAness” phenotype that can also respond to PARP inhibition [194]. This led to the development of the idea of a “pharmacologically induced” BRCAness phenotype in HR-proficient tumors using novel therapeutics [195].

Fatty acid nitroalkenes are endogenously produced products of nitric oxide- and nitrite-dependent nitration of unsaturated fatty acids. By virtue of kinetically rapid and reversible Michael addition, fatty acid nitroalkenes will mediate the PTM of susceptible cysteine residues of proteins,

in some cases modifying protein function and inducing signaling responses via pleiotropic mechanisms [139, 140, 148, 196]. This dissertation discusses the potential of the nitroalkene OA-NO₂ as a drug to pharmacologically induce BRCAness in HR-positive, BRCA wildtype TNBC to confer sensitivity to PARP inhibition.

In Chapter 3, the impact of OA-NO₂ on the proliferation of TNBC cells was evaluated as both a single agent and when in combination with DNA-targeted cancer therapies. In an orthotopic xenograft mouse model, OA-NO₂ reduced tumor growth and induced γ H2AX staining indicating DNA damaging capabilities. *In vitro*, OA-NO₂ was co-administered with clinically-relevant DNA-directed therapeutics doxorubicin, cisplatin or olaparib conferring sensitivity in three TNBC cell lines MM231, BT549 and Hs578T in an ATP based 3-day cell survival assay. Furthermore, OA-NO₂ sensitized MM231 cells to IR therapy that was shown by both increased γ H2AX staining and by inhibiting cell proliferation in a clonogenic outgrowth assay. In aggregate, OA-NO₂ displayed reduced TNBC tumor cell growth, induced DNA damage via γ H2AX and inhibited cell proliferation in vitro of three TNBC cell lines in combination with DNA-targeting therapies doxorubicin, cisplatin, olaparib or IR.

In Chapter 4, the impact of OA-NO₂ on DSB repair pathways was explored. Based on fluorescent based cell reporter assays evaluating DNA repair, OA-NO₂ was shown to inhibit post DNA resection DSB repair pathways HR, SSA, and alt-EJ but not NHEJ. These results reveal that OA-NO₂ is a viable candidate for inducing BRCAness in HR-proficient TNBC cells.

In Chapter 5, the mechanism by which OA-NO₂ blocks HR was explored. RAD51, being the central recombinase protein for HR and having a previously identified cysteine with a functional role was tested. Indeed, TNBC cells that were treated with IR to induce RAD51 foci using RAD51 immunofluorescence. This recruitment of IR mediated RAD51 foci was inhibited

by co-treatment with OA-NO₂. This led to DR-GFP reporter assay studies where overexpression of RAD51 in U2OS cells partially rescued HR inhibitory effects of OA-NO₂. Next, OA-NO₂ interaction with human RAD1 protein was shown via affinity-precipitation of RAD51 by biotin-OA-NO₂ in 293T cells and subsequently in TNBC cells MM231 and MM468. By showing no reactions of non-electrophilic control biotinylated OA or SA-NO₂, it was deduced that the electrophilic nature of this fatty acid nitroalkene was required for RAD51 binding. This interaction was Cys319 specific due to abrogation of this interaction in C319S mutant RAD51 protein but not with C312S mutant RAD51 protein. Furthermore, the impact of OA-NO₂ on RAD51 and ssDNA binding was evaluated using an FP based assay. With increasing concentrations of OA-NO₂, relative polarization signal was reduced in the reaction mix containing Alexa 488 ssDNA and human RAD51 protein, indicating inhibitory effect of OA-NO₂ on RAD51 DNA binding *in vitro*. Taken together, these results provide evidence that the inhibition of RAD51 is achieved by OA-NO₂ through direct physical interaction between RAD51 C319 residue and OA-NO₂ to repress the HR pathway.

In chapter 6, the effects of combination treatments of OA-NO₂ with PARP inhibitors were explored both *in vitro* and *in vivo*. In an *in vitro* ATP-based cell survival assay, talazoparib in combination with OA-NO₂ displayed higher levels of synergistic growth inhibition of MM231 compared to olaparib. In an orthotopic mouse xenograft model where TNBC cell line MM231 was used, talazoparib in combination with OA-NO₂ reduced relative tumor growth compared to vehicle, PARPi or OA-NO₂ *in vivo*.

In chapter 7 of this dissertation, the effects of nitroalkene substituents at different positions along the fatty acid chain were investigated for an ability to inhibit TNBC cell growth and HR efficiency. The derivatives that had the electrophilic carbon closer to the carboxylate, NFA5,

NFA8 and NFA12, had lower IC50 values compared to OA-NO₂ whereas the nitroalkene derivative NFA21 that had the electrophilic carbon at the omega end of the fatty acid had an IC50 value comparable to the IC50 value of OA-NO₂. In addition, the degree of HR efficiency inhibition by NFA8 was 5-fold higher compared to OA-NO₂ in U2OS cells.

Even though PARPi is a promising therapeutic approach for breast cancer patients, there are important limitations. First, only a small subset of patients benefit from this treatment, the ones that have BRCA mutations. Second, patients reportedly acquire resistant mechanisms such as elevated RAD51 levels, acquiring genetic reversion of BRCA1 and BRCA2, and inactivating the p53-binding protein 1 (53BP1). These resistance mechanisms converge on re-establishing functional HR, often identified with formation of RAD51 foci. Additionally, usage of high concentrations of PARPi as a monotherapy can be limited by toxicities and prevent maximal clinical benefit [197]. In summary, this dissertation provides a basis for OA-NO₂ use to pharmacologically induce BRCAness, thus representing a viable treatment strategy for all TNBC patients who are HR-proficient either inherently or through resistance mechanisms.

8.2 Future Directions

When it comes to DSB repair, OA-NO₂ does not only inhibit HR, it also inhibits SSA and alt-EJ but has no effect on NHEJ. Interestingly, SSA increases in cells where RAD51 is mutated or knocked down [198, 199]. In addition, RAD51 protein is not required for SSA pathway where RAD52 is the central protein [200]. This suggests that the inhibition of SSA by OA-NO₂ is through an interaction independent of RAD51. Since OA-NO₂ only inhibits post-resection DSB repair pathways, additional possible targets of OA-NO₂ are downstream of DSB resection. Future

experiments should include defining DNA repair proteins targeted by nitroalkenes, via mass spectrometry (MS) analysis of TNBC cell protein adducts with nitroalkenes (Appendix A). Additionally, immunofluorescence experiments are underway to identify whether RAD51 and its inhibition has an impact on nuclear localization of DSB repair proteins such as 53BP1, BRCA1, BRCA2, CtIP, XPF and NBS1.

For future *in vivo* studies, rather than only using the caliper tool to measure tumor volume, the IVIS Spectrum *in vivo* imaging system should be used to perform bioluminescence imaging for measuring tumor volume and monitor disease progression. TNBC cell lines with luciferase transfection can then be used to distinguish bioluminescence. One of the advantages of using bioluminescent imaging for tumor growth is that the treatment can start at an earlier time point therefore being potentially more effective and more clinically relevant. With caliper measurements, tumors must be at least 50 mm³ for precise measurements. Additionally, OA-NO₂ plus PARPi should be investigated in additional *in vivo* mouse models with attention to dose-response relationships. Patient-derived xenografts (PDX) can have additional and more applicable results for the clinic. As opposed to cell lines such as MDA-MB-231 that were utilized in the xenograft model, PDX models have tumors that are derived from primary human tumors and represent many important features of the human disease such as growth kinetics, therapy responses and metastatic capabilities [201, 202]. Specifically, tumors with known HR defects such as lack of RAD51 foci should be used in addition to HR-proficient tumors in these PDX studies and their sensitivity to OA-NO₂ will be compared to acquire additional pre-clinical results [203].

Finally, OA-NO₂ and its combinatorial therapeutic effects with PARPi are currently being evaluated for ovarian cancer. PARP inhibitors olaparib and rucaparib acquired Food and Drug Administration (FDA) approvals for treatment of BRCA-associated ovarian cancer in 2014 and

2016, respectively [204-207]. Additionally, niraparib, olaparib and rucaparib have received FDA approval as maintenance therapy post-platinum-base chemotherapy [208-214]. Although PARPi is gaining significant traction for ovarian cancer therapy, about 50% of the patients are insensitive due to resistance mechanisms heightening the need for additional interventions [215]. OA-NO₂ in combination with PARPi is thus a promising therapeutic solution for PARPi insensitive ovarian cancer patients.

Appendix – List of Potential OA-NO₂ Targets in DNA Repair Pathways

	Pathway	Protein	UniProtKB identifier	Length	Mass (Da)
1	NHEJ	RIF1	Q5UIP0-1	2472	274466
2		53BP1	Q12888-1	1972	213574
3		XRCC6	P12956-1	609	69843
4		XRCC5	P13010-1	732	82705
5		PRKDC	P78527-1	4128	469089
6		DNALI4	P49917-1	911	103971
7		XRCC4	Q13426-1	336	38287
8		NHEJ1	Q9H9Q4-1	299	33337
9		DCR1C	Q96SD1-1	692	78436
10		POLL	Q9UGP5-1	575	63482
11		POLM	Q9NP87-1	494	54816
12		DNTT	P04053-1	509	58536
13	HR	RAD50	Q92878-1	1,312	153,892
14		MRE11	P49959-1	708	80,593
15		NBS1	O60934-1	754	84,959
16		ATM	Q13315-1	3056	350687
17		TOPBP1	Q92547-1	1522	170679
18		BRIP1	Q9BX63-1	1249	140867
19		BRCA1	P48754-1	1,812	198,795
20		BARD1	Q99728-1	777	86,448
21		CtIP	Q99708-1	897	101,942
22		USP4	Q13107-1	963	108,565
23		ABRX1	Q6UWZ7-1	409	46663
24		UIMC1	Q96RL1-1	719	79727
25		BABA1	Q9NWX8-1	329	36560
26		BABA2	Q9NXR7-2	383	43552
27		BRCC3	P46736-1	316	36072
28		PALB2	Q86YC2-1	1186	131295
29		BRCA2	P51587-1	3418	384202
30		SEM1	P60896-1	70	8278
31		SYCP3	Q8IZU3-1	236	27729
32		RPA1	P27694-1	616	68138
33		RPA2	P15927-1	270	29247

	Pathway	Protein	UniProtKB identifier	Length	Mass (Da)
34		RPA3	P35244-1	121	13569
35		RAD51	Q06609-1	339	36966
36		RAD52	P43351-1	418	46169
37		RAD51B	O15315-3	384	42196
38		RAD51C	O43502-1	376	42190
39		RAD51D	O75771-1	328	35049
40		XRCC2	O43543-1	280	31956
41		XRCC3	O43542-1	346	37850
42		RAD54	Q92698-1	747	84352
43		EXO1	Q9UQ84-1	846	94,103
44		DNA2	P51530-1	1,060	120,415
45		BLM	P54132-1	1,417	159,000
46		XRCC1	P18887-1	633	69477
47		DNLI3	P49916-1	1009	112907
48		ERCC1	P07992-1	297	32562
49		XPF	Q92889-1	916	104486
50		TOP3	Q13472-1	1001	112372
51		MUS81	Q96NY9-1	551	61173
52		EME1	Q96AY2-1	570	63252
53		POLD1	P28340-1	1107	123631
54		POLD2	P49005-1	469	51289
55		POLD3	Q15054-1	466	51400
56		POLD4	Q9HCU8-1	107	12433
57		SMARCAD1	Q9H4L7-1	1026	117402
58		SRCAP	Q6ZRS2-1	3230	343555
59		USP11	P51784-1	963	109817
60		RAD54B	Q9Y620-1	910	102967
61		RMI1	Q9H9A7-1	625	70144
62		RMI2	Q96E14-1	147	15865
63		RECQ5	O94762-1	991	108858
64		RTEL1	Q9NZ71-1	1219	133683
65		GEN1	Q17RS7-1	908	102884
66		SLX1	Q9BQ83-1	275	30771

	Pathway	Protein	UniProtKB identifier	Length	Mass (Da)
67		SLX4	Q8IY92-1	1834	200012
68		PARI	Q9NWS1-1	579	65054
69		FBH1	Q8NFX0-1	1043	117686
70		FANCM	Q8IYD8-1	2048	232191
71		FANCD2	Q9BXW9-2	1451	164128
72		RECQ1	P46063-1	649	73457
73		WRN	Q14191-1	1432	162461
74		MDC1	Q14676-1	2089	226666
75		RNF8	O76064-1	485	55518
76		RNF168	Q8IYW5-1	571	65020
77		CHK2	O96017-1	543	60915
78		ATR	Q13535-1	2644	301367
79		CHK1	O14757-1	476	54434
80		CLASPIN	Q9HAW4-1	1339	151094
81		ATRIP	Q8WXE1-1	791	85838
82		RAD17	O75943-1	681	77055
83		RFC2	P35250-1	354	39157
84		RFC5	P40937-1	340	38497
85		RAD9	Q99638-1	391	42547
86		HUS1	O60921-1	280	31691
87		RAD1	O60671-1	282	31827
88		P53	P04637-1	393	43653
89		RHNO1	Q9BSD3-1	238	26709
90		WEE1	P30291-1	646	71597
91		GADD45	P24522-1	165	18336
92	BER	APE1	P27695-1	318	35555
93		PARP1	P09874-1	1014	113084
94		LIG1	P18858-1	919	101736
95		LIG3	P49916-1	1009	112907
96		FEN1	P39748-1	380	42593
97		PCNA	P12004-1	261	28769
98		APE2	Q9UBZ4-1	518	57401
99		POLB	P06746-1	335	38178

	Pathway	Protein	UniProtKB identifier	Length	Mass (Da)
100		POLE	Q07864-1	2286	261518
101		UNG	P13051-1	313	34645
102		MUTYH	Q9UIF7-1	546	60069
103		SMUG1	Q53HV7-1	270	29862
104		MPG	P29372-1	298	32869
105		MBD4	O95243-1	580	66051
106		TDG	Q13569-1	410	46053
107	MMR	MSH2	P43246-1	934	104743
108		MSH3	P20585-1	1137	127412
109		MSH6	P52701-1	1360	152786
110		MLH1	P40692-1	756	84601
111		PMS2	P54278-1	862	95797
112		MLH3	Q9UHC1-1	1453	163711
113		RFC1	P35251-1	1148	128255
114		PMS1	P54277-1	932	105830
115	NER	XPB	P19447-1	782	89278
116		XPD	P18074-1	760	86909
117		XPA	P23025-1	273	31368
118		XPC	Q01831-1	940	105953
119		RAD23B	P54727-1	409	43171
120		CSA	Q13216-1	396	44055
121		CSB	Q03468-1	1493	168416
122		XPG	P28715-1	1186	133108
123		RBX1	P62877-1	108	12274
124		CUL4A	Q13619-1	759	87680
125		DDB1	Q16531-1	1140	126968
126		DDB2	Q92466-1	427	47864
127		CETN2	P41208-1	172	19738
128		CDK7	P50613-1	346	39038
129		MNAT1	P51948-1	309	35823
130		CCNH	P51946-1	323	37643
131		TTDA	Q6ZYL4-1	71	8053

Bibliography

1. Curtin, N.J., *DNA repair dysregulation from cancer driver to therapeutic target*. Nat Rev Cancer, 2012. **12**(12): p. 801-17.
2. Kaina, B., et al., *MGMT: key node in the battle against genotoxicity, carcinogenicity and apoptosis induced by alkylating agents*. DNA Repair (Amst), 2007. **6**(8): p. 1079-99.
3. Fleck, O. and O. Nielsen, *DNA repair*. J Cell Sci, 2004. **117**(Pt 4): p. 515-7.
4. Luo, M., et al., *Redox regulation of DNA repair: implications for human health and cancer therapeutic development*. Antioxid Redox Signal, 2010. **12**(11): p. 1247-69.
5. Sancar, A., et al., *Molecular mechanisms of mammalian DNA repair and the DNA damage checkpoints*. Annu Rev Biochem, 2004. **73**: p. 39-85.
6. Bai, P., *Biology of Poly(ADP-Ribose) Polymerases: The Factotums of Cell Maintenance*. Mol Cell, 2015. **58**(6): p. 947-58.
7. Burkle, A., *Poly(ADP-ribosyl)ation, a DNA damage-driven protein modification and regulator of genomic instability*. Cancer Lett, 2001. **163**(1): p. 1-5.
8. Guarne, A. and J.B. Charbonnier, *Insights from a decade of biophysical studies on MutL: Roles in strand discrimination and mismatch removal*. Prog Biophys Mol Biol, 2015. **117**(2-3): p. 149-156.
9. Martin, S.A., C.J. Lord, and A. Ashworth, *Therapeutic targeting of the DNA mismatch repair pathway*. Clin Cancer Res, 2010. **16**(21): p. 5107-13.
10. Costa, R.M., et al., *The eukaryotic nucleotide excision repair pathway*. Biochimie, 2003. **85**(11): p. 1083-99.
11. Shuck, S.C., E.A. Short, and J.J. Turchi, *Eukaryotic nucleotide excision repair: from understanding mechanisms to influencing biology*. Cell Res, 2008. **18**(1): p. 64-72.
12. Dip, R., U. Camenisch, and H. Naegeli, *Mechanisms of DNA damage recognition and strand discrimination in human nucleotide excision repair*. DNA Repair (Amst), 2004. **3**(11): p. 1409-23.
13. Latimer, J.J., et al., *Nucleotide excision repair deficiency is intrinsic in sporadic stage I breast cancer*. Proc Natl Acad Sci U S A, 2010. **107**(50): p. 21725-30.
14. Mechanic, L.E., et al., *Polymorphisms in nucleotide excision repair genes, smoking and breast cancer in African Americans and whites: a population-based case-control study*. Carcinogenesis, 2006. **27**(7): p. 1377-85.

15. Aparicio, T., R. Baer, and J. Gautier, *DNA double-strand break repair pathway choice and cancer*. DNA Repair (Amst), 2014. **19**: p. 169-75.
16. Helleday, T., et al., *DNA double-strand break repair: from mechanistic understanding to cancer treatment*. DNA Repair (Amst), 2007. **6**(7): p. 923-35.
17. Hoeijmakers, J.H., *DNA damage, aging, and cancer*. N Engl J Med, 2009. **361**(15): p. 1475-85.
18. Chen, J. and J. Stubbe, *Bleomycins: towards better therapeutics*. Nat Rev Cancer, 2005. **5**(2): p. 102-12.
19. Dasari, S. and P.B. Tchounwou, *Cisplatin in cancer therapy: molecular mechanisms of action*. Eur J Pharmacol, 2014. **740**: p. 364-78.
20. Thompson, L.H., *Recognition, signaling, and repair of DNA double-strand breaks produced by ionizing radiation in mammalian cells: the molecular choreography*. Mutat Res, 2012. **751**(2): p. 158-246.
21. Su, T.T., *Cellular responses to DNA damage: one signal, multiple choices*. Annu Rev Genet, 2006. **40**: p. 187-208.
22. Kim, J.S., et al., *Independent and sequential recruitment of NHEJ and HR factors to DNA damage sites in mammalian cells*. J Cell Biol, 2005. **170**(3): p. 341-7.
23. Bakkenist, C.J. and M.B. Kastan, *DNA damage activates ATM through intermolecular autophosphorylation and dimer dissociation*. Nature, 2003. **421**(6922): p. 499-506.
24. Georgoulis, A., et al., *Genome Instability and gammaH2AX*. Int J Mol Sci, 2017. **18**(9).
25. Moynahan, M.E. and M. Jasin, *Mitotic homologous recombination maintains genomic stability and suppresses tumorigenesis*. Nat Rev Mol Cell Biol, 2010. **11**(3): p. 196-207.
26. Deriano, L. and D.B. Roth, *Modernizing the nonhomologous end-joining repertoire: alternative and classical NHEJ share the stage*. Annu Rev Genet, 2013. **47**: p. 433-55.
27. Cejka, P., *DNA End Resection: Nucleases Team Up with the Right Partners to Initiate Homologous Recombination*. J Biol Chem, 2015. **290**(38): p. 22931-8.
28. Buck, D., et al., *Cernunnos, a novel nonhomologous end-joining factor, is mutated in human immunodeficiency with microcephaly*. Cell, 2006. **124**(2): p. 287-99.
29. Kakarougkas, A. and P.A. Jeggo, *DNA DSB repair pathway choice: an orchestrated handover mechanism*. Br J Radiol, 2014. **87**(1035): p. 20130685.
30. Grundy, G.J., et al., *One ring to bring them all--the role of Ku in mammalian non-homologous end joining*. DNA Repair (Amst), 2014. **17**: p. 30-8.

31. Gottlieb, T.M. and S.P. Jackson, *The DNA-dependent protein kinase: requirement for DNA ends and association with Ku antigen*. Cell, 1993. **72**(1): p. 131-42.
32. Cary, R.B., et al., *DNA looping by Ku and the DNA-dependent protein kinase*. Proc Natl Acad Sci U S A, 1997. **94**(9): p. 4267-72.
33. Davis, A.J. and D.J. Chen, *DNA double strand break repair via non-homologous end-joining*. Transl Cancer Res, 2013. **2**(3): p. 130-143.
34. Leber, R., et al., *The XRCC4 gene product is a target for and interacts with the DNA-dependent protein kinase*. J Biol Chem, 1998. **273**(3): p. 1794-801.
35. Macheret, M. and T.D. Halazonetis, *DNA replication stress as a hallmark of cancer*. Annu Rev Pathol, 2015. **10**: p. 425-48.
36. Maher, R.L., A.M. Branagan, and S.W. Morrical, *Coordination of DNA replication and recombination activities in the maintenance of genome stability*. J Cell Biochem, 2011. **112**(10): p. 2672-82.
37. Panier, S. and S.J. Boulton, *Double-strand break repair: 53BP1 comes into focus*. Nat Rev Mol Cell Biol, 2014. **15**(1): p. 7-18.
38. Isono, M., et al., *BRCA1 Directs the Repair Pathway to Homologous Recombination by Promoting 53BP1 Dephosphorylation*. Cell Rep, 2017. **18**(2): p. 520-532.
39. Cannavo, E. and P. Cejka, *Sae2 promotes dsDNA endonuclease activity within Mre11-Rad50-Xrs2 to resect DNA breaks*. Nature, 2014. **514**(7520): p. 122-5.
40. Symington, L.S., *End resection at double-strand breaks: mechanism and regulation*. Cold Spring Harb Perspect Biol, 2014. **6**(8).
41. Ma, C.J., et al., *Protein dynamics of human RPA and RAD51 on ssDNA during assembly and disassembly of the RAD51 filament*. Nucleic Acids Res, 2017. **45**(2): p. 749-761.
42. Prakash, R., et al., *Homologous recombination and human health: the roles of BRCA1, BRCA2, and associated proteins*. Cold Spring Harb Perspect Biol, 2015. **7**(4): p. a016600.
43. Zhang, F., et al., *PALB2 functionally connects the breast cancer susceptibility proteins BRCA1 and BRCA2*. Mol Cancer Res, 2009. **7**(7): p. 1110-8.
44. Orthwein, A., et al., *A mechanism for the suppression of homologous recombination in G1 cells*. Nature, 2015. **528**(7582): p. 422-6.
45. Carreira, A. and S.C. Kowalczykowski, *Two classes of BRC repeats in BRCA2 promote RAD51 nucleoprotein filament function by distinct mechanisms*. Proc Natl Acad Sci U S A, 2011. **108**(26): p. 10448-53.

46. Esashi, F., et al., *CDK-dependent phosphorylation of BRCA2 as a regulatory mechanism for recombinational repair*. *Nature*, 2005. **434**(7033): p. 598-604.
47. Jensen, R.B., *BRCA2: one small step for DNA repair, one giant protein purified*. *Yale J Biol Med*, 2013. **86**(4): p. 479-89.
48. Godin, S.K., M.R. Sullivan, and K.A. Bernstein, *Novel insights into RAD51 activity and regulation during homologous recombination and DNA replication*. *Biochem Cell Biol*, 2016. **94**(5): p. 407-418.
49. Taylor, M.R.G., et al., *Rad51 Paralogs Remodel Pre-synaptic Rad51 Filaments to Stimulate Homologous Recombination*. *Cell*, 2015. **162**(2): p. 271-286.
50. Amunugama, R., J. Groden, and R. Fishel, *The HsRAD51B-HsRAD51C stabilizes the HsRAD51 nucleoprotein filament*. *DNA Repair (Amst)*, 2013. **12**(9): p. 723-32.
51. Ma, C.J., et al., *Human RAD52 interactions with replication protein A and the RAD51 presynaptic complex*. *J Biol Chem*, 2017. **292**(28): p. 11702-11713.
52. Feng, Z., et al., *Rad52 inactivation is synthetically lethal with BRCA2 deficiency*. *Proc Natl Acad Sci U S A*, 2011. **108**(2): p. 686-91.
53. Kadyk, L.C. and L.H. Hartwell, *Sister chromatids are preferred over homologs as substrates for recombinational repair in Saccharomyces cerevisiae*. *Genetics*, 1992. **132**(2): p. 387-402.
54. Morrical, S.W., *DNA-pairing and annealing processes in homologous recombination and homology-directed repair*. *Cold Spring Harb Perspect Biol*, 2015. **7**(2): p. a016444.
55. Heyer, W.D., K.T. Ehmsen, and J. Liu, *Regulation of homologous recombination in eukaryotes*. *Annu Rev Genet*, 2010. **44**: p. 113-39.
56. Sung, P., *Function of yeast Rad52 protein as a mediator between replication protein A and the Rad51 recombinase*. *J Biol Chem*, 1997. **272**(45): p. 28194-7.
57. Motycka, T.A., et al., *Physical and functional interaction between the XPF/ERCC1 endonuclease and hRad52*. *J Biol Chem*, 2004. **279**(14): p. 13634-9.
58. Bennardo, N., et al., *Alternative-NHEJ is a mechanistically distinct pathway of mammalian chromosome break repair*. *PLoS Genet*, 2008. **4**(6): p. e1000110.
59. Kojic, M., et al., *Compensatory role for Rad52 during recombinational repair in Ustilago maydis*. *Mol Microbiol*, 2008. **67**(5): p. 1156-68.
60. Lok, B.H., et al., *RAD52 inactivation is synthetically lethal with deficiencies in BRCA1 and PALB2 in addition to BRCA2 through RAD51-mediated homologous recombination*. *Oncogene*, 2013. **32**(30): p. 3552-8.

61. Bunting, S.F. and A. Nussenzweig, *End-joining, translocations and cancer*. Nat Rev Cancer, 2013. **13**(7): p. 443-54.
62. Mateos-Gomez, P.A., et al., *Mammalian polymerase theta promotes alternative NHEJ and suppresses recombination*. Nature, 2015. **518**(7538): p. 254-7.
63. Audebert, M., B. Salles, and P. Calsou, *Effect of double-strand break DNA sequence on the PARP-1 NHEJ pathway*. Biochem Biophys Res Commun, 2008. **369**(3): p. 982-8.
64. Ceccaldi, R., et al., *Homologous-recombination-deficient tumours are dependent on Poltheta-mediated repair*. Nature, 2015. **518**(7538): p. 258-62.
65. Hanahan, D. and R.A. Weinberg, *Hallmarks of cancer: the next generation*. Cell, 2011. **144**(5): p. 646-74.
66. Miki, Y., et al., *A strong candidate for the breast and ovarian cancer susceptibility gene BRCA1*. Science, 1994. **266**(5182): p. 66-71.
67. Wooster, R., et al., *Identification of the breast cancer susceptibility gene BRCA2*. Nature, 1995. **378**(6559): p. 789-92.
68. Couch, F.J., K.L. Nathanson, and K. Offit, *Two decades after BRCA: setting paradigms in personalized cancer care and prevention*. Science, 2014. **343**(6178): p. 1466-70.
69. Loveday, C., et al., *Germline mutations in RAD51D confer susceptibility to ovarian cancer*. Nat Genet, 2011. **43**(9): p. 879-882.
70. Meindl, A., et al., *Germline mutations in breast and ovarian cancer pedigrees establish RAD51C as a human cancer susceptibility gene*. Nat Genet, 2010. **42**(5): p. 410-4.
71. Turnbull, C. and N. Rahman, *Genetic predisposition to breast cancer: past, present, and future*. Annu Rev Genomics Hum Genet, 2008. **9**: p. 321-45.
72. Hottiger, M.O., et al., *Toward a unified nomenclature for mammalian ADP-ribosyltransferases*. Trends Biochem Sci, 2010. **35**(4): p. 208-19.
73. De Vos, M., V. Schreiber, and F. Dantzer, *The diverse roles and clinical relevance of PARPs in DNA damage repair: current state of the art*. Biochem Pharmacol, 2012. **84**(2): p. 137-46.
74. Harper, J.W. and S.J. Elledge, *The DNA damage response: ten years after*. Mol Cell, 2007. **28**(5): p. 739-45.
75. Zhao, Y., et al., *Preclinical evaluation of a potent novel DNA-dependent protein kinase inhibitor NU7441*. Cancer Res, 2006. **66**(10): p. 5354-62.
76. Shiloh, Y. and Y. Ziv, *The ATM protein kinase: regulating the cellular response to genotoxic stress, and more*. Nat Rev Mol Cell Biol, 2013. **14**(4): p. 197-210.

77. Batey, M.A., et al., *Preclinical evaluation of a novel ATM inhibitor, KU59403, in vitro and in vivo in p53 functional and dysfunctional models of human cancer*. *Mol Cancer Ther*, 2013. **12**(6): p. 959-67.
78. Zou, L., D. Liu, and S.J. Elledge, *Replication protein A-mediated recruitment and activation of Rad17 complexes*. *Proc Natl Acad Sci U S A*, 2003. **100**(24): p. 13827-32.
79. Acevedo, J., S. Yan, and W.M. Michael, *Direct Binding to Replication Protein A (RPA)-coated Single-stranded DNA Allows Recruitment of the ATR Activator TopBP1 to Sites of DNA Damage*. *J Biol Chem*, 2016. **291**(25): p. 13124-31.
80. Stracker, T.H., T. Usui, and J.H. Petrini, *Taking the time to make important decisions: the checkpoint effector kinases Chk1 and Chk2 and the DNA damage response*. *DNA Repair (Amst)*, 2009. **8**(9): p. 1047-54.
81. Hall, A.B., et al., *Potentiation of tumor responses to DNA damaging therapy by the selective ATR inhibitor VX-970*. *Oncotarget*, 2014. **5**(14): p. 5674-85.
82. Villaruz, L.C., et al., *ATM protein is deficient in over 40% of lung adenocarcinomas*. *Oncotarget*, 2016. **7**(36): p. 57714-57725.
83. Vendetti, F.P., et al., *ATR kinase inhibitor AZD6738 potentiates CD8+ T cell-dependent antitumor activity following radiation*. *J Clin Invest*, 2018. **128**(9): p. 3926-3940.
84. Lengauer, C., K.W. Kinzler, and B. Vogelstein, *Genetic instabilities in human cancers*. *Nature*, 1998. **396**(6712): p. 643-9.
85. Muggia, F.M., et al., *Platinum Antitumor Complexes: 50 Years Since Barnett Rosenberg's Discovery*. *J Clin Oncol*, 2015. **33**(35): p. 4219-26.
86. Chetrit, A., et al., *Effect of BRCA1/2 mutations on long-term survival of patients with invasive ovarian cancer: the national Israeli study of ovarian cancer*. *J Clin Oncol*, 2008. **26**(1): p. 20-5.
87. Turner, N., A. Tutt, and A. Ashworth, *Targeting the DNA repair defect of BRCA tumours*. *Curr Opin Pharmacol*, 2005. **5**(4): p. 388-93.
88. O'Malley, B.W., Jr., et al., *Molecular disruption of the MRN(95) complex induces radiation sensitivity in head and neck cancer*. *Laryngoscope*, 2003. **113**(9): p. 1588-94.
89. Abuzeid, W.M., et al., *Molecular disruption of RAD50 sensitizes human tumor cells to cisplatin-based chemotherapy*. *J Clin Invest*, 2009. **119**(7): p. 1974-85.
90. Ibrahim, Y.H., et al., *PI3K inhibition impairs BRCA1/2 expression and sensitizes BRCA-proficient triple-negative breast cancer to PARP inhibition*. *Cancer Discov*, 2012. **2**(11): p. 1036-47.

91. Ward, A., K.K. Khanna, and A.P. Wiegman, *Targeting homologous recombination, new pre-clinical and clinical therapeutic combinations inhibiting RAD51*. *Cancer Treat Rev*, 2015. **41**(1): p. 35-45.
92. Maacke, H., et al., *Over-expression of wild-type Rad51 correlates with histological grading of invasive ductal breast cancer*. *Int J Cancer*, 2000. **88**(6): p. 907-13.
93. Wiegman, A.P., et al., *Rad51 supports triple negative breast cancer metastasis*. *Oncotarget*, 2014. **5**(10): p. 3261-72.
94. Graeser, M., et al., *A marker of homologous recombination predicts pathologic complete response to neoadjuvant chemotherapy in primary breast cancer*. *Clin Cancer Res*, 2010. **16**(24): p. 6159-68.
95. Asakawa, H., et al., *Prediction of breast cancer sensitivity to neoadjuvant chemotherapy based on status of DNA damage repair proteins*. *Breast Cancer Res*, 2010. **12**(2): p. R17.
96. Huang, F. and A.V. Mazin, *A small molecule inhibitor of human RAD51 potentiates breast cancer cell killing by therapeutic agents in mouse xenografts*. *PLoS One*, 2014. **9**(6): p. e100993.
97. Huang, F., et al., *Identification of specific inhibitors of human RAD51 recombinase using high-throughput screening*. *ACS Chem Biol*, 2011. **6**(6): p. 628-35.
98. Budke, B., et al., *An optimized RAD51 inhibitor that disrupts homologous recombination without requiring Michael acceptor reactivity*. *J Med Chem*, 2013. **56**(1): p. 254-63.
99. Zhu, J., et al., *Synthesis, molecular modeling, and biological evaluation of novel RAD51 inhibitors*. *Eur J Med Chem*, 2015. **96**: p. 196-208.
100. American Cancer Society., *Cancer facts & figures*. The Society: Atlanta, GA. p. volumes.
101. Bray, F., et al., *Global cancer statistics 2018: GLOBOCAN estimates of incidence and mortality worldwide for 36 cancers in 185 countries*. *CA Cancer J Clin*, 2018. **68**(6): p. 394-424.
102. Edwards, B.K., et al., *Annual Report to the Nation on the status of cancer, 1975-2010, featuring prevalence of comorbidity and impact on survival among persons with lung, colorectal, breast, or prostate cancer*. *Cancer*, 2014. **120**(9): p. 1290-314.
103. Curtis, C., et al., *The genomic and transcriptomic architecture of 2,000 breast tumours reveals novel subgroups*. *Nature*, 2012. **486**(7403): p. 346-52.
104. Perou, C.M., et al., *Molecular portraits of human breast tumours*. *Nature*, 2000. **406**(6797): p. 747-52.

105. Sorlie, T., et al., *Gene expression patterns of breast carcinomas distinguish tumor subclasses with clinical implications*. Proc Natl Acad Sci U S A, 2001. **98**(19): p. 10869-74.
106. Arnedos, M., et al., *Triple-negative breast cancer: are we making headway at least?* Ther Adv Med Oncol, 2012. **4**(4): p. 195-210.
107. Bauer, K.R., et al., *Descriptive analysis of estrogen receptor (ER)-negative, progesterone receptor (PR)-negative, and HER2-negative invasive breast cancer, the so-called triple-negative phenotype: a population-based study from the California cancer Registry*. Cancer, 2007. **109**(9): p. 1721-8.
108. Foulkes, W.D., I.E. Smith, and J.S. Reis-Filho, *Triple-negative breast cancer*. N Engl J Med, 2010. **363**(20): p. 1938-48.
109. Dent, R., et al., *Triple-negative breast cancer: clinical features and patterns of recurrence*. Clin Cancer Res, 2007. **13**(15 Pt 1): p. 4429-34.
110. Carey, L.A., et al., *The triple negative paradox: primary tumor chemosensitivity of breast cancer subtypes*. Clin Cancer Res, 2007. **13**(8): p. 2329-34.
111. Henderson, I.C., et al., *Improved outcomes from adding sequential Paclitaxel but not from escalating Doxorubicin dose in an adjuvant chemotherapy regimen for patients with node-positive primary breast cancer*. J Clin Oncol, 2003. **21**(6): p. 976-83.
112. Guarneri, V., M.V. Dieci, and P. Conte, *Relapsed triple-negative breast cancer: challenges and treatment strategies*. Drugs, 2013. **73**(12): p. 1257-65.
113. Bianchini, G., et al., *Triple-negative breast cancer: challenges and opportunities of a heterogeneous disease*. Nat Rev Clin Oncol, 2016. **13**(11): p. 674-690.
114. Bonotto, M., et al., *Measures of outcome in metastatic breast cancer: insights from a real-world scenario*. Oncologist, 2014. **19**(6): p. 608-15.
115. Cancer Genome Atlas, N., *Comprehensive molecular portraits of human breast tumours*. Nature, 2012. **490**(7418): p. 61-70.
116. Antoniou, A., et al., *Average risks of breast and ovarian cancer associated with BRCA1 or BRCA2 mutations detected in case Series unselected for family history: a combined analysis of 22 studies*. Am J Hum Genet, 2003. **72**(5): p. 1117-30.
117. Lips, E.H., et al., *Triple-negative breast cancer: BRCAness and concordance of clinical features with BRCA1-mutation carriers*. Br J Cancer, 2013. **108**(10): p. 2172-7.
118. Alexandrov, L.B., et al., *Signatures of mutational processes in human cancer*. Nature, 2013. **500**(7463): p. 415-21.

119. Polak, P., et al., *A mutational signature reveals alterations underlying deficient homologous recombination repair in breast cancer*. Nat Genet, 2017. **49**(10): p. 1476-1486.
120. Lord, C.J. and A. Ashworth, *BRCAness revisited*. Nat Rev Cancer, 2016. **16**(2): p. 110-20.
121. Timms, K.M., et al., *Association of BRCA1/2 defects with genomic scores predictive of DNA damage repair deficiency among breast cancer subtypes*. Breast Cancer Res, 2014. **16**(6): p. 475.
122. Naipal, K.A., et al., *Functional ex vivo assay to select homologous recombination-deficient breast tumors for PARP inhibitor treatment*. Clin Cancer Res, 2014. **20**(18): p. 4816-26.
123. Meijer, T.G., et al., *Functional Ex Vivo Assay Reveals Homologous Recombination Deficiency in Breast Cancer Beyond BRCA Gene Defects*. Clin Cancer Res, 2018. **24**(24): p. 6277-6287.
124. Davies, H., et al., *HRDetect is a predictor of BRCA1 and BRCA2 deficiency based on mutational signatures*. Nat Med, 2017. **23**(4): p. 517-525.
125. Nagahashi, M., et al., *Next generation sequencing-based gene panel tests for the management of solid tumors*. Cancer Sci, 2019. **110**(1): p. 6-15.
126. Farmer, H., et al., *Targeting the DNA repair defect in BRCA mutant cells as a therapeutic strategy*. Nature, 2005. **434**(7035): p. 917-21.
127. Robson, M., et al., *Olaparib for Metastatic Breast Cancer in Patients with a Germline BRCA Mutation*. N Engl J Med, 2017. **377**(6): p. 523-533.
128. Ettl, J., et al., *Quality of life with talazoparib versus physician's choice of chemotherapy in patients with advanced breast cancer and germline BRCA1/2 mutation: patient-reported outcomes from the EMBRACA phase III trial*. Ann Oncol, 2018. **29**(9): p. 1939-1947.
129. Murai, J., et al., *Trapping of PARP1 and PARP2 by Clinical PARP Inhibitors*. Cancer Res, 2012. **72**(21): p. 5588-99.
130. Jones, P., *Profiling PARP inhibitors*. Nat Biotechnol, 2012. **30**(3): p. 249-50.
131. Chattaraj, P.K., U. Sarkar, and D.R. Roy, *Electrophilicity index*. Chem Rev, 2006. **106**(6): p. 2065-91.
132. Ayers, P.W., R.G. Parr, and R.G. Pearson, *Elucidating the hard/soft acid/base principle: a perspective based on half-reactions*. J Chem Phys, 2006. **124**(19): p. 194107.
133. Lopachin, R.M., et al., *Application of the Hard and Soft, Acids and Bases (HSAB) theory to toxicant--target interactions*. Chem Res Toxicol, 2012. **25**(2): p. 239-51.

134. Batthyany, C., et al., *Reversible post-translational modification of proteins by nitrated fatty acids in vivo*. J Biol Chem, 2006. **281**(29): p. 20450-63.
135. Groeger, A.L. and B.A. Freeman, *Signaling actions of electrophiles: anti-inflammatory therapeutic candidates*. Mol Interv, 2010. **10**(1): p. 39-50.
136. Abedi, E. and M.A. Sahari, *Long-chain polyunsaturated fatty acid sources and evaluation of their nutritional and functional properties*. Food Sci Nutr, 2014. **2**(5): p. 443-63.
137. Baker, L.M., et al., *Nitro-fatty acid reaction with glutathione and cysteine. Kinetic analysis of thiol alkylation by a Michael addition reaction*. J Biol Chem, 2007. **282**(42): p. 31085-93.
138. Fazzari, M., et al., *Generation and esterification of electrophilic fatty acid nitroalkenes in triacylglycerides*. Free Radic Biol Med, 2015. **87**: p. 113-24.
139. Schopfer, F.J., C. Cipollina, and B.A. Freeman, *Formation and signaling actions of electrophilic lipids*. Chem Rev, 2011. **111**(10): p. 5997-6021.
140. Delmastro-Greenwood, M., B.A. Freeman, and S.G. Wendell, *Redox-dependent anti-inflammatory signaling actions of unsaturated fatty acids*. Annu Rev Physiol, 2014. **76**: p. 79-105.
141. Tak, P.P. and G.S. Firestein, *NF-kappaB: a key role in inflammatory diseases*. J Clin Invest, 2001. **107**(1): p. 7-11.
142. Cui, T., et al., *Nitrated fatty acids: Endogenous anti-inflammatory signaling mediators*. J Biol Chem, 2006. **281**(47): p. 35686-98.
143. Itoh, K., K.I. Tong, and M. Yamamoto, *Molecular mechanism activating Nrf2-Keap1 pathway in regulation of adaptive response to electrophiles*. Free Radic Biol Med, 2004. **36**(10): p. 1208-13.
144. Kansanen, E., et al., *Electrophilic nitro-fatty acids activate NRF2 by a KEAP1 cysteine 151-independent mechanism*. J Biol Chem, 2011. **286**(16): p. 14019-27.
145. Tontonoz, P. and B.M. Spiegelman, *Fat and beyond: the diverse biology of PPARgamma*. Annu Rev Biochem, 2008. **77**: p. 289-312.
146. Schopfer, F.J., et al., *Covalent peroxisome proliferator-activated receptor gamma adduction by nitro-fatty acids: selective ligand activity and anti-diabetic signaling actions*. J Biol Chem, 2010. **285**(16): p. 12321-33.
147. Woodcock, C.C., et al., *Nitro-fatty acid inhibition of triple-negative breast cancer cell viability, migration, invasion, and tumor growth*. J Biol Chem, 2018. **293**(4): p. 1120-1137.

148. Baker, P.R., et al., *Fatty acid transduction of nitric oxide signaling: multiple nitrated unsaturated fatty acid derivatives exist in human blood and urine and serve as endogenous peroxisome proliferator-activated receptor ligands*. J Biol Chem, 2005. **280**(51): p. 42464-75.
149. Woodcock, S.R., et al., *Synthesis of nitrolipids. All four possible diastereomers of nitrooleic acids: (E)- and (Z)-, 9- and 10-nitro-octadec-9-enoic acids*. Org Lett, 2006. **8**(18): p. 3931-4.
150. Woodcock, S.R., et al., *Nitrated fatty acids: synthesis and measurement*. Free Radic Biol Med, 2013. **59**: p. 14-26.
151. Dunphy, K.A., L. Tao, and D.J. Jerry, *Mammary epithelial transplant procedure*. J Vis Exp, 2010(40).
152. Moynahan, M.E., A.J. Pierce, and M. Jasin, *BRCA2 is required for homology-directed repair of chromosomal breaks*. Mol Cell, 2001. **7**(2): p. 263-72.
153. Richardson, C., M.E. Moynahan, and M. Jasin, *Double-strand break repair by interchromosomal recombination: suppression of chromosomal translocations*. Genes Dev, 1998. **12**(24): p. 3831-42.
154. Gunn, A. and J.M. Stark, *I-SceI-based assays to examine distinct repair outcomes of mammalian chromosomal double strand breaks*. Methods Mol Biol, 2012. **920**: p. 379-91.
155. Woodcock, C.C., et al., *Nitro-fatty acid inhibition of triple negative breast cancer cell viability, migration, invasion and tumor growth*. J Biol Chem, 2017.
156. Campbell, K.J., et al., *Cisplatin mimics ARF tumor suppressor regulation of RelA (p65) nuclear factor-kappaB transactivation*. Cancer Res, 2006. **66**(2): p. 929-35.
157. Ahmed, K.M. and J.J. Li, *ATM-NF-kappaB connection as a target for tumor radiosensitization*. Curr Cancer Drug Targets, 2007. **7**(4): p. 335-42.
158. Rogakou, E.P., et al., *Megabase chromatin domains involved in DNA double-strand breaks in vivo*. J Cell Biol, 1999. **146**(5): p. 905-16.
159. Stiff, T., et al., *ATM and DNA-PK function redundantly to phosphorylate H2AX after exposure to ionizing radiation*. Cancer Res, 2004. **64**(7): p. 2390-6.
160. Scully, R. and A. Xie, *Double strand break repair functions of histone H2AX*. Mutat Res, 2013. **750**(1-2): p. 5-14.
161. Sharma, P., *Update on the Treatment of Early-Stage Triple-Negative Breast Cancer*. Curr Treat Options Oncol, 2018. **19**(5): p. 22.
162. Thorn, C.F., et al., *Doxorubicin pathways: pharmacodynamics and adverse effects*. Pharmacogenet Genomics, 2011. **21**(7): p. 440-6.

163. Dziadkowiec, K.N., et al., *PARP inhibitors: review of mechanisms of action and BRCA1/2 mutation targeting*. *Prz Menopauzalny*, 2016. **15**(4): p. 215-219.
164. Powell, S.N. and R.S. Bindra, *Targeting the DNA damage response for cancer therapy*. *DNA Repair (Amst)*, 2009. **8**(9): p. 1153-65.
165. Mao, Z., et al., *DNA repair by homologous recombination, but not by nonhomologous end joining, is elevated in breast cancer cells*. *Neoplasia*, 2009. **11**(7): p. 683-91.
166. Bhattacharyya, A., et al., *The breast cancer susceptibility gene BRCA1 is required for subnuclear assembly of Rad51 and survival following treatment with the DNA cross-linking agent cisplatin*. *J Biol Chem*, 2000. **275**(31): p. 23899-903.
167. Xu, Z.Y., et al., *Xrcc3 induces cisplatin resistance by stimulation of Rad51-related recombinational repair, S-phase checkpoint activation, and reduced apoptosis*. *J Pharmacol Exp Ther*, 2005. **314**(2): p. 495-505.
168. Ceccaldi, R., B. Rondinelli, and A.D. D'Andrea, *Repair Pathway Choices and Consequences at the Double-Strand Break*. *Trends Cell Biol*, 2016. **26**(1): p. 52-64.
169. Li, J. and X. Xu, *DNA double-strand break repair: a tale of pathway choices*. *Acta Biochim Biophys Sin (Shanghai)*, 2016. **48**(7): p. 641-6.
170. Robert, M., et al., *Olaparib for the treatment of breast cancer*. *Expert Opin Investig Drugs*, 2017. **26**(6): p. 751-759.
171. Sullivan, M.R. and K.A. Bernstein, *RAD-ical New Insights into RAD51 Regulation*. *Genes (Basel)*, 2018. **9**(12).
172. Modesti, M., et al., *Fluorescent human RAD51 reveals multiple nucleation sites and filament segments tightly associated along a single DNA molecule*. *Structure*, 2007. **15**(5): p. 599-609.
173. Budke, B., et al., *RI-1: a chemical inhibitor of RAD51 that disrupts homologous recombination in human cells*. *Nucleic Acids Res*, 2012. **40**(15): p. 7347-57.
174. Kuroda, S., et al., *Telomerase-dependent oncolytic adenovirus sensitizes human cancer cells to ionizing radiation via inhibition of DNA repair machinery*. *Cancer Res*, 2010. **70**(22): p. 9339-48.
175. Dupre, A., et al., *A forward chemical genetic screen reveals an inhibitor of the Mre11-Rad50-Nbs1 complex*. *Nat Chem Biol*, 2008. **4**(2): p. 119-25.
176. Lamont, K.R., et al., *Attenuating homologous recombination stimulates an AID-induced antileukemic effect*. *J Exp Med*, 2013. **210**(5): p. 1021-33.

177. Alagpulinsa, D.A., S. Ayyadevara, and R.J. Shmookler Reis, *A Small-Molecule Inhibitor of RAD51 Reduces Homologous Recombination and Sensitizes Multiple Myeloma Cells to Doxorubicin*. *Front Oncol*, 2014. **4**: p. 289.
178. Zhu, J., et al., *A novel small molecule RAD51 inactivator overcomes imatinib-resistance in chronic myeloid leukaemia*. *EMBO Mol Med*, 2013. **5**(3): p. 353-65.
179. Klein, H.L., *The consequences of Rad51 overexpression for normal and tumor cells*. *DNA Repair (Amst)*, 2008. **7**(5): p. 686-93.
180. Martin, R.W., et al., *RAD51 up-regulation bypasses BRCA1 function and is a common feature of BRCA1-deficient breast tumors*. *Cancer Res*, 2007. **67**(20): p. 9658-65.
181. Brouwer, I., et al., *Two distinct conformational states define the interaction of human RAD51-ATP with single-stranded DNA*. *EMBO J*, 2018. **37**(7).
182. Shen, Y., et al., *BMN 673, a novel and highly potent PARP1/2 inhibitor for the treatment of human cancers with DNA repair deficiency*. *Clin Cancer Res*, 2013. **19**(18): p. 5003-15.
183. Rouleau, M., et al., *PARP inhibition: PARP1 and beyond*. *Nat Rev Cancer*, 2010. **10**(4): p. 293-301.
184. Murai, J., et al., *Stereospecific PARP trapping by BMN 673 and comparison with olaparib and rucaparib*. *Mol Cancer Ther*, 2014. **13**(2): p. 433-43.
185. Litton, J.K., et al., *Talazoparib in Patients with Advanced Breast Cancer and a Germline BRCA Mutation*. *N Engl J Med*, 2018. **379**(8): p. 753-763.
186. Muvarak, N.E., et al., *Enhancing the Cytotoxic Effects of PARP Inhibitors with DNA Demethylating Agents - A Potential Therapy for Cancer*. *Cancer Cell*, 2016. **30**(4): p. 637-650.
187. Cardillo, T.M., et al., *Synthetic Lethality Exploitation by an Anti-Trop-2-SN-38 Antibody-Drug Conjugate, IMMU-132, Plus PARP Inhibitors in BRCA1/2-wild-type Triple-Negative Breast Cancer*. *Clin Cancer Res*, 2017. **23**(13): p. 3405-3415.
188. Liu, Y., et al., *RAD51 Mediates Resistance of Cancer Stem Cells to PARP Inhibition in Triple-Negative Breast Cancer*. *Clin Cancer Res*, 2017. **23**(2): p. 514-522.
189. D'Amore, A., et al., *Nitro-Oleic Acid (NO₂-OA) Release Enhances Regional Angiogenesis in a Rat Abdominal Wall Defect Model*. *Tissue Eng Part A*, 2018. **24**(11-12): p. 889-904.
190. Ferlay, J., et al., *Cancer incidence and mortality worldwide: sources, methods and major patterns in GLOBOCAN 2012*. *Int J Cancer*, 2015. **136**(5): p. E359-86.
191. Jamdade, V.S., et al., *Therapeutic targets of triple-negative breast cancer: a review*. *Br J Pharmacol*, 2015. **172**(17): p. 4228-37.

192. Abramson, V.G., et al., *Subtyping of triple-negative breast cancer: implications for therapy*. *Cancer*, 2015. **121**(1): p. 8-16.
193. Geenen, J.J.J., et al., *PARP Inhibitors in the Treatment of Triple-Negative Breast Cancer*. *Clin Pharmacokinet*, 2018. **57**(4): p. 427-437.
194. Turner, N., A. Tutt, and A. Ashworth, *Hallmarks of 'BRCAness' in sporadic cancers*. *Nat Rev Cancer*, 2004. **4**(10): p. 814-9.
195. Edessa, D. and M. Sisay, *Recent advances of cyclin-dependent kinases as potential therapeutic targets in HR+/HER2- metastatic breast cancer: a focus on ribociclib*. *Breast Cancer (Dove Med Press)*, 2017. **9**: p. 567-579.
196. Baker, P.R., et al., *Red cell membrane and plasma linoleic acid nitration products: synthesis, clinical identification, and quantitation*. *Proc Natl Acad Sci U S A*, 2004. **101**(32): p. 11577-82.
197. LaFargue, C.J., et al., *Exploring and comparing adverse events between PARP inhibitors*. *Lancet Oncol*, 2019. **20**(1): p. e15-e28.
198. Mansour, W.Y., et al., *Hierarchy of nonhomologous end-joining, single-strand annealing and gene conversion at site-directed DNA double-strand breaks*. *Nucleic Acids Res*, 2008. **36**(12): p. 4088-98.
199. Stark, J.M., et al., *Genetic steps of mammalian homologous repair with distinct mutagenic consequences*. *Mol Cell Biol*, 2004. **24**(21): p. 9305-16.
200. Symington, L.S., *Role of RAD52 epistasis group genes in homologous recombination and double-strand break repair*. *Microbiol Mol Biol Rev*, 2002. **66**(4): p. 630-70, table of contents.
201. Yano, S., et al., *In Vivo Selection of Intermediately- and Highly-Malignant Variants of Triple-negative Breast Cancer in Orthotopic Nude Mouse Models*. *Anticancer Res*, 2016. **36**(12): p. 6273-6277.
202. Holen, I., et al., *In vivo models in breast cancer research: progress, challenges and future directions*. *Dis Model Mech*, 2017. **10**(4): p. 359-371.
203. Castroviejo-Bermejo, M., et al., *A RAD51 assay feasible in routine tumor samples calls PARP inhibitor response beyond BRCA mutation*. *EMBO Mol Med*, 2018. **10**(12).
204. Kaufman, B., et al., *Olaparib monotherapy in patients with advanced cancer and a germline BRCA1/2 mutation*. *J Clin Oncol*, 2015. **33**(3): p. 244-50.
205. Domchek, S.M., et al., *Efficacy and safety of olaparib monotherapy in germline BRCA1/2 mutation carriers with advanced ovarian cancer and three or more lines of prior therapy*. *Gynecol Oncol*, 2016. **140**(2): p. 199-203.

206. Kaye, S.B., et al., *Phase II, open-label, randomized, multicenter study comparing the efficacy and safety of olaparib, a poly (ADP-ribose) polymerase inhibitor, and pegylated liposomal doxorubicin in patients with BRCA1 or BRCA2 mutations and recurrent ovarian cancer*. J Clin Oncol, 2012. **30**(4): p. 372-9.
207. Drew, Y., et al., *Phase 2 multicentre trial investigating intermittent and continuous dosing schedules of the poly(ADP-ribose) polymerase inhibitor rucaparib in germline BRCA mutation carriers with advanced ovarian and breast cancer*. Br J Cancer, 2016. **114**(12): p. e21.
208. Mirza, M.R., et al., *Niraparib Maintenance Therapy in Platinum-Sensitive, Recurrent Ovarian Cancer*. N Engl J Med, 2016. **375**(22): p. 2154-2164.
209. Zhong, L., et al., *Cost-Effectiveness of Niraparib and Olaparib as Maintenance Therapy for Patients with Platinum-Sensitive Recurrent Ovarian Cancer*. J Manag Care Spec Pharm, 2018. **24**(12): p. 1219-1228.
210. Ledermann, J., et al., *Olaparib maintenance therapy in platinum-sensitive relapsed ovarian cancer*. N Engl J Med, 2012. **366**(15): p. 1382-92.
211. Ledermann, J., et al., *Olaparib maintenance therapy in patients with platinum-sensitive relapsed serous ovarian cancer: a preplanned retrospective analysis of outcomes by BRCA status in a randomised phase 2 trial*. Lancet Oncol, 2014. **15**(8): p. 852-61.
212. Ledermann, J., P. Harter, and C. Gourley, *Correction to Lancet Oncol 2014; 15: 856. Olaparib maintenance therapy in patients with platinum-sensitive relapsed serous ovarian cancer: a preplanned retrospective analysis of outcomes by BRCA status in a randomised phase 2 trial*. Lancet Oncol, 2015. **16**(4): p. e158.
213. Pujade-Lauraine, E., et al., *Olaparib tablets as maintenance therapy in patients with platinum-sensitive, relapsed ovarian cancer and a BRCA1/2 mutation (SOLO2/ENGOT-Ov21): a double-blind, randomised, placebo-controlled, phase 3 trial*. Lancet Oncol, 2017. **18**(9): p. 1274-1284.
214. Coleman, R.L., et al., *Rucaparib maintenance treatment for recurrent ovarian carcinoma after response to platinum therapy (ARIEL3): a randomised, double-blind, placebo-controlled, phase 3 trial*. Lancet, 2017. **390**(10106): p. 1949-1961.
215. Cancer Genome Atlas Research, N., *Integrated genomic analyses of ovarian carcinoma*. Nature, 2011. **474**(7353): p. 609-15.